3/25

SANDIA REPORT

SAND96–0551 • UC–704
Unlimited Release
Printed March 1996

Shock Compression Profiles in Ceramics

D. E. Grady, R. L. Moody

Prepared by
Sandia National Laboratories
Albuquerque, New Mexico 87185 and Livermore, California 94550
for the United States Department of Energy
under Contract DE-AC04-94AL85000

Issued by Sandia National Laboratories, operated for the United States Department of Energy by Sandia Corporation.

Available to DOE and DOE contractors from
Office of Scientific and Technical Information
PO Box 62
Oak Ridge, TN 37831

Prices available from (615) 576-8401, FTS 626-8401

Available to the public from
National Technical Information Service
US Department of Commerce
5285 Port Royal Rd
Springfield, VA 22161

NTIS price codes
Printed copy: A08
Microfiche copy: A01

Distribution
Category UC-704

SAND96-0551
Unlimited Release
Printed March -1996

SHOCK COMPRESSION PROFILES IN CERAMICS

D.E. GRADY and R.L. MOODY
Experimental Impact Physics Department 1433
Sandia National Laboratories
Albuquerque, NM 87185-0821

Abstract

An investigation of the shock compression properties of high-strength ceramics has been performed using controlled planar impact techniques. In a typical experimental configuration, a ceramic target disc is held stationary, and it is struck by plates of either a similar ceramic or by plates of a well-characterized metal. All tests were performed using either a single-stage propellant gun or a two-stage light-gas gun. Particle velocity histories were measured with laser velocity inteferometry (VISAR) at the interface between the back of the target ceramic and a calibrated VISAR window material. Peak impact stresses achieved in these experiments range from about 3 to 70 GPa. Ceramics tested under shock impact loading include: Al_2O_3, AlN, B_4C, SiC, Si_3N_4, TiB_2, WC and ZrO_2. This report compiles the VISAR wave profiles and experimental impact parameters within a database–useful for response model development, computational model validation studies, and independent assessment of the physics of dynamic deformation on high-strength, brittle solids.

Contents

1. Introduction

Planar impact experiments provide the backbone data for the development of dynamic material response models used in computational simulation and engineering analysis of the high-velocity interaction of materials and structures. While such techniques do not exhaustively examine the stress-strain-time states achieved in high-velocity impact events, they do target the high-confining-stress and high-strain-rate deformation characteristics of such interactions. In addition, the technology of planar-impact, material-response studies and the concomitant high-resolution diagnostics of such technology has achieved a maturity not available in other dynamic test methods.

Over the past several years, the Impact Physics Department at Sandia National Laboratories has actively pursued a study of the dynamic mechanical and equation-of-state properties of high-strength ceramics through controlled-launch impact experiments. To date, a large number of experiments have been completed upon a range of relevant ceramics. As these data unfold, their critical material response features are emerging, and results are impacting the development of constitutive models for ceramics. High-resolution wave profile measurements have been provided exclusively by time-resolved interferometry (VISAR) diagnostics. Through novel implementation of such experiments, the critical features concerning dynamic compressibility, strength, flow, and fracture are being explored.

Some unique examples of important effects revealed through shock profile studies on ceramic materials include:

- The Hugoniot elastic limit for more recent silicon carbides is more than a factor-of-two higher than values reported in earlier literature, an indication of substantial improvements in ceramic preparation techniques over the past several decades.

- The compressive wave observed in titanium diboride exhibits a three-wave structure, indicative of either phase transformation or of a complex two-mechanism yield in this material.

- In stark contrast to other ceramics that show neutral or hardening post-yield shear strength more reminiscent of the shock behavior of metals, boron carbide shows a substantial loss of shear strength, after the initial dynamic yield.

- In contrast to other ceramics studied, transformation-toughened zirconium dioxide exhibits a 1.6 to 1.8 GPa spall strength. This is comparable with many metals, suggesting that the toughening mechanism plays a critical role in the transient spall process.

- An irreversible, 20 percent-by-volume phase transition in aluminum nitride, at approximately 20 GPa, leads to a complex shock profile structure and large dissipation properties for this ceramic.

- Examination of the evolution of precursor wave profiles with propagation distance indicates that initial yield and post-yield characteristics of most ceramics are relatively rate insensitive.

- Unusually high compression hardening is observed in tungsten carbide, probably manifesting the liquid-phase, sintered microstructure of this material.

- The release properties of most ceramics appear to be extremely dispersive, as compared to metals shocked to similar pressures.

In addition to those features noted above and other physical features of ceramic materials are being extracted from wave-profile measurements, providing insight into both dynamic response and critical data for constitutive model development. Reports and papers which address in more detail the material response issues outlined above are provided in the references.

It is not the intention of this document, however, to explore the very rich dynamic properties characteristic of ceramic materials, as revealed by shock wave experiments. The more modest purposes of this report are to document the extensive database of wave profile measurements which have been made on ceramic materials and to make this data available for the development of material response models and the validation of predictive computational codes.

This report is organized as follows: After the brief introduction, a section is included that discusses, in some detail, the experimental impact procedures and the VISAR-diagnostics methods used to acquire the present wave profile data. Following the experimental section, the wave profile data are presented. In alphabetical order, the data for each ceramic investigated are fully provided. A preliminary section for each ceramic discusses the source–or sources–for the ceramics tested, necessary material properties not provided later, and some of the salient dynamic characteristics that have been uncovered in analysis studies to date. Some qualifying comments about specific wave profile features or anomalies exhibited by the data to follow are also included, where they are deemed useful.

Following this initial summary for a specific ceramic, data sheets for each test on that ceramic–one test per page–are provided. The upper half of the page includes a table of relevant experimental properties and dimensions. The measured-interface velocity profile is provided on the lower half of page. Test numbering cross-references, ceramic densities, and ultrasonic properties are provided in appendices.

2. Experimental Methods

Controlled planar impact experiments were used in all cases to obtain the wave-profile data provided in this report. Variations in both impact geometry and in ancillary impact materials were often used to achieve specific loading conditions or to enhance profile features characteristic of particular deformation properties of the target material. The baseline experimental configuration is described here in detail. Any variations to this baseline configuration are identified with the associated experiment, and the intended purpose of the variation is discussed. For example, PMMA (polymethyl methacrylate) VISAR windows were often substituted for lithium fluoride windows when a more intense dynamic spall environment was desired. More complex multiple plate geometries were used on the projectile when double shock loading was investigated.

Uniaxial-strain, compressive shock and release waves were produced in the ceramic test samples, using either a single-stage powder-gun or a two-stage light-gas gun. In particular, an 89 mm (inner-bore diameter), smooth-bore powder gun with a velocity range of 0.4 - 2.4 km/s was used for the largest portion of the shock-wave tests presented in this report. Some of the higher shock-pressure data were acquired with a 20 mm (inner-bore diameter), two-stage, light-gas gun.

On the powder-gun facility, three electrical self-shorting pins are used to measure the velocity of the projectile at impact. Accuracy of the velocity measurement for these experiments is typically $\pm$1% or better. Where measurement difficulties indicate larger uncertainties, those uncertainties are noted in the individual data sheets.

Four similar pins are mounted flush to the impact plane and are used to monitor the planarity of impact. These pins are also used to trigger diagnostic equipment, including transient digitizers and counters. Deviations from planarity at impact are typically about 10^{-3} radians.

The baseline target configuration is shown in Figure 1. Either a disc of the ceramic being tested or another material of known shock properties–usually a metal–is mounted on the projectile, and it is typically backed by a lower shock impedance material, such as polyurethane foam or PMMA. This produces the subsequent decompression wave that follows the initial impact-induced shock wave. To provide an impact surface for the shorting pins within the impact plane when the impactor is less than full projectile diameter, an aluminum ring that encloses the impactor is used.

For the target, a similar disc of the ceramic is mounted in a stationary supporting target fixture. An optical-quality disc of single crystal lithium fluoride–or other VISAR

window material–is intimately bonded with epoxy to the back of this ceramic sample. All critical surfaces are lapped and polished, and they are typically flat to within a few bands of sodium light. The surface of the lithium fluoride that is to be bonded is first lightly diffused, and then it is plated by vapor-deposition with about 100 nm of aluminum. The epoxy bond between the ceramic sample and the lithium fluoride window is typically 10 to 20 μm.

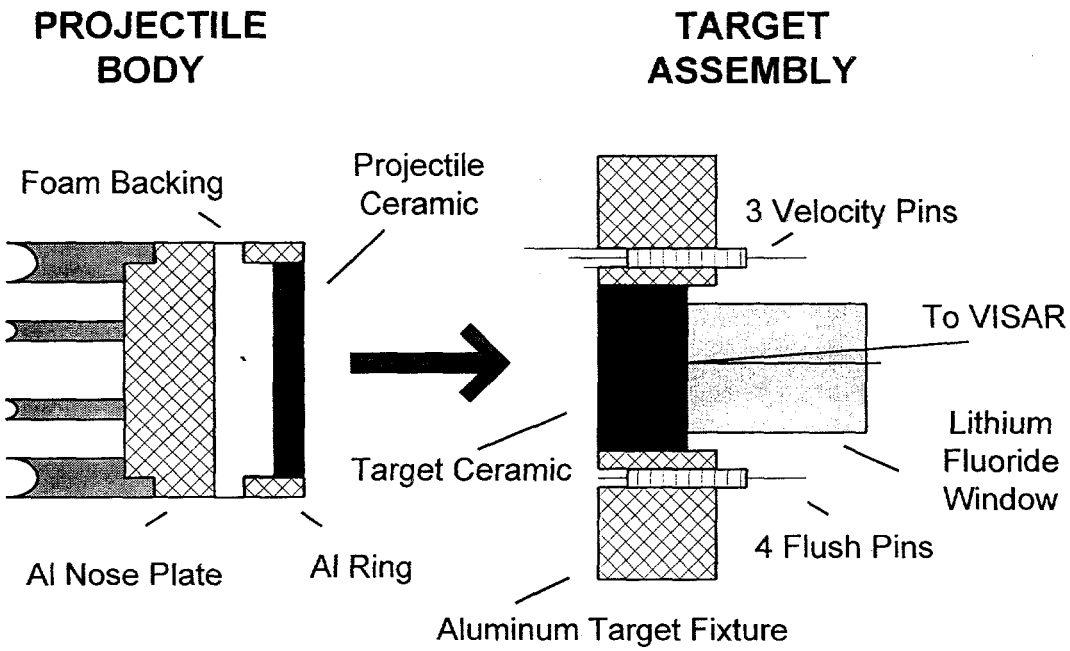

FIGURE 1. Experimental configuration for shock and release-wave experiments on ceramic

The ceramic-on-ceramic planar impact produces a compressive wave of uniaxial strain that propagates across the stationary ceramic specimen and through the ceramic/window interface. An equivalent compressive shock-wave propagates backwards through the projectile impactor specimen, and then it reflects at the low-impedance foam interface, becoming a release wave which unloads the compressed ceramic. (This wave can become, instead, a reflected recompression wave, if a higher impedance backing material is used.) Dimensions of the sample and impactor discs are selected such that lateral release waves from the boundaries of the discs do not interfere with the central uniaxial motion of the material until after the experimental measurement is completed.

In a typical shock wave experiment, four materials are usually responsible for determining the characteristics of the measured interface wave-profile, and they

must be accounted for in a one-dimensional computational simulation of the experiment. These four materials are the impactor and backing materials of the projectile and the sample and window materials of the target. A simplified experimental configuration is illustrated in Figure 2. Critical parameters for these four experimental materials are provided at the top of each experimental data sheet presented in this report.

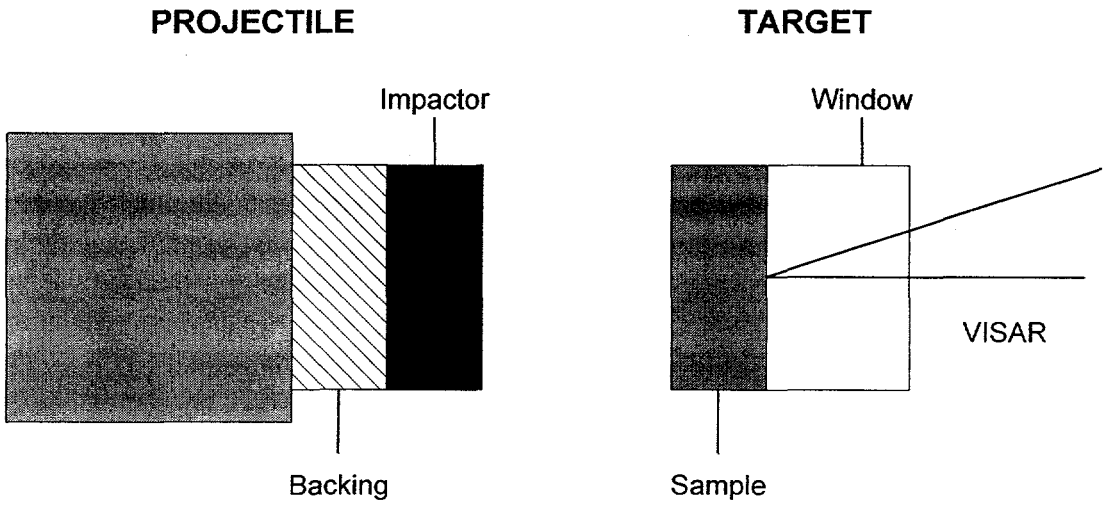

FIGURE 2. Simplified experimental configuration, identifying materials critical to the VISAR wave profile measurement

Using laser velocity interferometry techniques (VISAR, Barker and Hollenbach, 1972), the compression and release wave behavior are measured by monitoring the time-resolved longitudinal motion at the center of the ceramic/window interface. Typically, the illuminated spot size of the incoming laser beam is 50 to 100 μm in diameter. Transient digitizers–with a sample period of 0.742 ns per data point–are used to record the measurements. Although its mechanical impedance is somewhat lower than that of the ceramics being tested, lithium fluoride is the predominant choice for the laser window material. This is because it is the only material which has been optically calibrated and which remains transparent when subjected to the 5 to 50 GPa shock stresses generated in the laser windows used in these experiments (Wise and Chhabildas, 1986).

The interference fringes measured by the VISAR system are converted to time-resolved histories of the velocity of the interface using the method originally developed by Barker and Hollenbach (1972). Amplitude resolution is approximately

2% for one fringe. Typically, two to three fringes are achieved in the interface acceleration through the compressive shock front.

It is also important to note that the transit times of the first arrival was not measured in these tests, and the profiles are not necessarily aligned in time with expected elastic precursor velocities.

Occasionally, shock jumps exceed the frequency response of the VISAR instrumentation, and the fringes corresponding to the velocity change are not recorded. These points are easily recognized by contrast dips in the VISAR reduction process. Integral fringes–typically one or two fringes–are added at these points to accommodate missing jumps in velocity. The required, approximate, amplitude of the missing velocity jump must be determined from other experimental and physical constraints. Each data sheet in this report indicates the experimental velocity-per-fringe constant and, in some cases, when an addition of fringes at a shock jump was necessary.

In general, the interactions of the evolving wave in the sample with the lower-impedance window material results in the complex wave structure monitored by the VISAR. Numerical simulations are commonly employed to recreate the wave structure in the sample.

The ceramics investigated in this report were acquired from a number of sources. Usually, the quality of the ceramic being investigated was high. However, because of the empirical nature and evolving technology of the sintering and hot-pressing methods used to produce such ceramics, features relating to microstructure and added chemical impurities are not usually constant from supplier to supplier. To support analysis and material model development, information about the supplier, microstructure, and chemical properties is discussed, where this information is available.

Density and ultrasonic properties for the ceramics are provided in Appendix A. Elastic properties have also been calculated from ultrasonic wave speeds, assuming elastic isotropy. The latter assumption is known to be incorrect for some of the hot-pressed ceramic where a degree of axial anisotropy apparently emerges from the preparation process.

In this document, a uniform system of test numbering has been used, which (in most cases) does not correspond to the original experiment numbers. Since many of the original test numbers appear in earlier reports and papers, an appropriate cross-reference is provided in Appendix B.

3. Aluminum Nitride Ceramics

Aluminum nitride exists under ambient conditions in the wurtzite (HCP) structure. Static compression experiments indicate a pressure-induced, non-recoverable volume, phase transformation to the rocksalt (FCC) structure [Volstädt, et al., 1990]. This transformation has also been observed to occur under shock-compression conditions [Kondo, et al., 1982; Nakamura and Mashimo, 1994; Kipp and Grady, 1994] at a shock stress of 20 to 22 GPa and a transformation volume change of approximately 20%. Under shock-wave conditions, this phase transformation leads to a complex shock-front structure with additional complications at the lithium fluoride interface, because of wave reflections [Kipp and Grady, 1994]. Above the 20 to 22 GPa shock-transition stress level, the material is extremely dissipative, leading to a rapid attenuation of the shock waves [Kipp and Grady, 1994]. A Hugoniot elastic limit of approximately 8 to 10 GPa characterizes the dynamic strength of fully-dense aluminum nitride [Brar, et al., 1992; Grady, 1994]. Shock studies for different sample thicknesses indicate a negligible elastic precursor attenuation with propagation distance [Grady, 1995]. Further equation-of-state and dynamic strength issues have been pursued by Dandekar, et al. (1994).

In this report, shock-wave profile data are reported on aluminum nitride ceramics that were provided by two different sources. The first material was provided by Dow Chemical Company, and it is the same material tested by Brar, et al. (1992). This hot-pressed ceramic was reported to have a porosity of approximately 1% and a grain size of about 2 μm. The nominal reference density is 3254 kg/m^3. Elastic, longitudinal and shear velocities are 10.73 km/s and 6.32 km/s, respectively. Sample to sample variations of about 2% in both density and wave velocities are believed to be an indication of material heterogeneity that was introduced in the ceramic production process. The second aluminum nitride ceramic was provided by T. Mashimo of Kumamoto University, Japan. This material was produced by Sumitomo Electric Industries Co., Ltd. It has a density of 3236 kg/m^3 and a porosity of 0.5 to 0.7%. Impurities were less than 100 ppm of Fe, Si, and Ca, with 0.03% wt C and 0.25% wt O. Elastic, longitudinal and shear wave velocities–measured ultrasonically–are 10.80 km/s and 6.34 km/s, respectively.

The majority (eleven) of the wave-profile measurements were made on the Dow Chemical Company material. Several of the profiles–AN3, AN8 and AN11–exhibited unduly noisy velocity profiles. One profile–AN1–revealed a lower amplitude double-wave that was not observed in other samples. This noisy behavior and inconsistency is not understood, but it may be related to the apparent non-uniformity of this material. In some cases, a very consistent sample-to-sample behavior was noted for the Dow material. For example, this behavior is observed in AN5, AN6, and AN10 that were investigated in Kipp and Grady (1994).

Spall strength data are provided by tests AN8, AN9, and possibly AN4. These data are discussed partially in Grady (1994a).

Three compression-only profiles were measured on the higher-quality Sumitomo Electric material; principally, to examine the Hugoniot elastic-limit strength and shock-induced phase transition properties of this ceramic. Wave features in these profiles are complicated by the impedance differences between window and ceramic materials.

Shot Number:	AN1	**Impact Velocity:**	1.780 km/s
Test Material:	Aluminum Nitride		
Supplier:	Dow Chemical Co.	**Velocity Per Fringe:**	430.92 m/s

	Material	Thickness (mm)	Diameter (mm)	Density (kg/m^3)
Sample	Aluminum Nitride	9.952	75.0	3261
Window	Lithium Flouride	25.4	50.8	2640
Impactor	Aluminum Nitride	4.971	87.4	3258
Backer	Polyurethane Foam	8.0	87.4	320

Comments: The first step, to approximately 0.2 km/s, was not seen in other aluminum nitride tests.

AN1 VELOCITY PROFILE

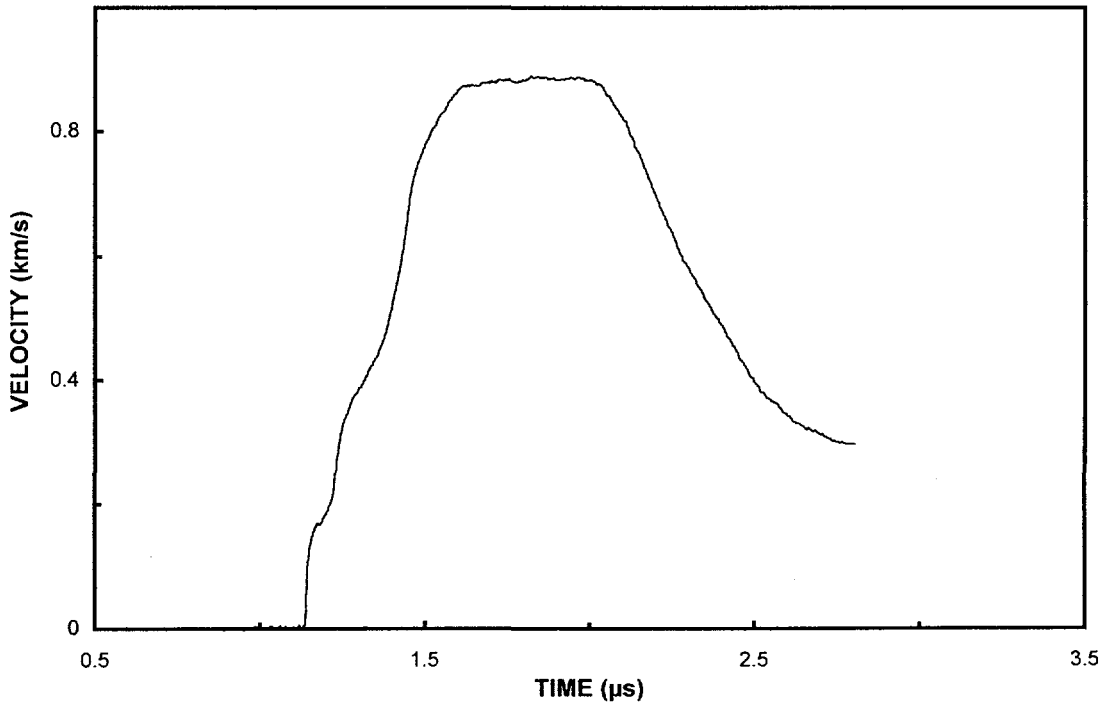

Shot Number:	AN2	**Impact Velocity:**	2.277 km/s
Test Material:	Aluminum Nitride		
Supplier:	Dow Chemical Co.	**Velocity Per Fringe:**	430.92 m/s

	Material	Thickness (mm)	Diameter (mm)	Density (kg/m^3)
Sample	Aluminum Nitride	9.952	75.0	3259
Window	Lithium Fluoride	25.4	50.8	2640
Impactor	Aluminum Nitride	4.923	88.1	3260
Backer	Polyurethane Foam	8.0	87.5	640

Comments:

AN2 VELOCITY PROFILE

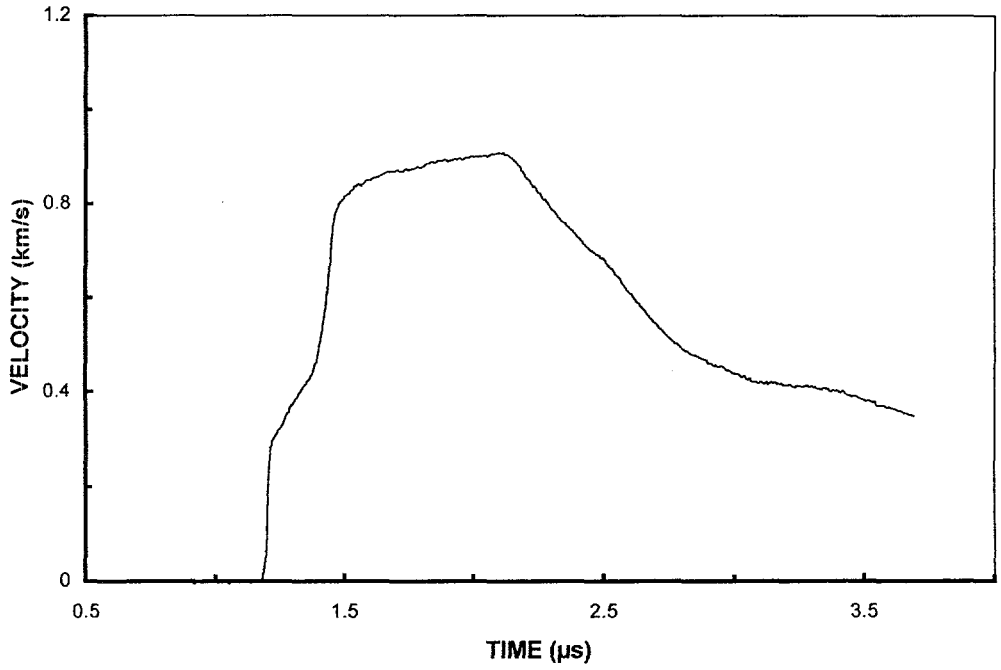

Shot Number:	AN3	**Impact Velocity:**	1.263 km/s ± 2%
Test Material:	Aluminum Nitride		
Supplier:	Dow Chemical Co.	**Velocity Per Fringe:**	430.92 m/s

	Material	Thickness (mm)	Diameter (mm)	Density (kg/m^3)
Sample	Aluminum Nitride	9.554	75.0	3262
Window	Lithium Fluoride	25.4	50.8	2640
Impactor	Aluminum Nitride	4.968	88.5	3258
Backer	Polyurethane Foam	8.0	87.5	320

Comments: The intial lead-in and noisy profile may be related to defects or inhomogeneities in the intial sample.

AN3 VELOCITY PROFILE

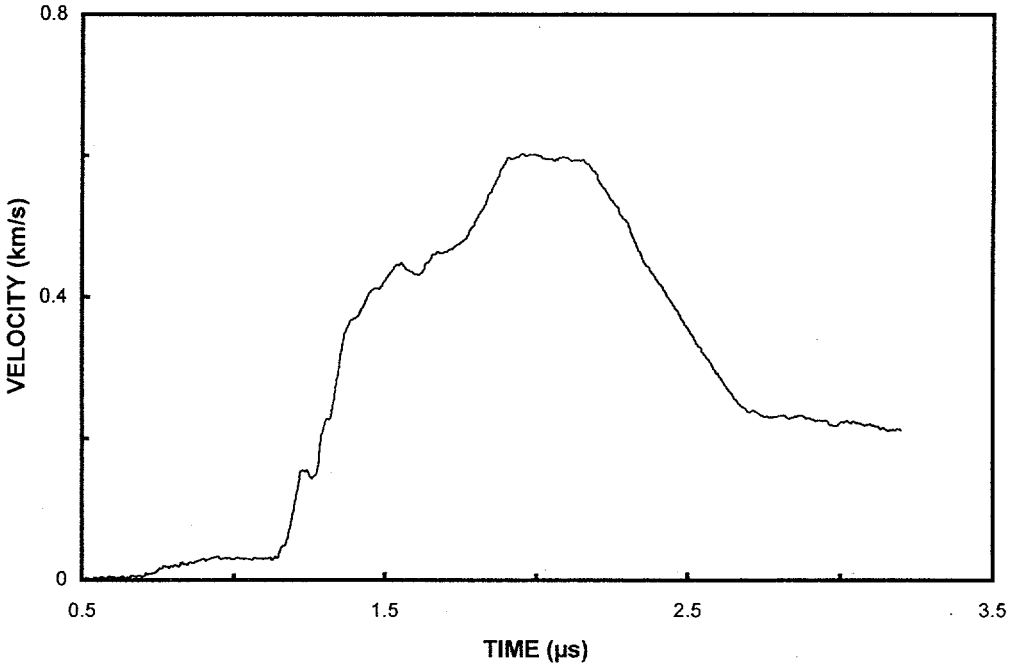

Shot Number:	AN4	**Impact Velocity:**	0.589 km/s
Test Material:	Aluminum Nitride		
Supplier:	Dow Chemical Co.	**Velocity Per Fringe:**	94.76 m/s

	Material	Thickness (mm)	Diameter (mm)	Density (kg/m^3)
Sample	Aluminum Nitride	9.954	74.9	3255
Window	Lithium Fluoride	25.4	50.8	2640
Impactor	Aluminum Nitride	4.975	87.5	3256
Backer	Polyurethane Foam	8.0	87.5	320

Comments:

AN4 VELOCITY PROFILE

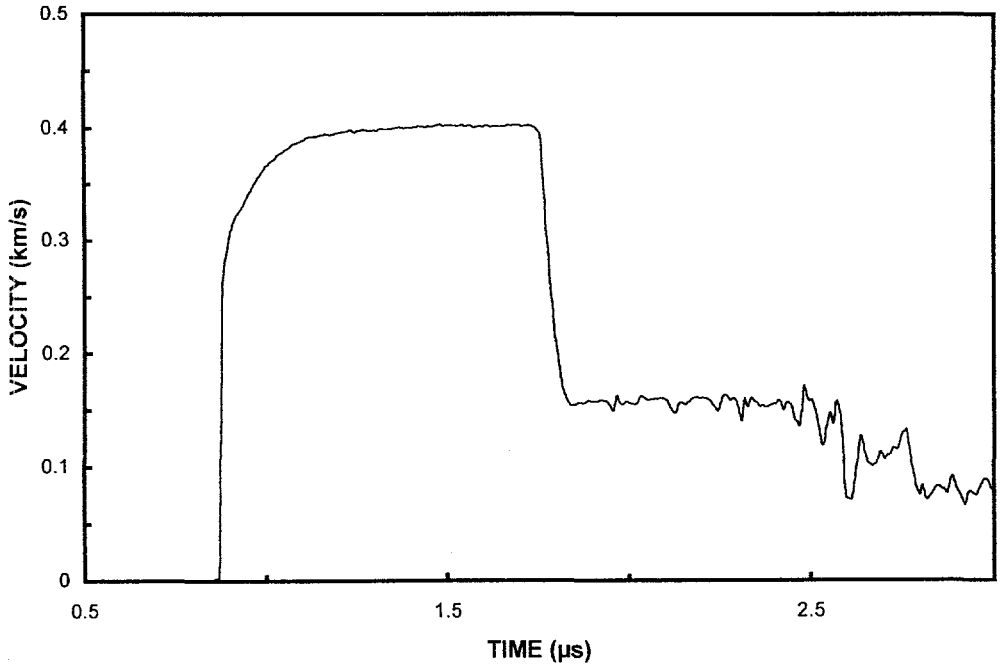

Shot Number:	AN5	**Impact Velocity:**	2.239 km/s
Test Material:	Aluminum Nitride		
Supplier:	Dow Chemical Co.	**Velocity Per Fringe:**	681.52 m/s

	Material	Thickness (mm)	Diameter (mm)	Density (kg/m^3)
Sample	Aluminum Nitride	9.567	75.0	3265
Window	Lithium Fluoride	25.4	50.7	2640
Impactor	Tantalum	1.508	87.5	16657
Backer	Polyurethane Foam	8.0	87.5	640

Comments: The small peak on top of the profile is the residual of the third wave in aluminum nitride, after rapid attenuation.

AN5 VELOCITY PROFILE

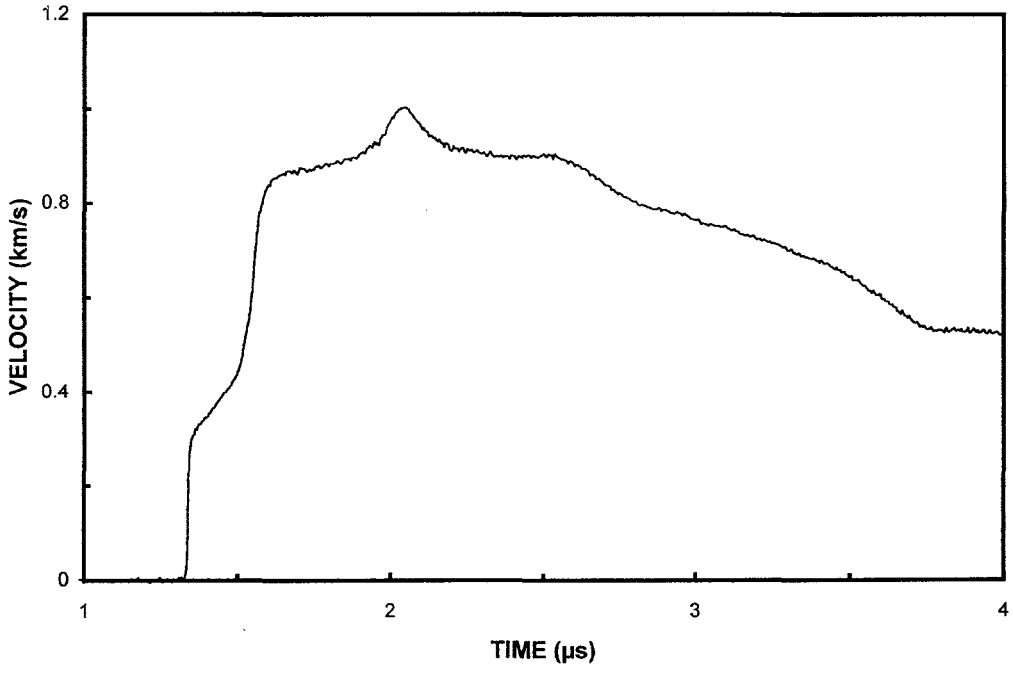

Shot Number:	AN6	**Impact Velocity:**	2.207 km/s
Test Material:	Aluminum Nitride		
Supplier:	Dow Chemical Co.	**Velocity Per Fringe:**	681.52 m/s

	Material	Thickness (mm)	Diameter (mm)	Density (kg/m^3)
Sample	Aluminum Nitride	2.510	76.5	3248
Window	Lithium Fluoride	25.5	50.8	2640
Impactor	Tantalum	1.528	87.5	16618
Backer	Polyurethane Foam	8.0	87.5	640

Comments: Computer simulations indicated complexities in the compression wave relate to impedance differences between sample and window.

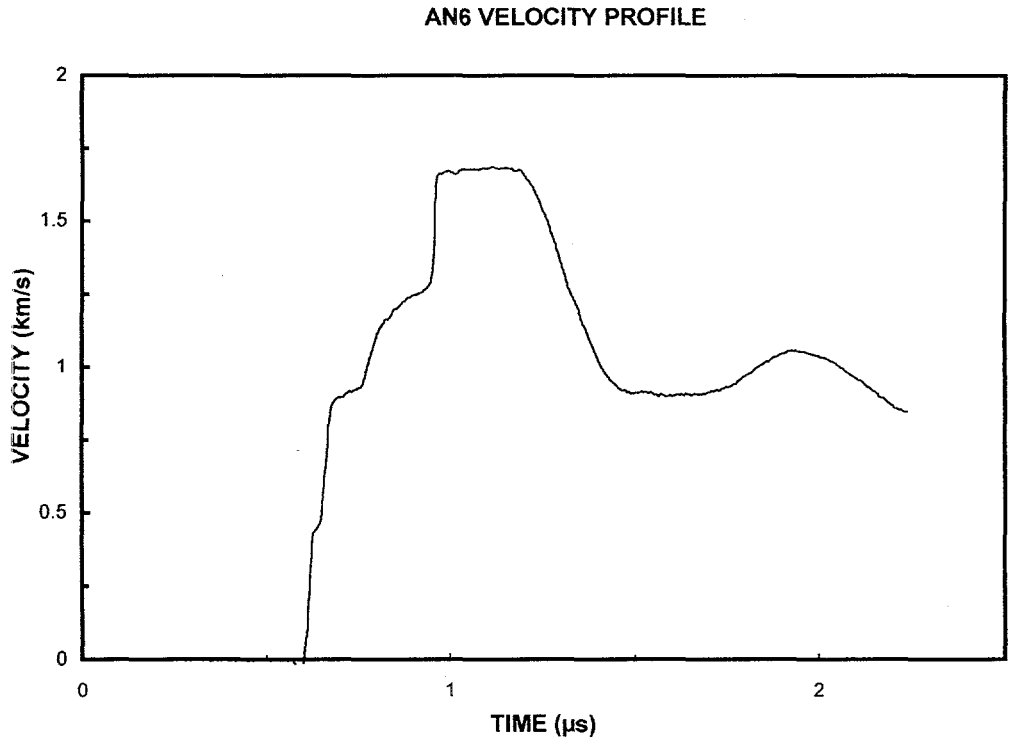

Shot Number:	AN7	**Impact Velocity:**	2.230 km/s
Test Material:	Aluminum Nitride		
Supplier:	Dow Chemical Co.	**Velocity Per Fringe:**	681.52 m/s

	Material	Thickness (mm)	Diameter (mm)	Density (kg/m^3)
Sample	Aluminum Nitride	2.507	76.5	3248
Window	Lithium Fluoride	25.5	50.9	2640
Impactor	Tungsten	1.502	87.5	19289
Backer	PMMA	6.4	87.5	1886

Comments: Highest impact-amplitude in aluminum nitride is achieved with a tungsten impactor.

AN7 VELOCITY PROFILE

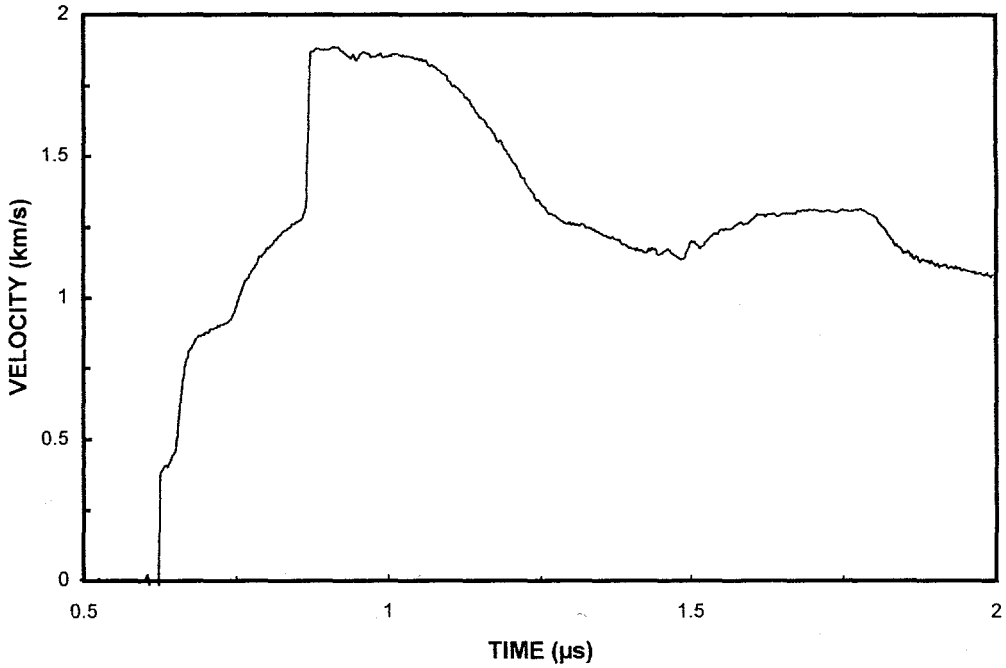

Shot Number:	AN8	**Impact Velocity:**	1.160 km/s ± 2%
Test Material:	Aluminum Nitride		
Supplier:	Dow Chemical Co.	**Velocity Per Fringe:**	94.76 m/s

	Material	Thickness (mm)	Diameter (mm)	Density (kg/m^3)
Sample	Aluminum Nitride	10.184	76.2	3258
Window	Lithium Fluoride	25.2	50.7	2640
Impactor	PMMA	2.004	87.5	1186
Backer	Polyurethane Foam	8.0	87.5	139

Comments: Spall strength experiment

AN8 VELOCITY PROFILE

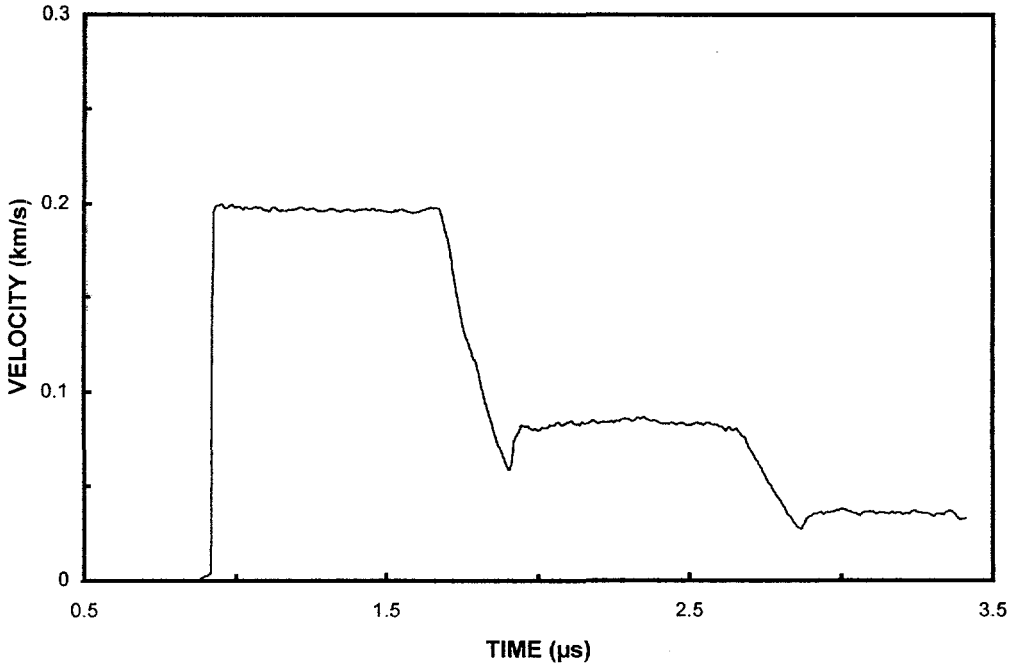

Shot Number:	AN9	**Impact Velocity:**	0.860 km/s
Test Material:	Aluminum Nitride		
Supplier:	Dow Chemical Co.	**Velocity Per Fringe:**	94.76 m/s

	Material	Thickness (mm)	Diameter (mm)	Density (kg/m^3)
Sample	Aluminum Nitride	9.552	75.0	3221
Window	Lithium Fluoride	25.5	50.7	2640
Impactor	PMMA	1.991	87.5	1186
Backer	Polyurethane Foam	7.9	87.5	139

Comments: Spall strength experiment

AN9 VELOCITY PROFILE

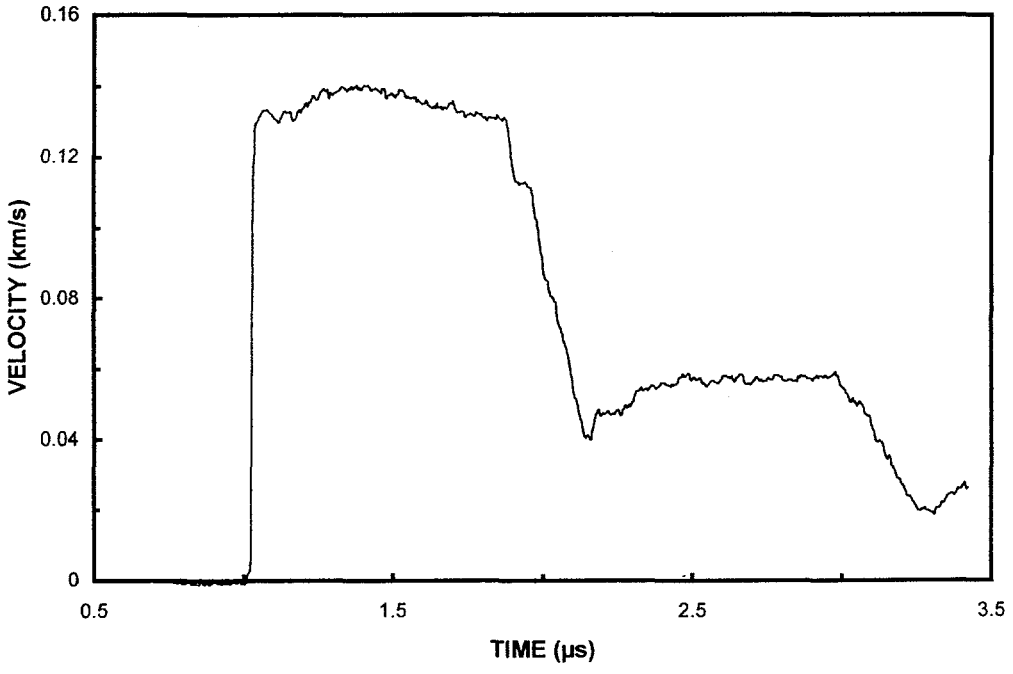

Shot Number:	AN10	**Impact Velocity:**	2.215 km/s
Test Material:	Aluminum Nitride		
Supplier:	Dow Chemical Co.	**Velocity Per Fringe:**	681.52 m/s

	Material	Thickness (mm)	Diameter (mm)	Density (kg/m^3)
Sample	Aluminum Nitride	4.183	76.5	3248
Window	Lithium Fluoride	31.9	50.8	2640
Impactor	Tantalum	1.526	87.5	16642
Backer	Polyurethane Foam	8.0	87.5	640

Comments: This is a repeat of test AN5, to better resolve the third wave by using a thinner sample.

AN10 VELOCITY PROFILE

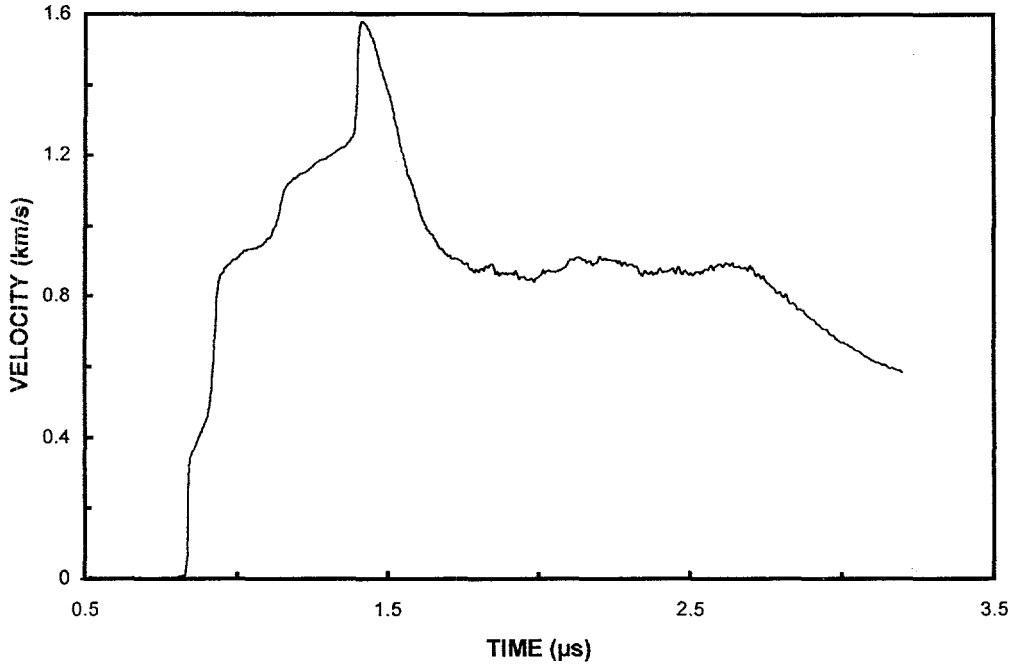

Shot Number:	AN11	**Impact Velocity:**	2.262 km/s
Test Material:	Aluminum Nitride		
Supplier:	Dow Chemical Co.	**Velocity Per Fringe:**	430.92 m/s

	Material	Thickness (mm)	Diameter (mm)	Density (kg/m^3)
Sample	Aluminum Nitride	4.182	76.5	3250
Window	Lithium Fluoride	37.8	50.8	2640
Impactor	Aluminum Nitride	4.181	76.5	3250
Backer	Polyurethane Foam	8.0	87.5	640

Comments: The noisy profile in this test was not understood.

AN11 VELOCITY PROFILE

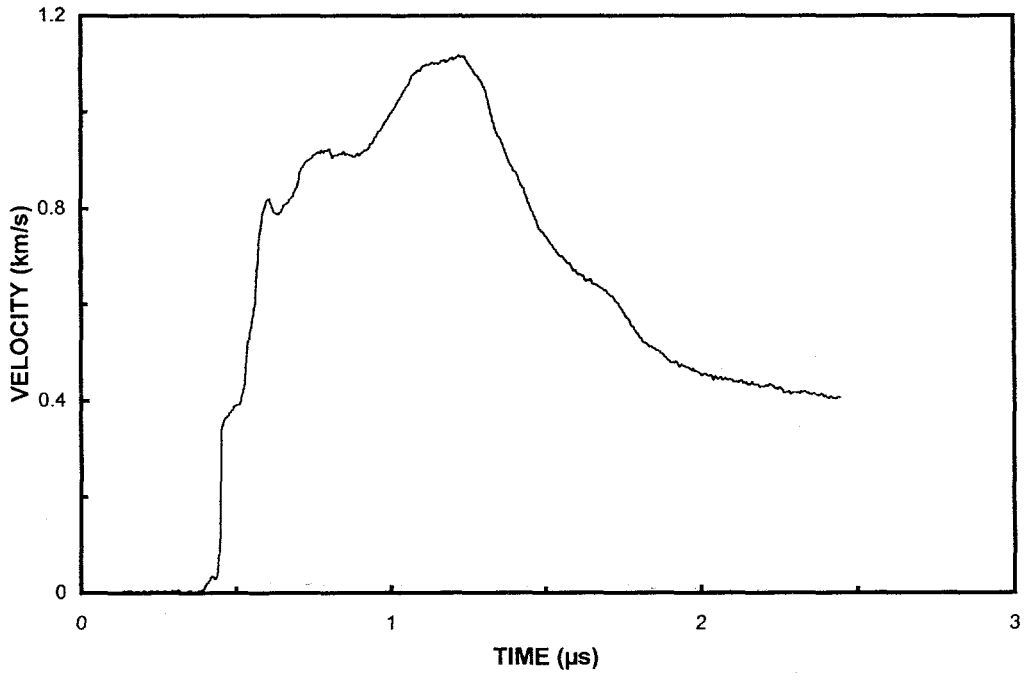

Shot Number:	AN12	**Impact Velocity:**	1.490 km/s
Test Material:	Aluminum Nitride		
Supplier:	Sumitomo Electric (Japan)	**Velocity Per Fringe:**	355.95 m/s

	Material	Thickness (mm)	Diameter (mm)	Density (kg/m^3)
Sample	Aluminum Nitride	4.343	See comment	3236
Window	Lithium Fluoride	18.9	38.1	2640
Impactor	Aluminum 6061-T6	12.7	87.5	2703
Backer	Free Surface			

Comments: Sample was a square, 30mm on a side.

AN12 VELOCITY PROFILE

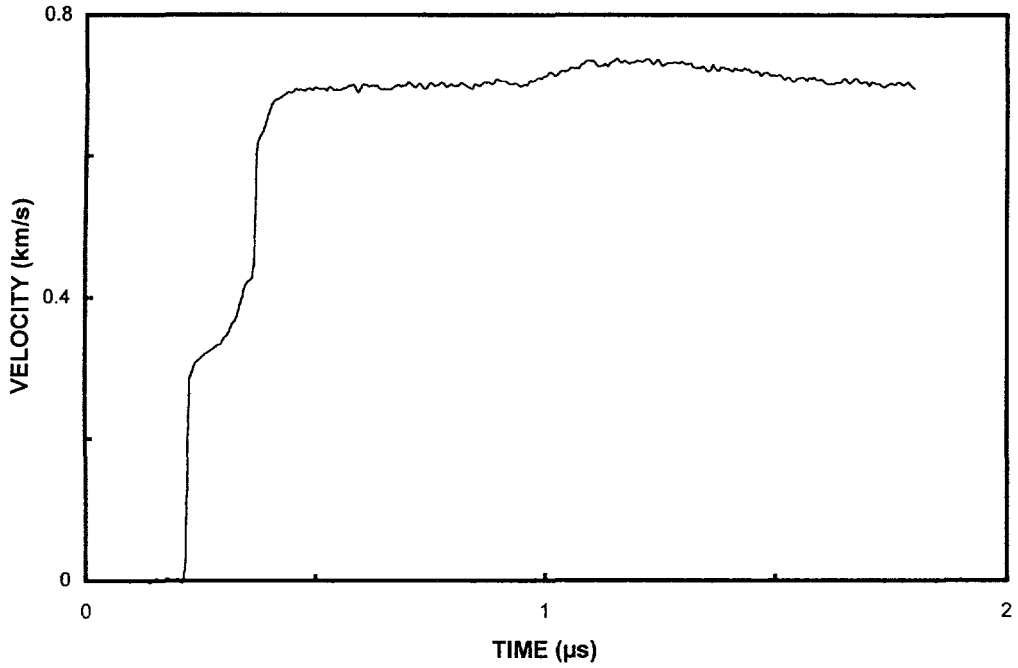

Shot Number:	AN13	**Impact Velocity:**	2.008 km/s
Test Material:	Aluminum Nitride		
Supplier:	Sumitomo Electric (Japan)	**Velocity Per Fringe:**	768.95 m/s

	Material	Thickness (mm)	Diameter (mm)	Density (kg/m^3)
Sample	Aluminum Nitride	4.34	See Comment	3219
Window	Lithium Fluoride	25.4	38.24	2640
Impactor	Copper OFHC	9.408	87.5	8930
Backer	Free Surface			

Comments: Sample was a square, 30mm on a side.

AN13 VELOCITY PROFILE

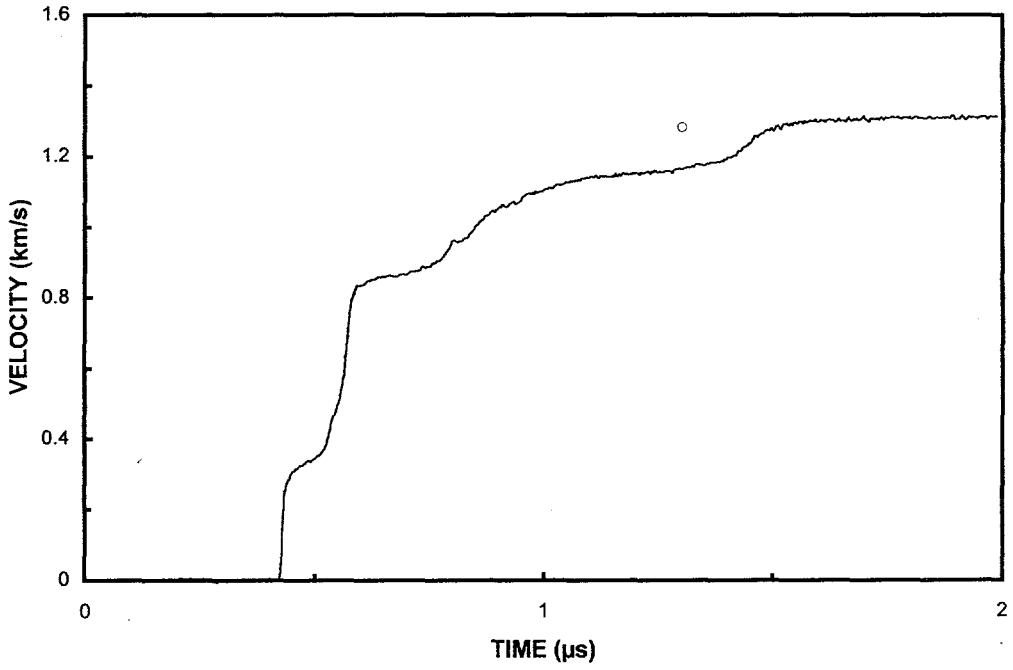

Shot Number:	AN14	**Impact Velocity:**	2.370 km/s
Test Material:	Aluminum Nitride		
Supplier:	Sumitomo Electric (Japan)	**Velocity Per Fringe:**	768.85 m/s

	Material	Thickness (mm)	Diameter (mm)	Density (kg/m^3)
Sample	Aluminum Nitride	4.340	See comment	3236
Window	Lithium Fluoride	19.1	38.1	2640
Impactor	Tantalum	3.898	50.8	16669
Backer	PMMA	6.77	87.5	1186

Comments: Sample was a square, 30mm on a side.

AN14 VELOCITY PROFILE

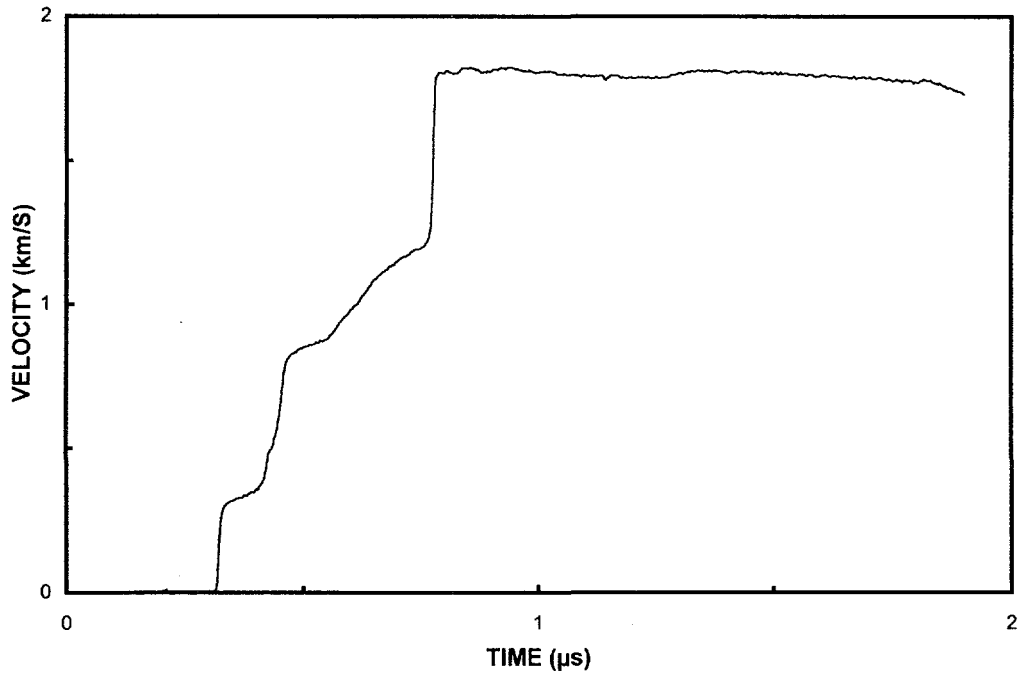

4. Aluminum Oxide Ceramics

Aluminum Oxide (Al_2O_3) ceramic is a widely used commercial ceramic because of its useful electrical, optical, and mechanical properties. It has been the most widely studied ceramic, in terms of its impact shock response. Sapphire, which is the single crystal form of Al_2O_3, has a rhombohedral-hexogonal crystal structure with close-packed oxygen ions. No phase transitions have been observed in this material while under shock or static loading pressures from 0 GPa to in excess of 100 GPa.

Because of its early and wide availability in good quality aluminum oxide ceramic or single crystal aluminum oxide forms, extensive shock-Hugoniot equation-of-state measurements have been performed upon this material. Early equation-of-state studies on single-crystal and polycrystalline aluminum oxide include the work of McQueen and Marsh (1960) and Ahrens, et al. (1968) to nearly 150 GPa, and the investigation of Graham and Brooks (1971) that included a determination of Hugoniot elastic limit with crystal orientation in single crystal Al_2O_3. A useful summary of this early shock data is included in the recent work of Mashimo, et al. (1988), along with new Hugoniot data on Al_2O_3.

Static X-ray diffraction data on aluminum oxide, to 12 GPa, have been provided by Sato and Akimoto (1979). This static compression data has been extrapolated to 30 GPa with a Birch-Murnaghan equation-of-state by Mashimo (1993), providing a reasonably confident measure of the hydrostatic compressibility of Al_2O_3.

The extensive shock-wave investigation of aluminum oxide by Gust and Royce (1971) is also noteworthy. Shock Hugoniot and strength data for four aluminum oxide ceramics–ranging in porosity from about 6% to near theoretical density–were provided to nearly 100 GPa. HEL strengths ranging from 6 to 13 GPa were reported, although a marked dependence of HEL value upon sample thickness was noted. Analysis of the dynamic-porosity crush process indicated a quadratic crush curve, with crush completing at about 30 GPa or 3 to 5 times the initial HEL.

The research of Cagnoux and Longy (1988) and Yeshurin, et al. (1988) on the shock deformation properties of aluminum oxide ceramic should also be noted. Both studies addressed the effects of microstructure upon dynamic yield strength, identifying microstructural heterogeneity–coarse grain structure or dissimilar second phases–as critical to the mode of failure. Homogeneous, fine-grain aluminum oxide yielded through dislocation plasticity, whereas heterogeneous material undergoes pervasive microcracking due to local tensile stresses in the dynamic failure process. Cagnoux and Longy (1988) observed no strain-rate dependence of the Hugoniot elastic limit in aluminum oxide ceramic over a range of about 5×10^5/s to 5×10^6/s.

This was similar to the rate insensitivity of the Hugoniot elastic-limit-strength for aluminum oxide, as well as other ceramics, observed by Grady (1995).

Velocity interferometry measurements of both compression and release waves have been taken on fully dense aluminum oxide by Munson and Lawrence (1979) to pressures of 16 GPa. Within this stress range–the measured HEL for the material studied was 9.1 GPa–the deformation wave is dispersive, presumably due to viscous effects brought about by the kinetics of the yield process. Release is reported to be fully elastic within this range. Dynamic yield is attributed to pervasive microfracture. This latter conclusion is based upon the observed lack of spall strength measured on release. Studies of compressive strength and spall on Coors AD995 aluminum oxide ceramic in the neighborhood of the HEL [Dandekar and Bartkowski, 1994] tend to support a compressive fracture mode of failure.

Two of the early profile measurements, in this report, were performed on a quite porous aluminum oxide prepared by the Italian manufacture, Industrie Bitossi, and supplied by the Los Alamos National Laboratory. The material was purported to be a Coors AD-90 equivalent with a theoretical density of 3.59 kg/m^3. A series of profile measurements were made on the AD-995 and AD-999 material supplied by the Coors Ceramic Company. These two aluminum oxide ceramics are reported to be 99.5% and 99.9% pure, respectively. Porosities are reported to be 2.3% and 0.6% respectively. The fourth material was supplied by the Michigan Technological Institute, and it was prepared through hot isostatic pressing of 99.99% pure α-Al_2O_3 powder [Staehler, et al., 1993]. No additives were included, thus minimizing the formation of second phases. A mean grain diameter of slightly less than one micrometer is characteristic of these samples. The samples were near the theoretical density, at 3970 kg/m^3. Densities and elastic properties for the aluminum oxide materials are provided in the Appendices.

The intial VISAR profiles are high-quality data on a material that is not well characterized, but they are characteristic of porous materials, in terms of their slow shock velocities and rapid overtaking of the decompressive wave. Tests AO3 through AO10 provide a systematic series of tests on Coors AD995, from just above the HEL to peak pressures approaching 50 GPa. Tests AO17 through AO19 are three additional tests addressing issues of precursor decay and spall. Tests AO13 through AO16 provide four comparable experiments on the higher density Coors AD999 ceramic. Tests AO11, AO12, AO20, and AO21 supported dynamic studies on the Michigan Technological Institute AL_2O_3 ceramic.

Shot Number:	AO1	**Impact Velocity:**	1.542 km/s
Test Material:	Aluminum Oxide		
Supplier:	Industrie Bitossi	**Velocity Per Fringe:**	430.92 m/s

	Material	Thickness (mm)	Diameter (mm)	Density (kg/m^3)
Sample	Aluminum Oxide	9.076	74.9	3555
Window	Lithium Fluoride	25.4	50.8	2640
Impactor	Aluminum Oxide	4.677	74.9	3554
Backer	Polyurethane Foam	6.0	87.5	320

Comments:

AO1 VELOCITY PROFILE

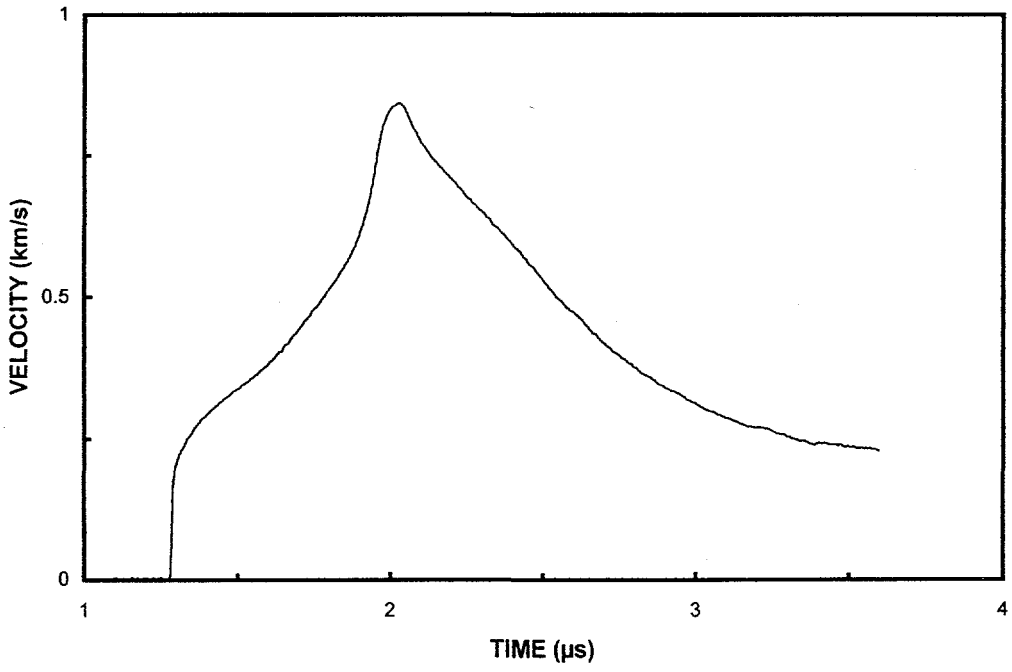

Shot Number:	AO2	**Impact Velocity:**	2.212 km/s
Test Material:	Aluminum Oxide		
Supplier:	Industrie Bitossi	**Velocity Per Fringe:**	430.92 m/s

	Material	Thickness (mm)	Diameter (mm)	Density (kg/m^3)
Sample	Aluminum Oxide	9.081	74.9	3555
Window	Lithium Fluoride	25.4	50.8	2640
Impactor	Aluminum Oxide	4.673	74.9	3555
Backer	Polyurethane Foam	6.0	87.5	640

Comments:

AO2 VELOCITY PROFILE

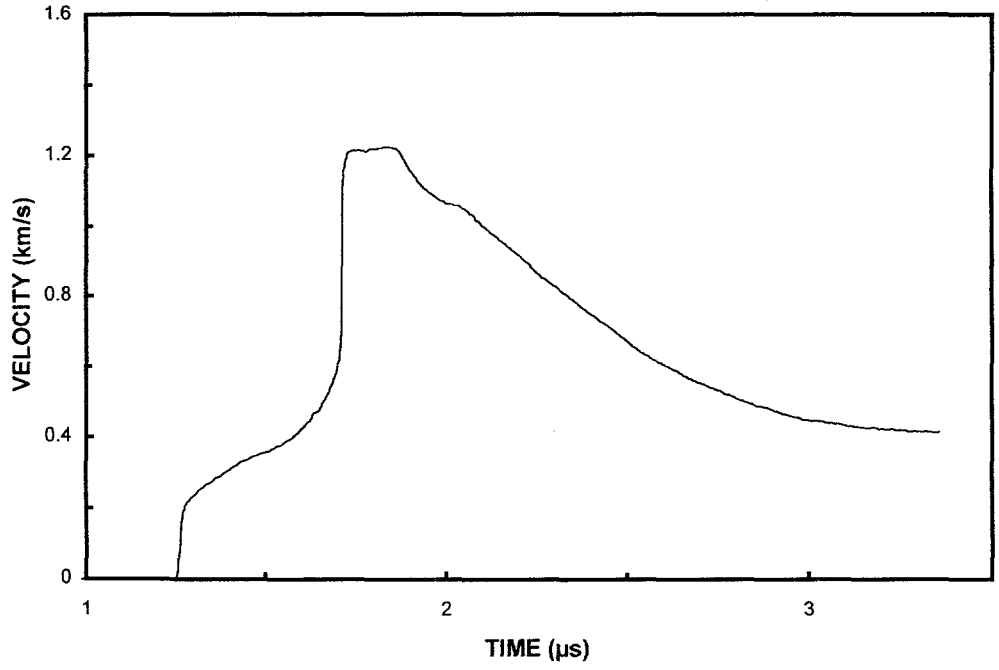

Shot Number:	AO3	**Impact Velocity:**	0.544 km/s
Test Material:	Aluminum Oxide (AD995)		
Supplier:	Coors Porcelain Co.	**Velocity Per Fringe:**	128.07 m/s

	Material	Thickness (mm)	Diameter (mm)	Density (kg/m^3)
Sample	Aluminum Oxide	10.007	76.2	3890
Window	Lithium Fluoride	25.4	50.8	2640
Impactor	Aluminum Oxide	5.008	87.5	3888
Backer	Polyurethane Foam	8.0	88.5	320

Comments:

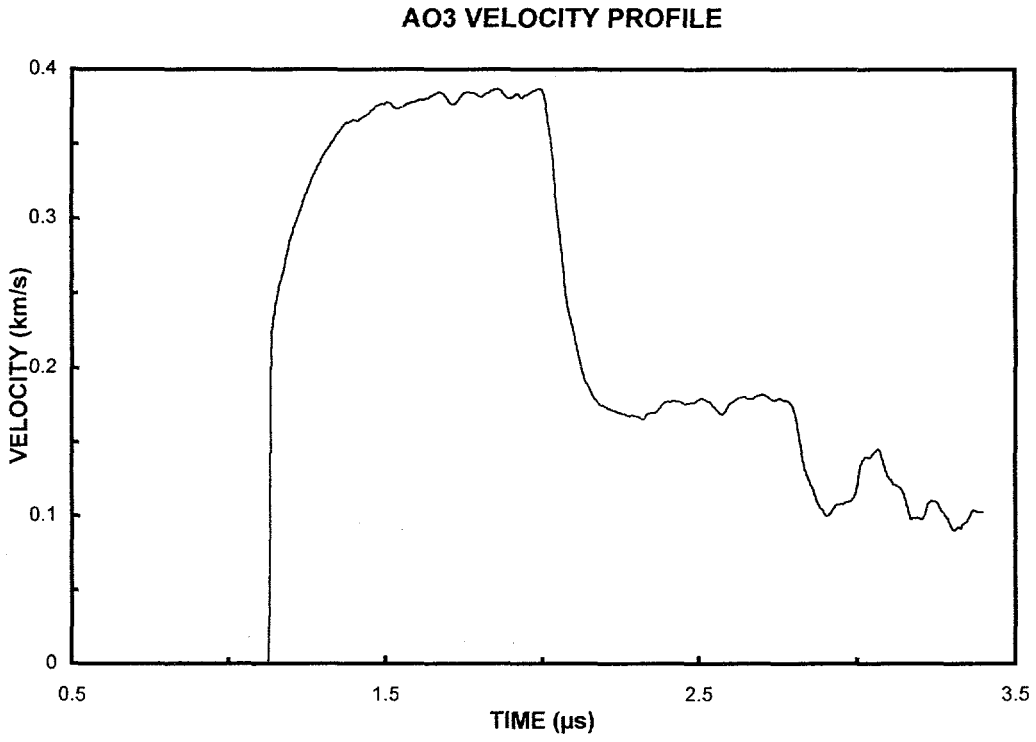

Shot Number:	AO4	**Impact Velocity:**	1.070 km/s
Test Material:	Aluminum Oxide (AD995)		
Supplier:	Coors Porcelain Co.	**Velocity Per Fringe:**	430.92 m/s

	Material	Thickness (mm)	Diameter (mm)	Density (kg/m^3)
Sample	Aluminum Oxide	10.006	76.2	3890
Window	Lithium Fluoride	25.4	50.8	2640
Impactor	Aluminum Oxide	5.019	87.5	3890
Backer	Polyurethane Foam	8.0	87.5	320

Comments:

AO4 VELOCITY PROFILE

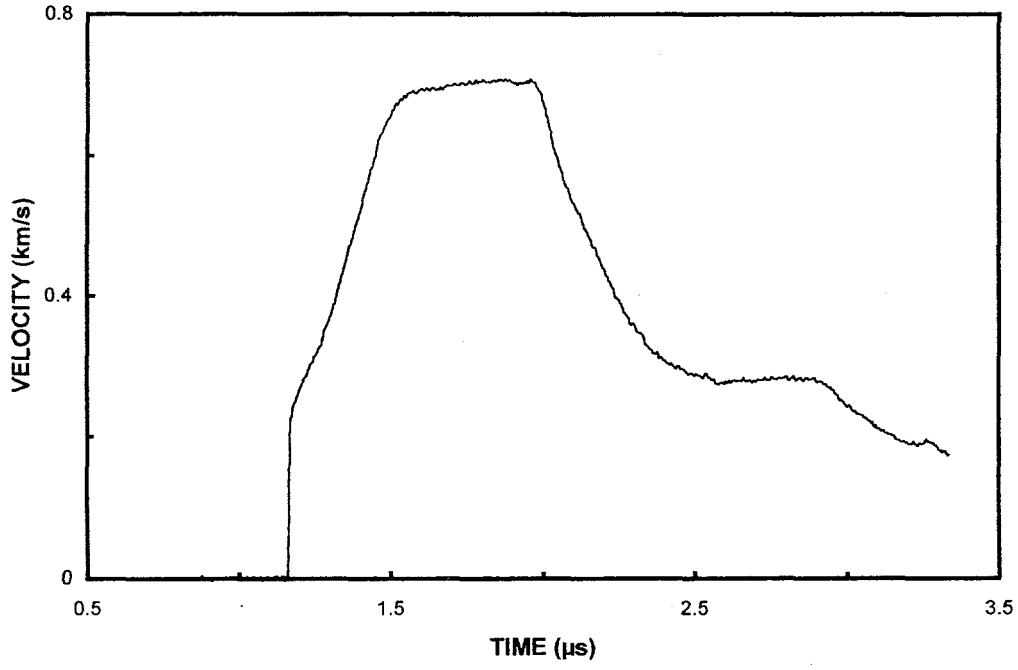

Shot Number:	AO5	**Impact Velocity:**	1.573 km/s
Test Material:	Aluminum Oxide (AD995)		
Supplier:	Coors Porcelain Co.	**Velocity Per Fringe:**	430.92 m/s

	Material	Thickness (mm)	Diameter (mm)	Density (kg/m^3)
Sample	Aluminum Oxide	10.008	76.2	3890
Window	Lithium Fluoride	25.4	50.8	2640
Impactor	Aluminum Oxide	5.008	87.5	3890
Backer	Polyurethane Foam	8.0	87.5	320

Comments:

AO5 VELOCITY PROFILE

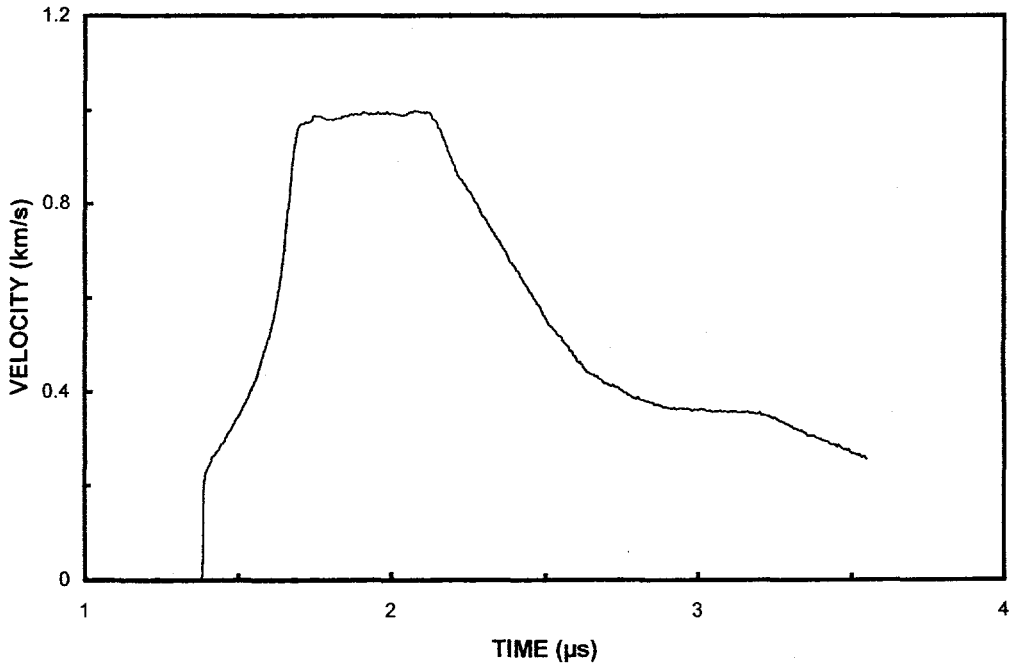

Shot Number:	AO6	**Impact Velocity:**	1.943 km/s
Test Material:	Aluminum Oxide (AD995)		
Supplier:	Coors Porcelain Co.	**Velocity Per Fringe:**	430.92 m/s

	Material	Thickness (mm)	Diameter (mm)	Density (kg/m^3)
Sample	Aluminum Oxide	10.007	76.2	3890
Window	Lithium Fluoride	25.4	50.8	2640
Impactor	Aluminum Oxide	5.013	87.5	3890
Backer	Polyurethane Foam	8.0	87.5	320

Comments:

AO6 VELOCITY PROFILE

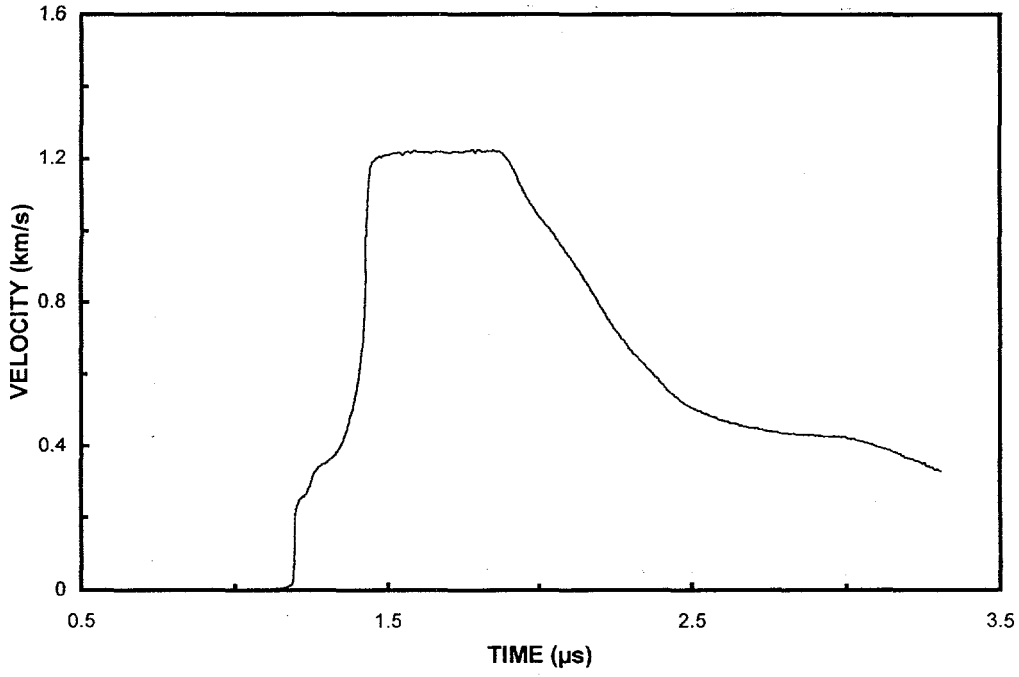

Shot Number:	AO7	**Impact Velocity:**	2.329 km/s
Test Material:	Aluminum Oxide (AD995)		
Supplier:	Coors Porcelain Co.	**Velocity Per Fringe:**	430.92 m/s

	Material	Thickness (mm)	Diameter (mm)	Density (kg/m^3)
Sample	Aluminum Oxide	9.998	76.2	3890
Window	Lithium Fluoride	25.4	50.8	2640
Impactor	Aluminum Oxide	5.005	87.5	3890
Backer	Polyurethane Foam	8.0	87.5	640

Comments:

AO7 VELOCITY PROFILE

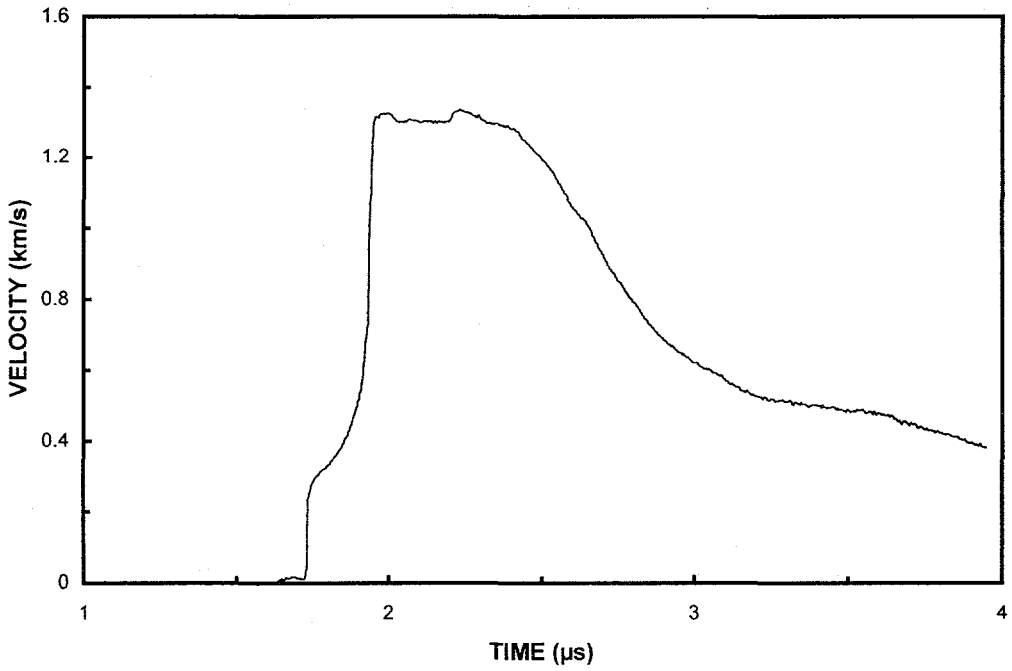

Shot Number:	AO8	**Impact Velocity:**	0.561 km/s
Test Material:	Aluminum Oxide (AD995)		
Supplier:	Coors Porcelain Co.	**Velocity Per Fringe:**	430.92 m/s

	Material	Thickness (mm)	Diameter (mm)	Density (kg/m^3)
Sample	Aluminum Oxide	9.987	76.2	3890
Window	Lithium Fluoride	25.4	50.8	2640
Impactor	Aluminum Oxide	4.989	87.5	3890
Backer	Polyurethane Foam	8.0	87.5	320

Comments:

AO8 VELOCITY PROFILE

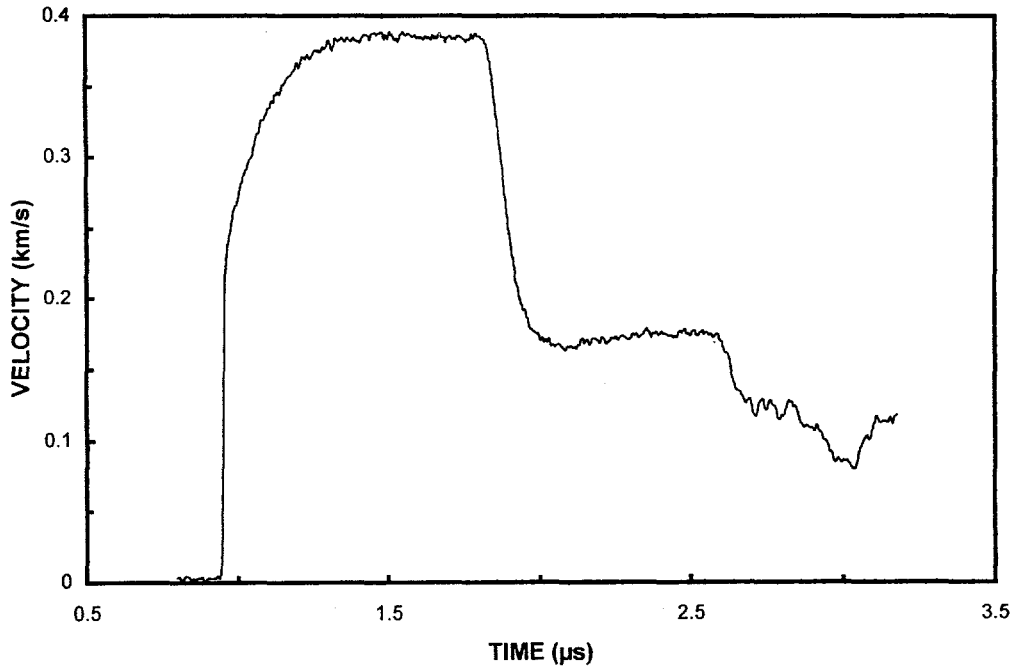

Shot Number:	AO9	**Impact Velocity:**	2.241 km/s
Test Material:	Aluminum Oxide (AD995)		
Supplier:	Coors Porcelain Co.	**Velocity Per Fringe:**	681.52 m/s

	Material	Thickness (mm)	Diameter (mm)	Density (kg/m^3)
Sample	Aluminum Oxide	5.008	76.2	3890
Window	Lithium Fluoride	25.5	50.7	2640
Impactor	Tantalum	1.555	87.5	16625
Backer	Polyurethane Foam	5.0	87.5	640

Comments:

AO9 VELOCITY PROFILE

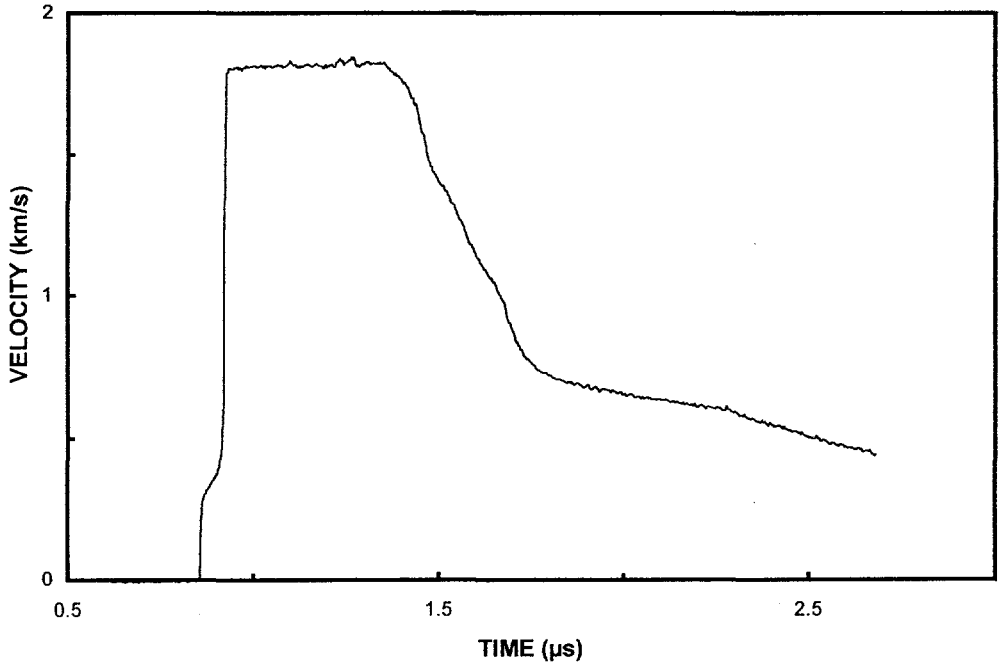

Shot Number:	AO10	**Impact Velocity:**	2.260 km/s
Test Material:	Aluminum Oxide (AD995)		
Supplier:	Coors Porcelain Co.	**Velocity Per Fringe:**	681.52 m/s

	Material	Thickness (mm)	Diameter (mm)	Density (kg/m^3)
Sample	Aluminum Oxide	5.008	76.2	3890
Window	Lithium Fluoride	25.6	50.8	2640
Impactor	Tungsten	1.501	87.5	19261
Backer	PMMA	6.34	87.5	1186

Comments:

AO10 VELOCITY PROFILE

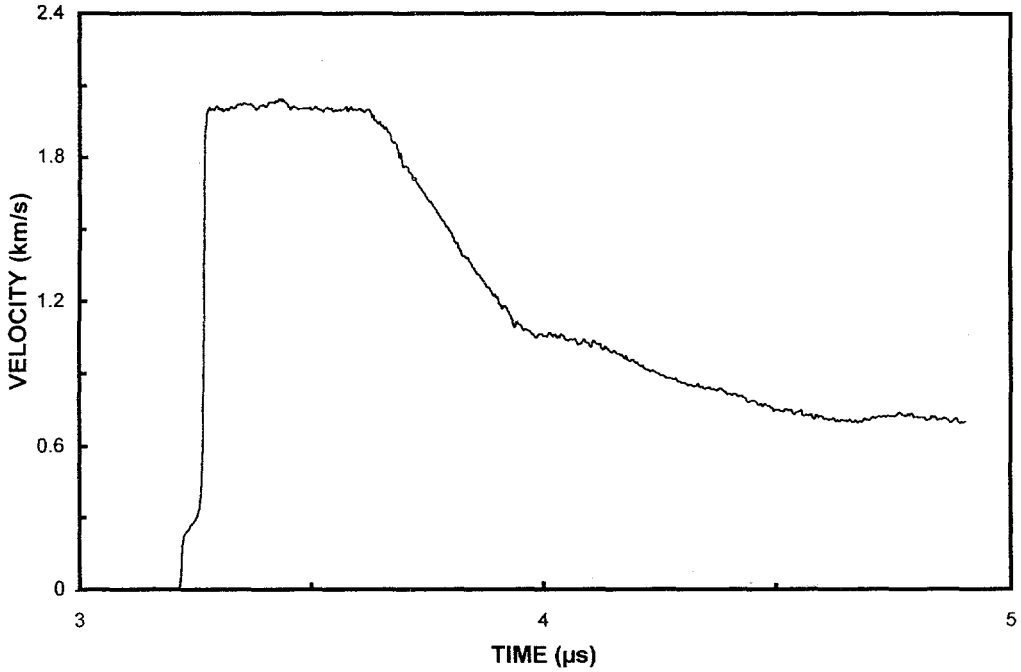

Shot Number:	AO11	**Impact Velocity:**	0.587 km/s ± 2%
Test Material:	Aluminum Oxide		
Supplier:	Michigan Tech. Univ.	**Velocity Per Fringe:**	128.07 m/s

	Material	Thickness (mm)	Diameter (mm)	Density (kg/m^3)
Sample	Aluminum Oxide	6.230	51.5	3970
Window	Lithium Fluoride	19.0	25.4	2640
Impactor	Aluminum Oxide	2.804	48.6	3970
Backer	Polyurethane Foam	8.0	87.5	145

Comments:

AO11 VELOCITY PROFILE

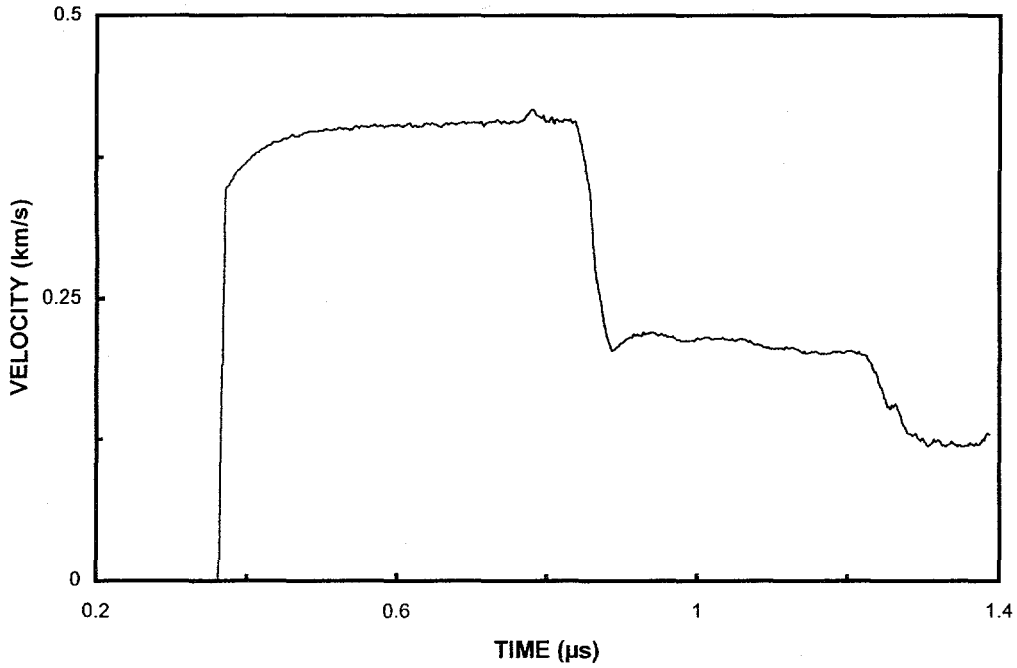

Shot Number:	AO12	**Impact Velocity:**	1.855 km/s
Test Material:	Aluminum Oxide		
Supplier:	Michigan Tech. Univ.	**Velocity Per Fringe:**	681.52 m/s

	Material	Thickness (mm)	Diameter (mm)	Density (kg/m^3)
Sample	Aluminum Oxide	6.261	51.5	3970
Window	Lithium Fluoride	19.1	25.4	2640
Impactor	Aluminum Oxide	2.802	48.8	3970
Backer	Polyurethane Foam	8.0	87.5	640

Comments: Details of the lead-in and rounding of the peak amplitude are a concern in this test

AO12 VELOCITY PROFILE

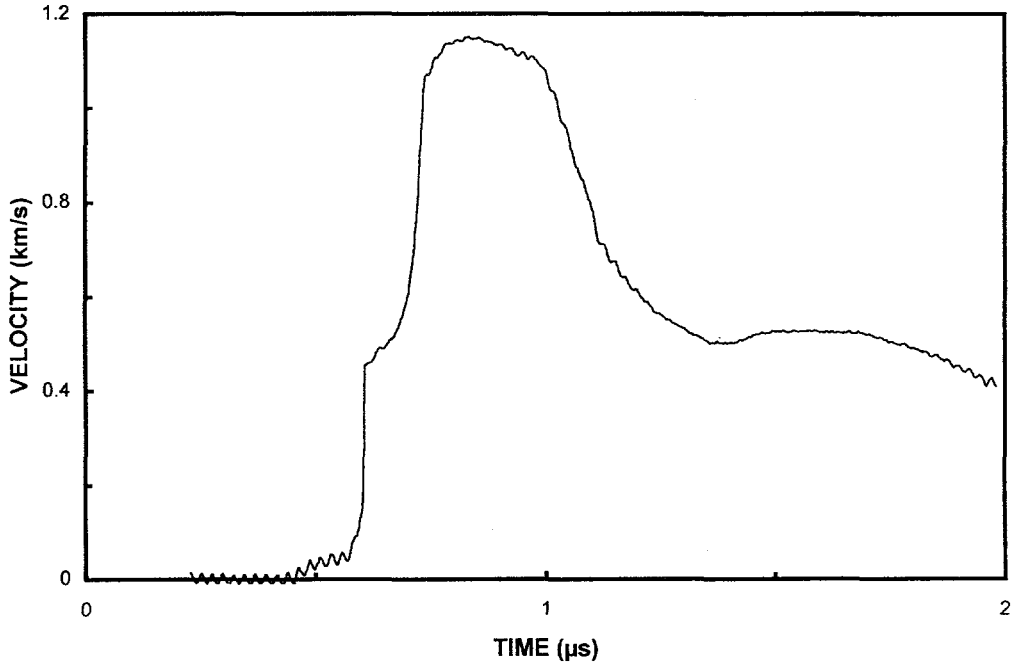

Shot Number:	AO13	**Impact Velocity:**	2.033 km/s
Test Material:	Aluminum Oxide (AD999)		
Supplier:	Coors Porcelain Co.	**Velocity Per Fringe:**	430.92 m/s

	Material	Thickness (mm)	Diameter (mm)	Density (kg/m^3)
Sample	Aluminum Oxide	9.909	76.4	3948
Window	Lithium Fluoride	25.6	50.8	2640
Impactor	Tantalum	1.497	87.6	16561
Backer	PMMA	2.0	87.5	1186

Comments:

AO13 VELOCITY PROFILE

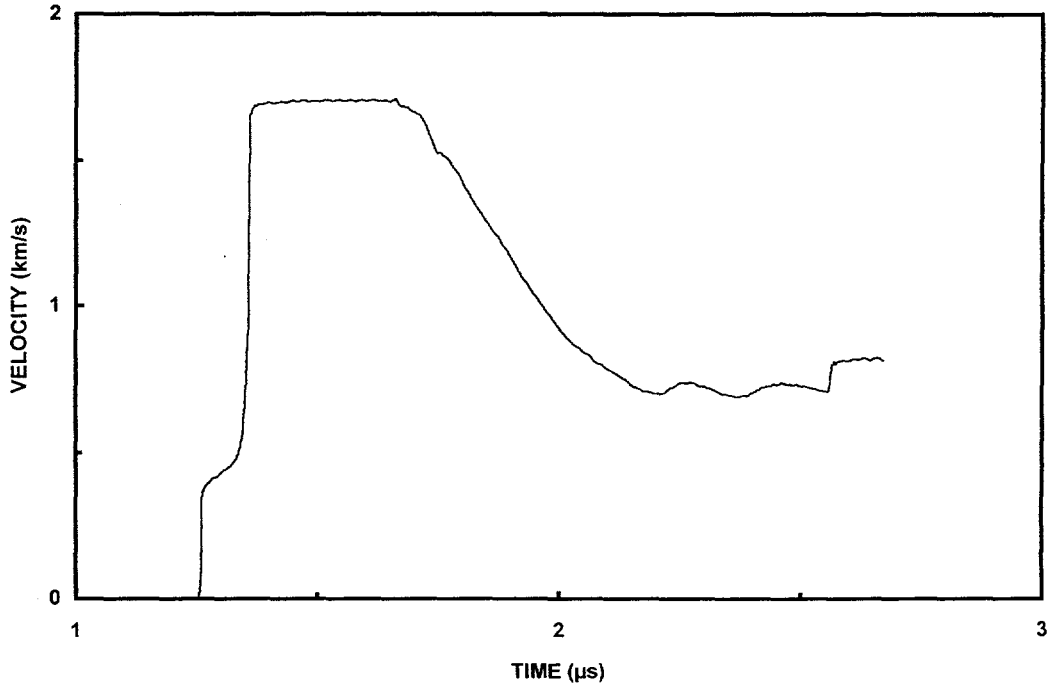

Shot Number:	AO14	**Impact Velocity:**	2.183 km/s
Test Material:	Aluminum Oxide (AD999)		
Supplier:	Coors Porcelain Co.	**Velocity Per Fringe:**	430.92 m/s

	Material	Thickness (mm)	Diameter (mm)	Density (kg/m^3)
Sample	Aluminum Oxide	10.009	77.3	3948
Window	Lithium Fluoride	25.4	50.7	2640
Impactor	Tungsten	1.414	87.5	19274
Backer	PMMA	2.0	87.5	1186

Comments:

AO14 VELOCITY PROFILE

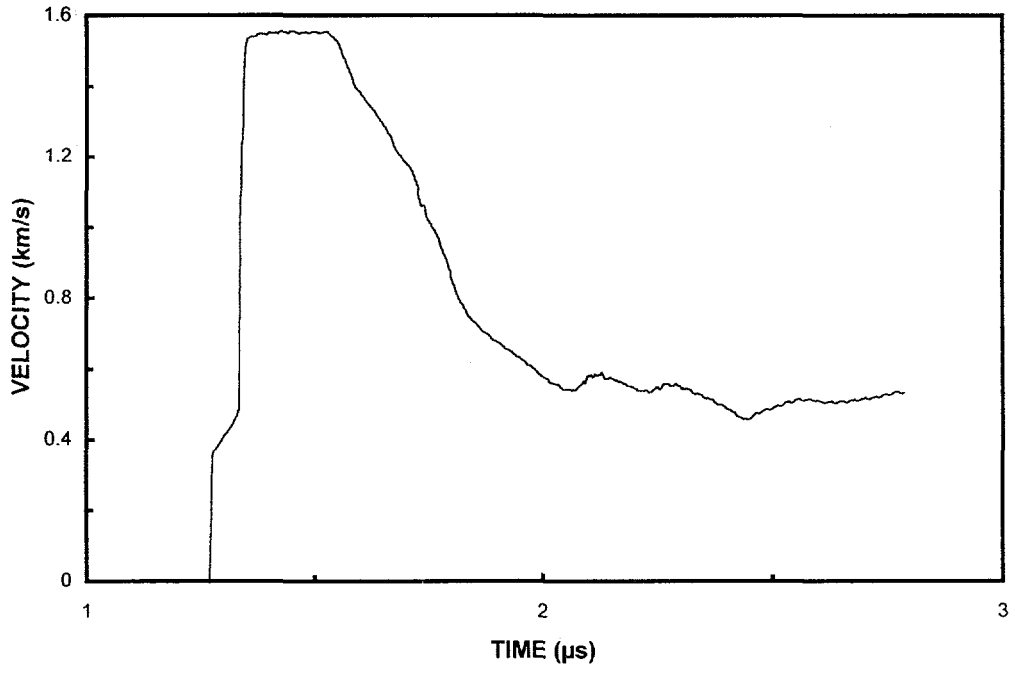

Shot Number:	AO15	**Impact Velocity:**	1.290 km/s
Test Material:	Aluminum Oxide (AD999)		
Supplier:	Coors Porcelain Co.	**Velocity Per Fringe:**	430.92 m/s

	Material	Thickness (mm)	Diameter (mm)	Density (kg/m^3)
Sample	Aluminum Oxide	10.026	76.0	3948
Window	Lithium Fluoride	25.6	50.8	2640
Impactor	Aluminum Oxide	5.118	90.0	3948
Backer	Polyurethane Foam	12.7	87.5	316

Comments:

AO15 VELOCITY PROFILE

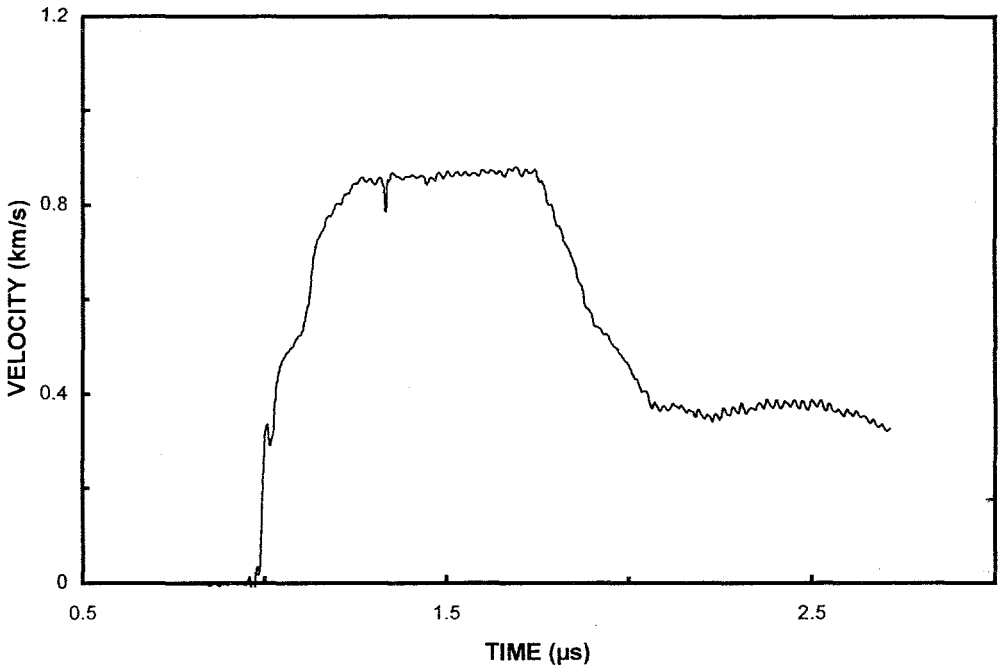

Shot Number:	AO16	**Impact Velocity:**	1.911 km/s ± 3%
Test Material:	Aluminum Oxide (AD999)		
Supplier:	Coors Porcelain Co.	**Velocity Per Fringe:**	430.92 m/s

	Material	Thickness (mm)	Diameter (mm)	Density (kg/m^3)
Sample	Aluminum Oxide	10.019	77.0	3948
Window	Lithium Fluoride	25.4	50.8	2640
Impactor	Aluminum Oxide	5.059	89.0	3948
Backer	Polyurethane Foam	12.7	87.5	313

Comments:

AO16 VELOCITY PROFILE

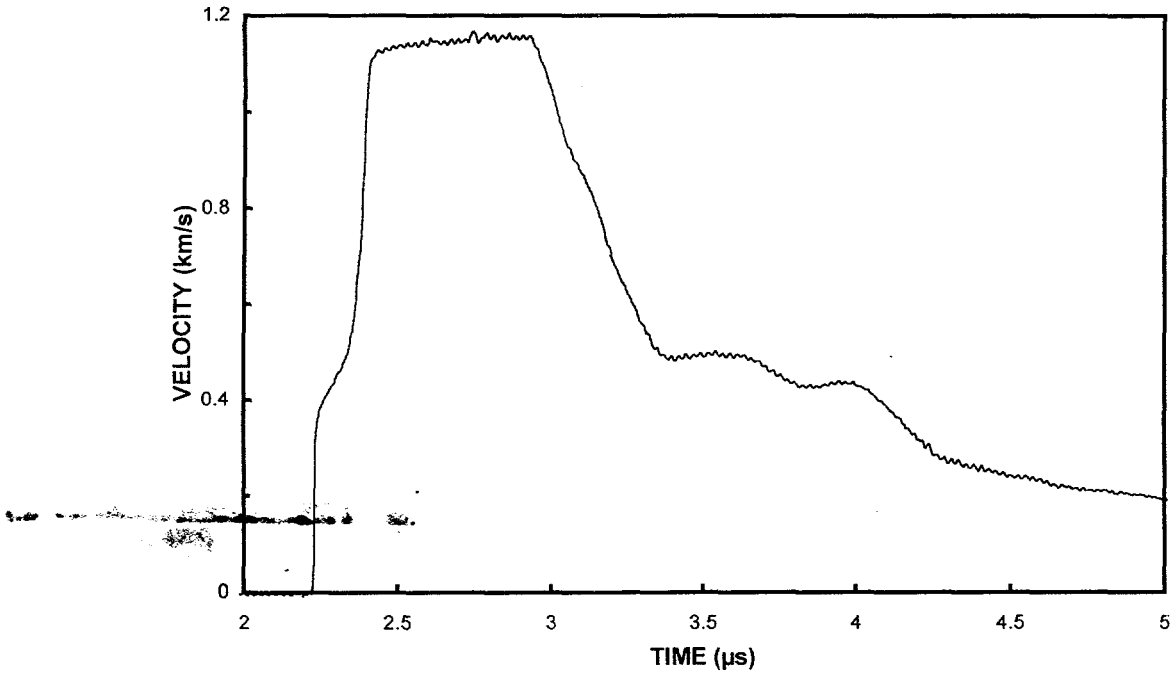

Shot Number:	AO17	**Impact Velocity:**	1.564 km/s
Test Material:	Aluminum Oxide (AD995)		
Supplier:	Coors Porcelain Co.	**Velocity Per Fringe:**	430.92 m/s

	Material	Thickness (mm)	Diameter (mm)	Density (kg/m^3)
Sample	Aluminum Oxide	4.762	76.2	3890
Window	Lithium Fluoride	25.4	38.1	2640
Impactor	Aluminum Oxide	2.475	76.31	3890
Backer	Polyurethane Foam	8.0	87.5	320

Comments:

AO17 VELOCITY PROFILE

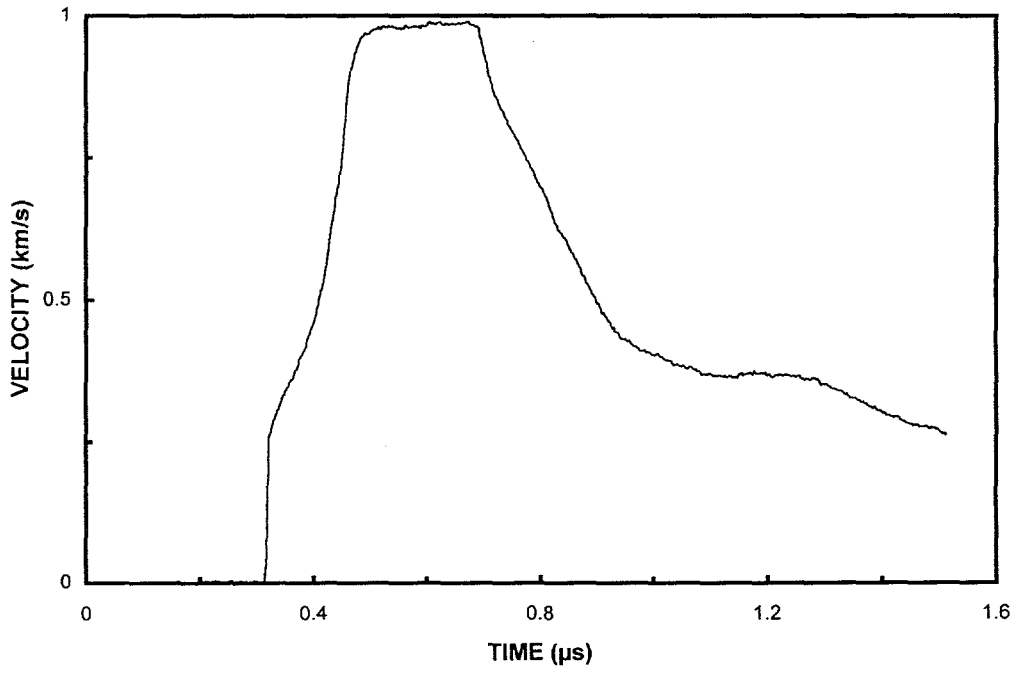

Shot Number:	AO18	**Impact Velocity:**	1.551 km/s
Test Material:	Aluminum Oxide (AD995)		
Supplier:	Coors Porcelain Co.	**Velocity Per Fringe:**	430.92 m/s

	Material	Thickness (mm)	Diameter (mm)	Density (kg/m^3)
Sample	Aluminum Oxide	2.478	76.3	3890
Window	Lithium Fluoride	25.4	38.1	2640
Impactor	Aluminum Oxide	2.477	76.2	3890
Backer	Polyurethane Foam	8.0	87.5	320

Comments:

AO18 VELOCITY PROFILE

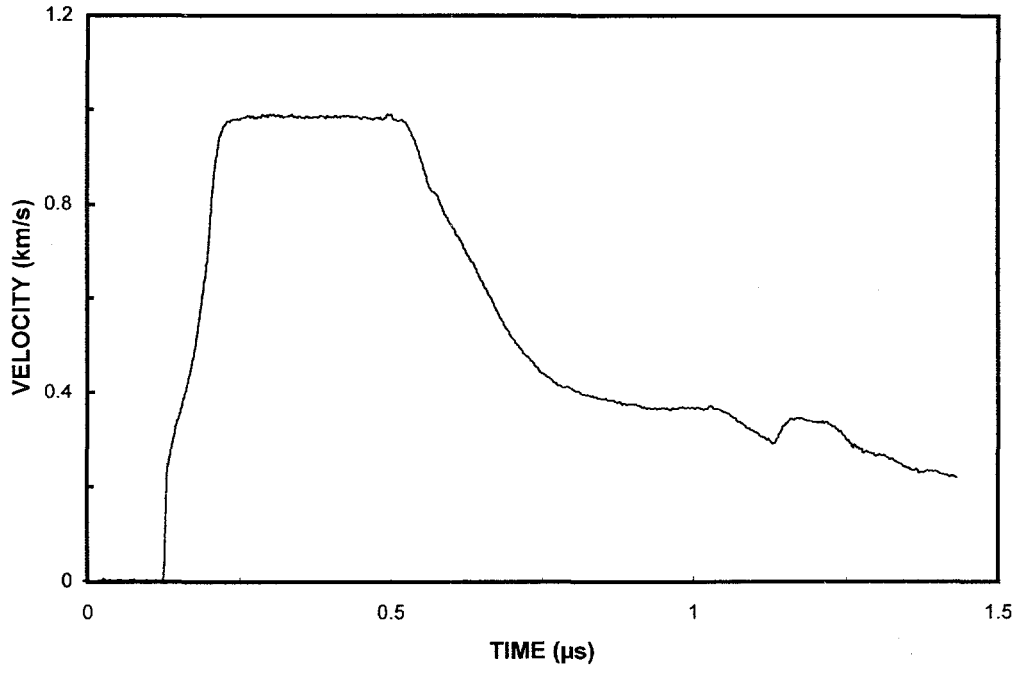

Shot Number:	AO19	**Impact Velocity:**	0.549 km/s
Test Material:	Aluminum Oxide (AD995)		
Supplier:	Coors Porcelain Co.	**Velocity Per Fringe:**	108.95 m/s

	Material	Thickness (mm)	Diameter (mm)	Density (kg/m^3)
Sample	Aluminum Oxide	4.698	76.3	3890
Window	Lithium Fluoride	25.3	38.1	2640
Impactor	Aluminum 6061-T6	1.493	50.7	2688
Backer	PMMA	6.370	87.5	1186

Comments:

AO19 VELOCITY PROFILE

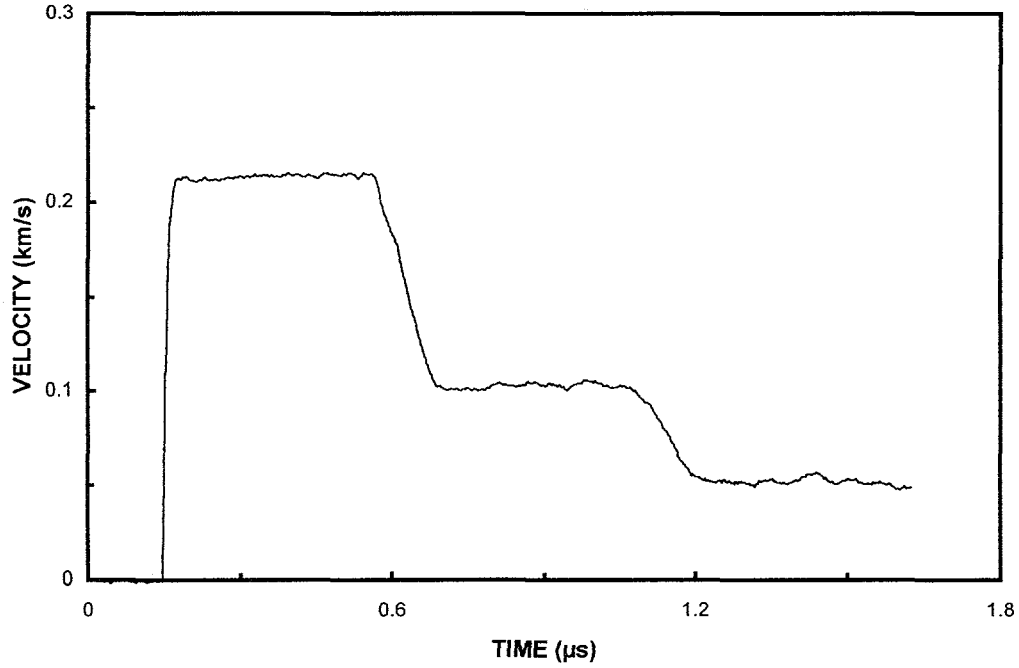

Shot Number:	AO20	**Impact Velocity:**	1.215 km/s
Test Material:	Aluminum Oxide		
Supplier:	Michigan Tech. Univ.	**Velocity Per Fringe:**	197.44 m/s

	Material	Thickness (mm)	Diameter (mm)	Density (kg/m^3)
Sample	Aluminum Oxide	5.990	49.3	3974
Window	Lithium Fluoride	25.4	38.0	2640
Impactor	Aluminum 6061-T6	1.510	50.8	2693
Backer	PMMA	6.3	87.5	1186

Comments:

AO20 VELOCITY PROFILE

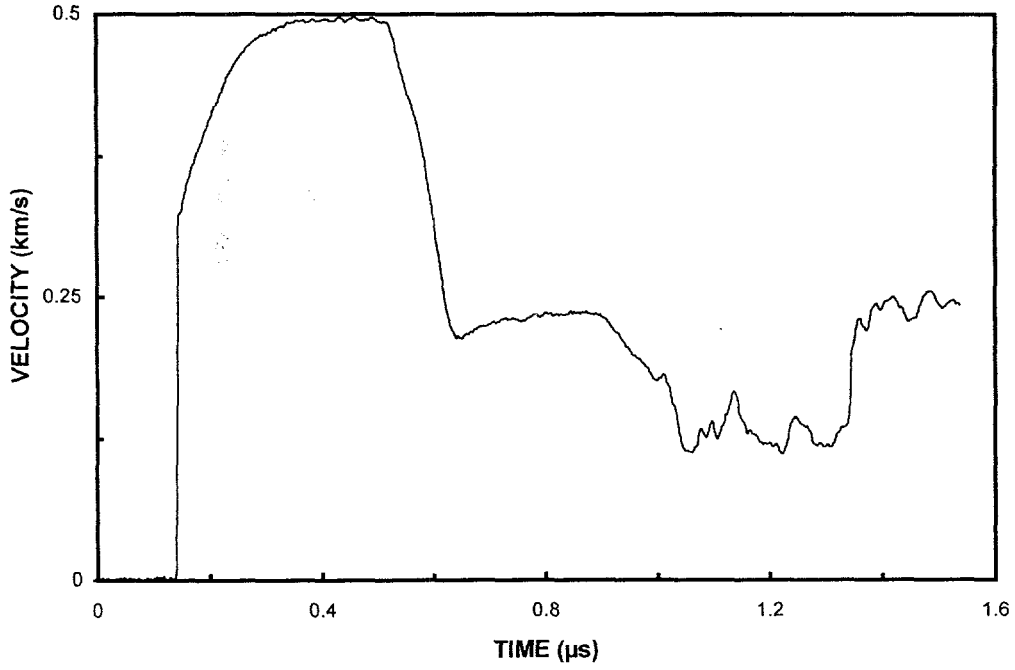

Shot Number:	AO21	**Impact Velocity:**	0.708 km/s
Test Material:	Aluminum Oxide		
Supplier:	Michigan Tech. Univ.	**Velocity Per Fringe:**	197.44 m/s

	Material	Thickness (mm)	Diameter (mm)	Density (kg/m^3)
Sample	Aluminum Oxide	5.990	49.3	3974
Window	Lithium Fluoride	25.4	38.0	2640
Impactor	Aluminum 6061-T6	1.523	50.8	2695
Backer	PMMA	6.3	87.5	1186

Comments:

AO21 VELOCITY PROFILE

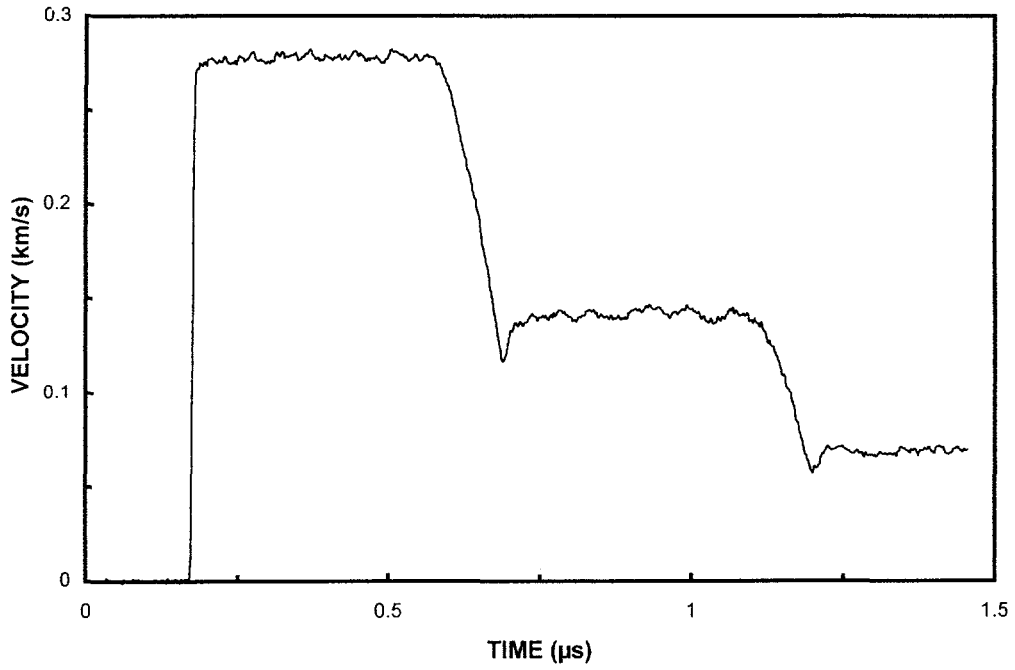

5. Boron Carbide Ceramics

Unusual shock-wave features were exhibited by boron carbide ceramics. In part, this behavior may be due to the notably different crystallographic structure of this material. Boron carbide has a very open rhombohedral structure of 12-atom clusters (icosahedral). This structure is a characteristic of boron, and it is unique to boron-rich solids [Emin, 1987]. High-pressure, Hugoniot data for boron carbide is provided by the early study of Gust and Royce (1971). Unique among the ceramics studied in this report, boron carbide exhibits a relaxing, elastic precursor-wave and Hugoniot states that lie on or near the hydrostatic compression curve, suggesting catastrophic loss of strength during shock compression [Grady, 1994b]. Release-wave profiles for boron carbide also contain features that are more consistent with a near fluid-like behavior [Grady, 1994b].

Boron carbide samples from two separate suppliers were tested in this work. Both of these ceramics were provided by Los Alamos National Laboratory. The first material was produced by Eagle Picher Industries, and it had a nominal grain size of 10 μm. Revealed by electron-probe microanalysis, the principal contaminant of this first ceramic is iron, which occurs within voids and other quite hetrogeneously distributed sites–relative to grain size–throughout this material. Dow Chemical Company produced the second boron carbide ceramic for these tests, and its nominal grain size is about 3 μm–determined by optical metallography.

Tests BC1 and BC2 provided the first exploratory shock-profile measurements on the Eagle Picher boron carbide material. Features of stress relaxation and ragged profile structure were observed, which have subsequently been found to be unique to boron carbide. All of the further tests on boron carbide (BC3 through BC11) were performed on the Dow Chemical material, which has a similar density. These further tests demonstrated that these features were not restricted to the Eagle Picher ceramic.

Several experiments achieved shock-compressive stresses below the elastic limit, and they were configured to test the spall strength of boron carbide (BC3, BC6, and BC8). Test BC9 was performed to examine the double shock properties of boron carbide, using lithium fluoride backed by tantalum to achieve the two-step impact loading. Several tests were conducted on boron carbide, using a small (20mm diameter launch tube) two-stage light gas gun (BC10 and BC11). The latter test (BC11) is a somewhat different equation-of-state configuration in which the boron carbide is placed in the projectile and the Hugoniot state is referenced to that of the aluminum material included in both the projectile and target.

Shot Number:	BC1	**Impact Velocity:**	1.546 km/s
Test Material:	Boron Carbide		
Supplier:	Eagle Picher Industries	**Velocity Per Fringe:**	430.92 m/s

	Material	Thickness (mm)	Diameter (mm)	Density (kg/m^3)
Sample	Boron Carbide	9.044	69.2	2517
Window	Lithium Fluoride	25.4	50.8	2640
Impactor	Boron Carbide	3.902	69.2	2517
Backer	Polyurethane Foam	6.0	87.5	320

Comments: Stess relaxation and erractic profile measurements are characteristic of boron carbide ceramic.

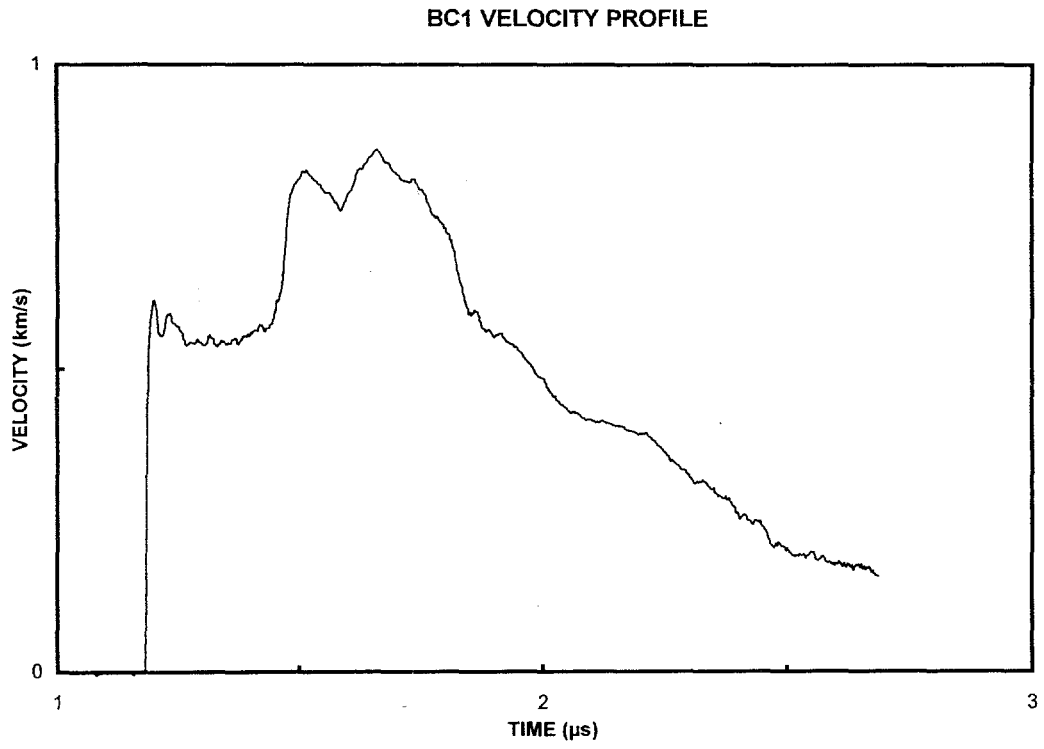

Shot Number:	BC2	**Impact Velocity:**	2.210 km/s
Test Material:	Boron Carbide		
Supplier:	Eagle Picher Industries	**Velocity Per Fringe:**	430.92 m/s

	Material	Thickness (mm)	Diameter (mm)	Density (k/m^3)
Sample	Boron Carbide	9.033	69.2	2517
Window	Lithium Fluoride	25.4	50.8	2640
Impactor	Boron Carbide	3.917	69.2	2517
Backer	Polyurethane Foam	6.0	87.5	640

Comments: Duplicate impact velocity measurements were not obtained in this test.

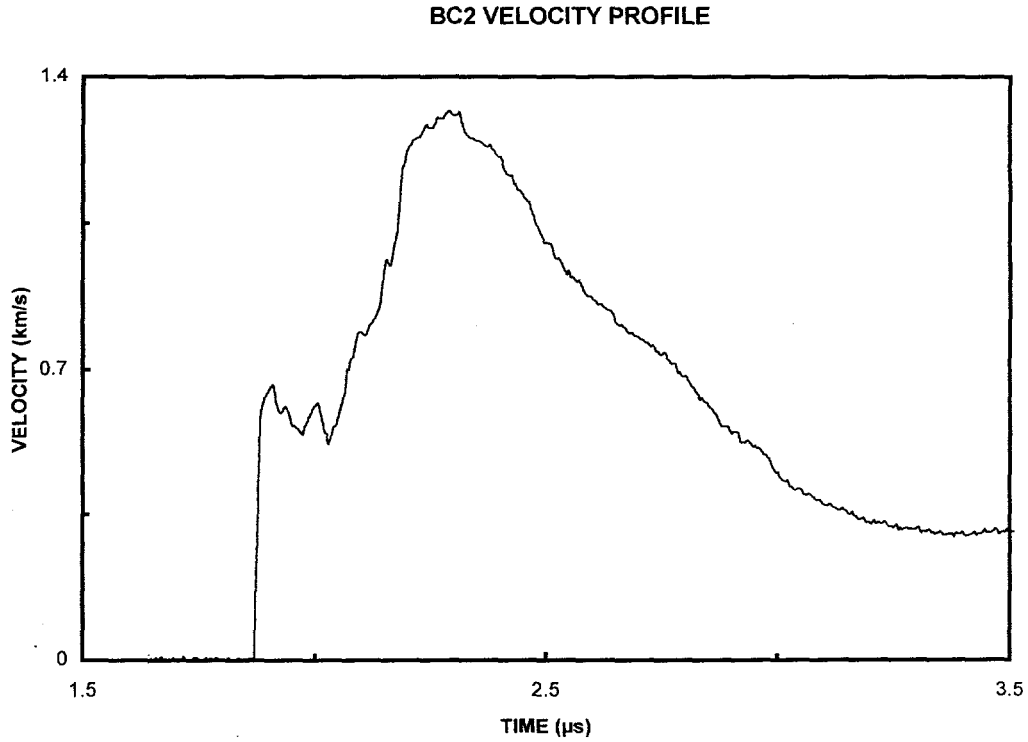

Shot Number:	BC3	**Impact Velocity:**	0.370 km/s
Test Material:	Boron Carbide		
Supplier:	DOW Chemical Company	**Velocity Per Fringe:**	121.34 m/s

	Material	Thickness (mm)	Diameter (mm)	Density (kg/m^3)
Sample	Boron Carbide	9.694	76.2	2506
Window	PMMA	25.4	50.8	1186
Impactor	Boron Carbide	4.924	76.2	2506
Backer	Polyurethane Foam	6.0	87.5	320

Comments: This is a spall experiment with a compressive amplitude below the elastic limit.

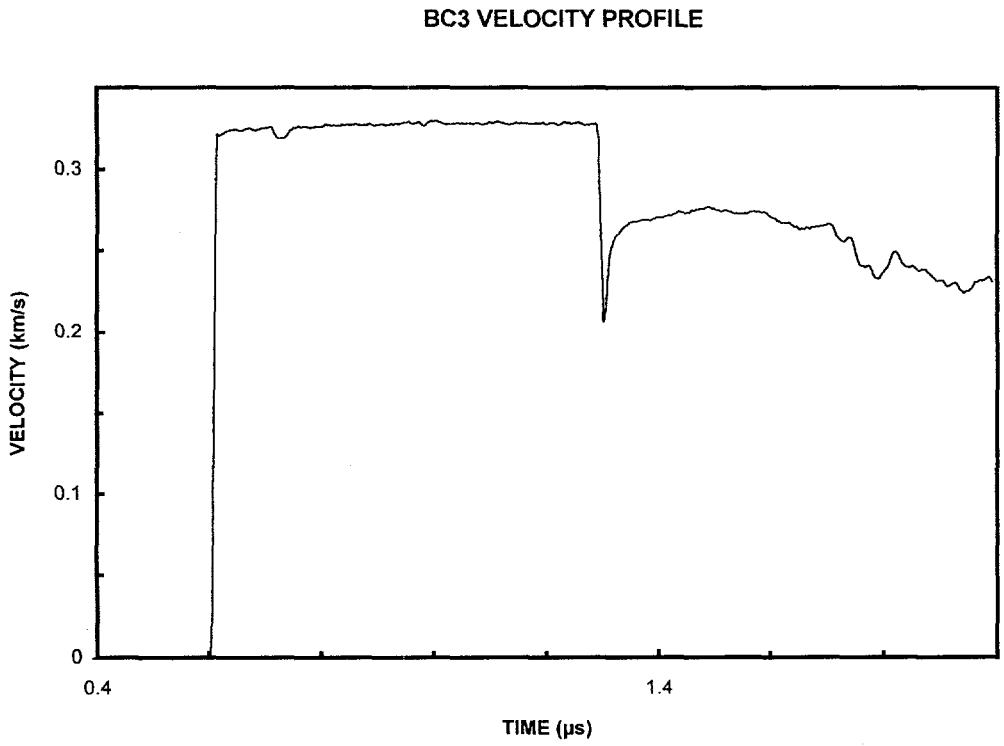

Shot Number:	BC4	**Impact Velocity:**	1.633 km/s
Test Material:	Boron Carbide		
Supplier:	DOW Chemical Company	**Velocity Per Fringe:**	430.92 km/s

	Material	Thickness (mm)	Diameter (mm)	Density (kg/m^3)
Sample	Boron Carbide	10.322	76.2	2506
Window	Lithium Fluoride	25.4	50.8	2640
Impactor	Boron Carbide	4.831	76.2	2506
Backer	Polyurethane Foam	6.0	87.5	320

Comments:

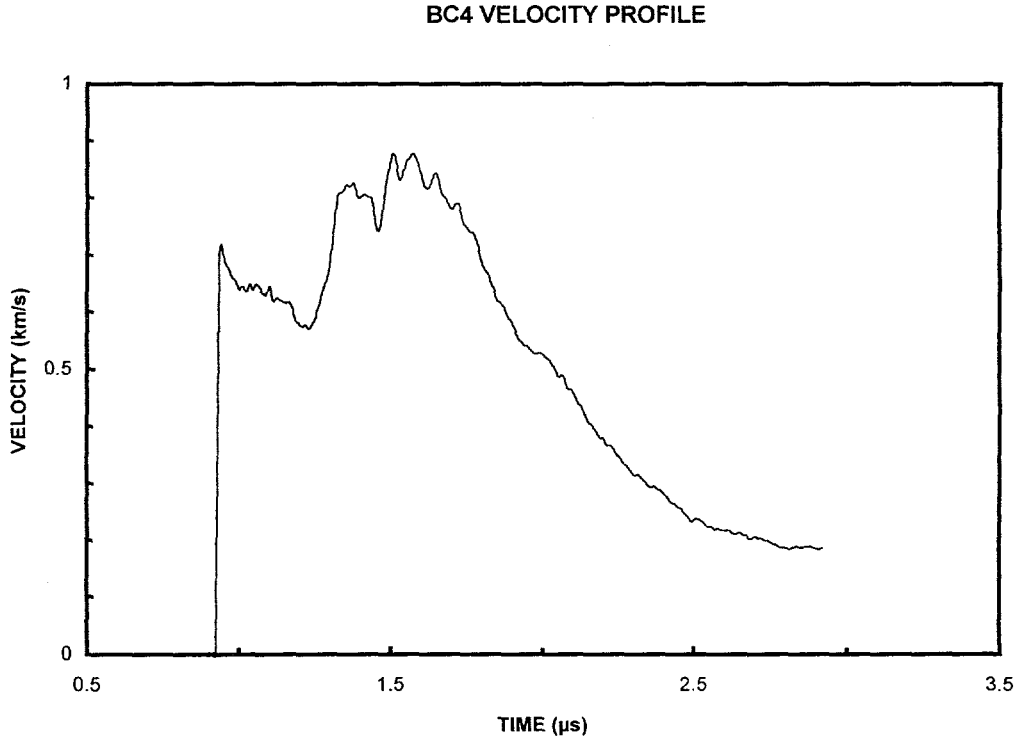

Shot Number:	BC5	**Impact Velocity:**	2.076 km/s
Test Material:	Boron Carbide		
Supplier:	DOW Chemical Company	**Velocity Per Fringe:**	430.92 m/s

	Material	Thickness (mm)	Diameter (mm)	Density (kg/m^3)
Sample	Boron Carbide	10.346	76.2	2506
Window	Lithium Fluoride	25.4	50.8	2640
Impactor	Boron Carbide	4.815	76.2	2506
Backer	Polyurethane Foam	6.0	87.5	640

Comments:

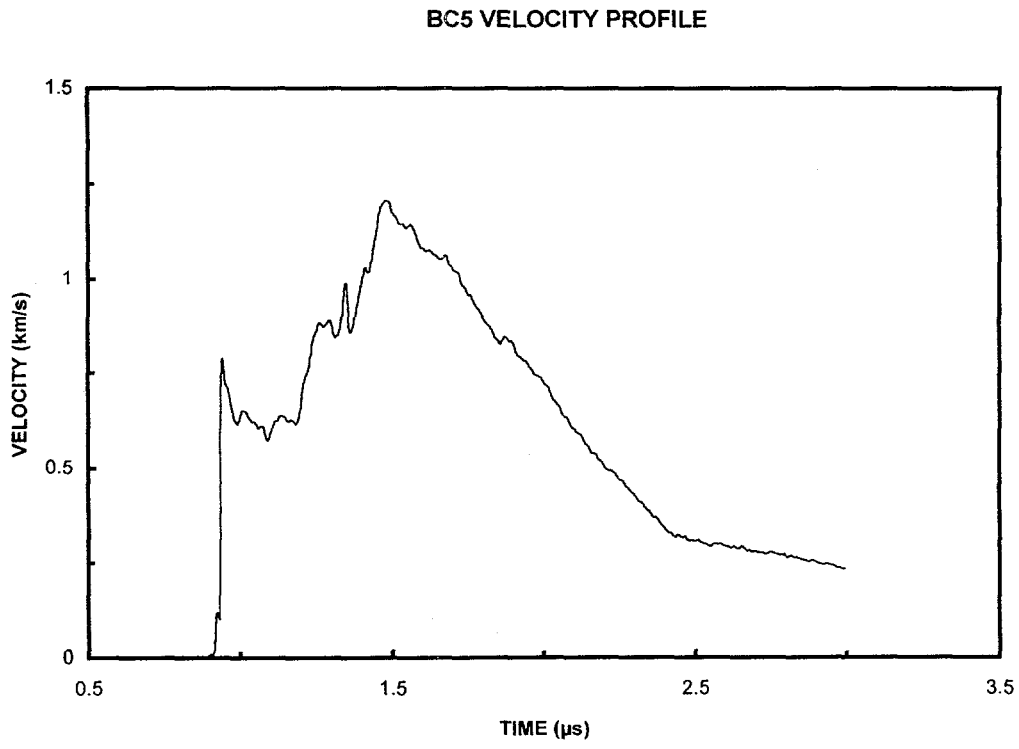

Shot Number:	BC6	**Impact Velocity:**	0.913 km/s
Test Material:	Boron Carbide		
Supplier:	DOW Chemical Company	**Velocity Per Fringe:**	121.34 m/s

	Material	Thickness (mm)	Diameter (mm)	Density (kg/m^3)
Sample	Boron Carbide	10.526	76.1	2506
Window	PMMA	24.2	76.1	1186
Impactor	PMMA	2.004	87.5	1186
Backer	Polyurethane Foam	8.0	87.5	160

Comments: Spall experiment

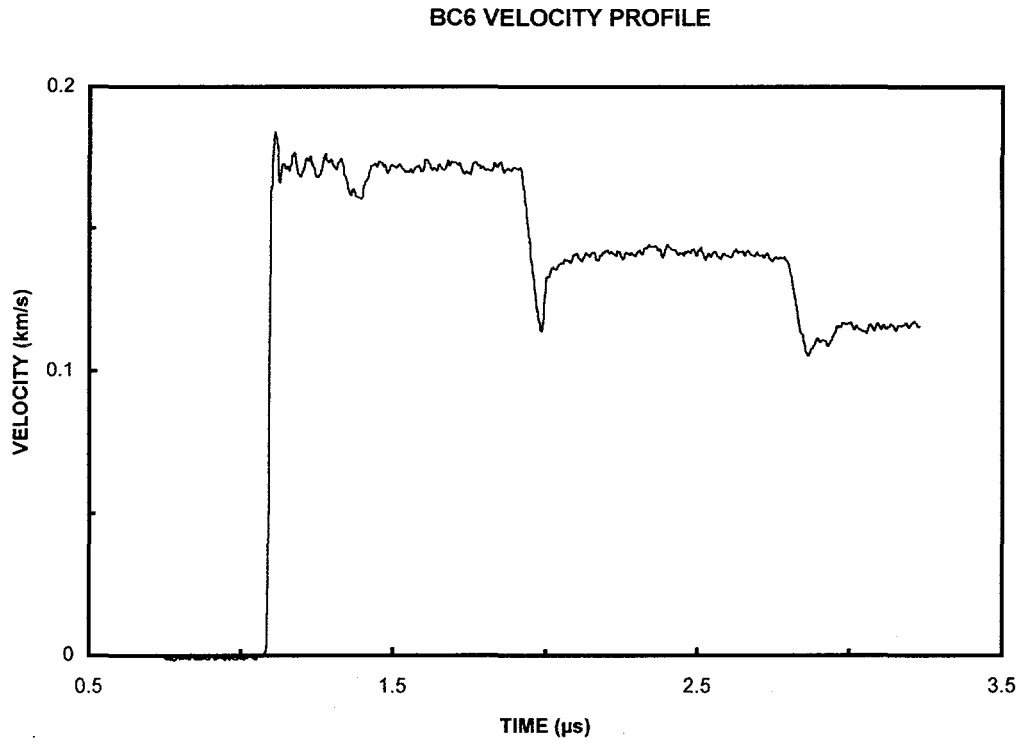

Shot Number:	BC7	**Impact Velocity:**	2.059 km/s
Test Material:	Boron Carbide		
Supplier:	DOW Chemical Company	**Velocity Per Fringe:**	681.52 m/s

	Material	Thickness (mm)	Diameter (mm)	Density (kg/m^3)
Sample	Boron Carbide	9.680	76.2	2506
Window	Lithium Fluoride	25.4	50.8	2640
Impactor	Tantalum	1.514	87.5	16659
Backer	Polyurethane Foam	6.0	87.5	640

Comments:

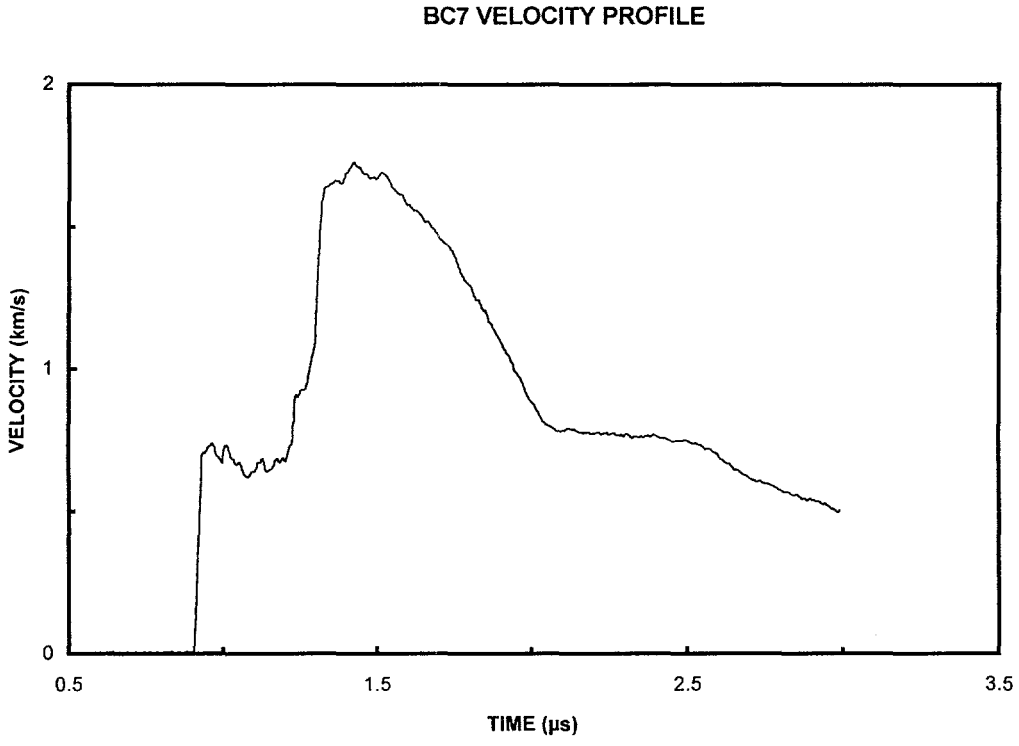

Shot Number:	BC8	**Impact Velocity:**	1.162 km/s
Test Material:	Boron Carbide		
Supplier:	DOW Chemical Company	**Velocity Per Fringe:**	121.34 m/s

	Material	Thickness (mm)	Diameter (mm)	Density (kg/m^3)
Sample	Boron Carbide	10.487	76.0	2506
Window	PMMA	24.2	50.8	1186
Impactor	PMMA	2.009	87.4	1186
Backer	Polyurethane Foam	8.0	87.5	160

Comments: Spall experiment

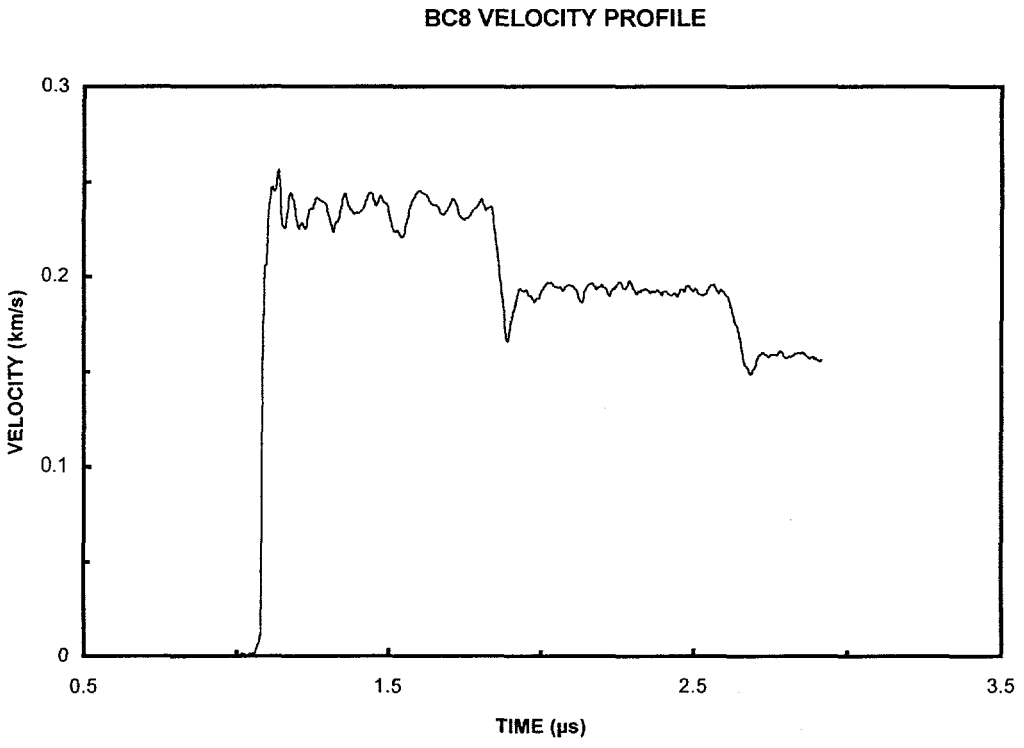

Shot Number:	BC9	**Impact Velocity:**	2.320 km/s
Test Material:	Boron Carbide		
Supplier:	DOW Chemical Company	**Velocity Per Fringe:**	430.92 m/s

	Material	Thickness (mm)	Diameter (mm)	Density (kg/m^3)
Sample	Boron Carbide	4.761	76.6	2506
Window	Lithium Fluoride	25.4	50.7	2640
Impactor	Lithium Fluoride	3.080	50.8	2640
Backer	Tantalum	1.505	87.5	16660

Comments: The impactor geometry provided a double shock in the boron carbide. The tantalum plate was backed by a 12 mm thick aluminum plate.

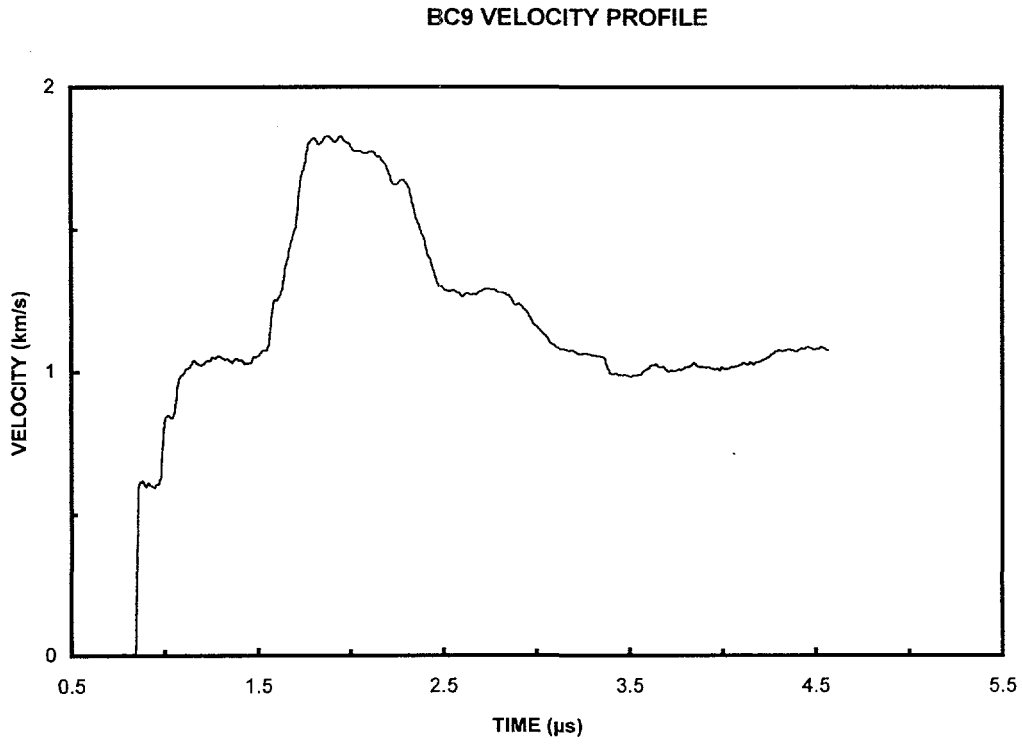

Shot Number:	BC10	**Impact Velocity:**	3.980 km/s
Test Material:	Boron Carbide		
Supplier:	DOW Chemical Company	**Velocity Per Fringe:**	681.52 m/s

	Material	Thickness (mm)	Diameter (mm)	Density (kg/m^3)
Sample	Boron Carbide	2.992	18.0	2506
Window	Lithium Fluoride	18.9	19.1	2640
Impactor	Boron Carbide	2.016	18.0	2506
Backer	PMMA	0.990	18.0	1186

Comments: This test performed on a two-stage light gas gun (20 mm bore diameter). A 0.5 mm aluminum disk backed the PMMA to activate the magnetic velocity system (MAVIS), and the remainder of the projectile sabot was PMMA.

BC10 VELOCITY PROFILE

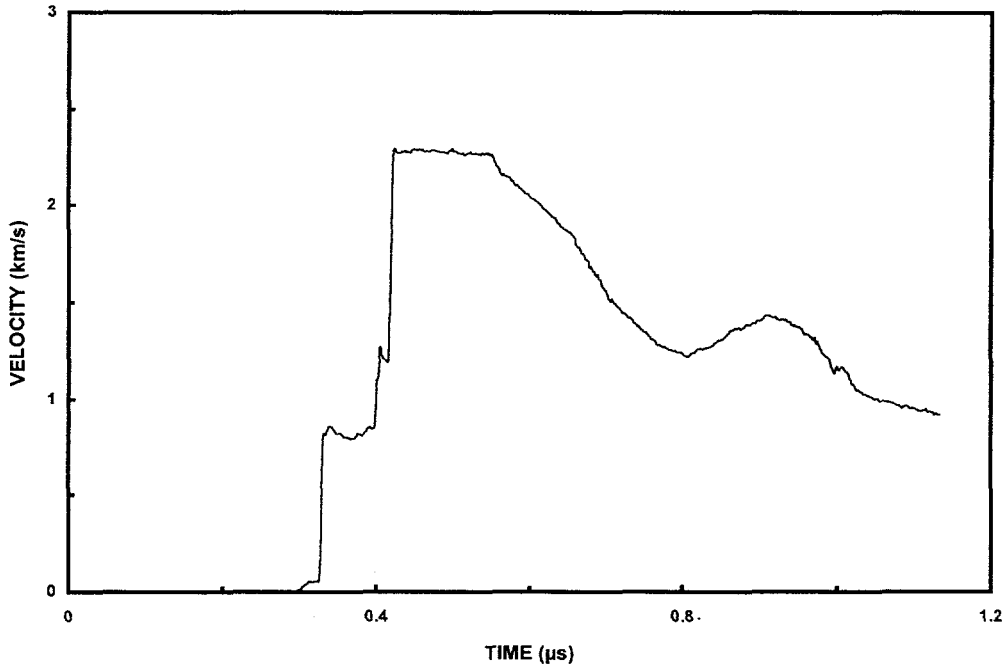

Shot Number:	BC11	**Impact Velocity:**	not measured
Test Material:	Boron Carbide		
Supplier:	DOW Chemical Company	**Velocity Per Fringe:**	681.52 m/s

	Material	Thickness (mm)	Diameter (mm)	Density (kg/m^3)
Sample	Aluminum	0.540	18.0	2703
Window	Lithium Fluoride	18.9	19.1	2640
Impactor	Aluminum	0.534	18.0	2703
Backer	Boron Carbide	3.001	18.0	2506

Comments: This was a reverse ballistic experiment on a two-stage light gas gun. Symmetric aluminum-aluminum impact provides projectile velocity.

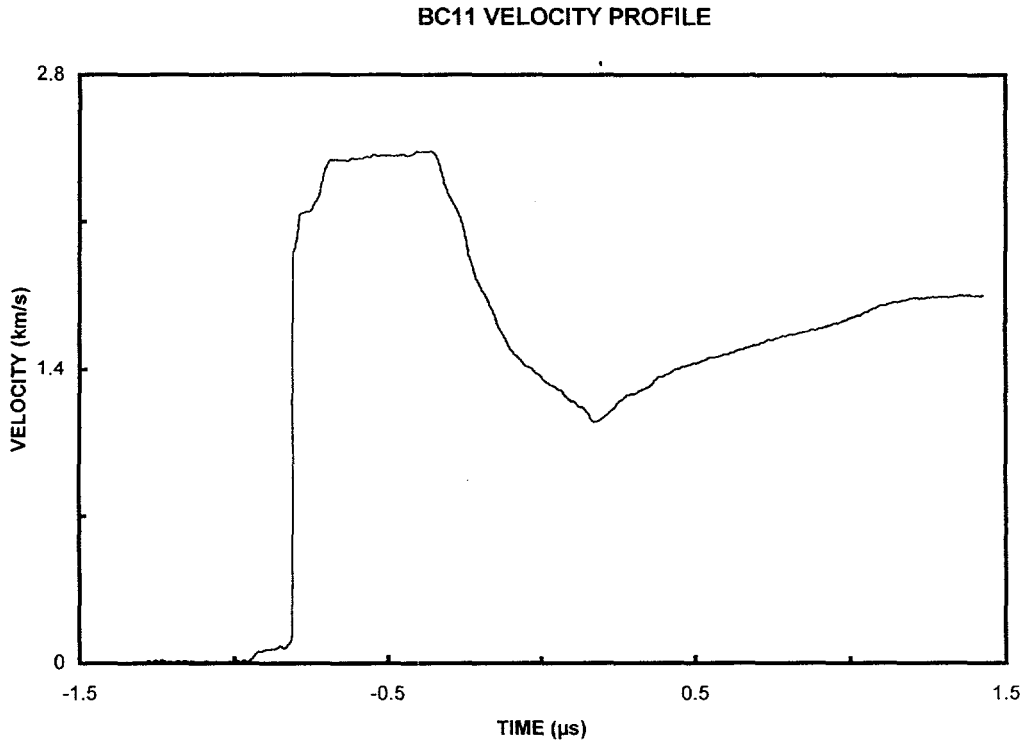

6. Silicon Carbide Ceramics

Silicon carbide ceramic exhibits features within the measured shock-wave profiles which are perhaps the most easily reproduced with numerical wave propagation codes and common, strain-hardening, metallic elastic-plastic models. Silicon carbide was one of the original suite of ceramics tested under strong shock compression by Gust et al. (1973), and ample high-pressure Hugoniot data is available for this material. Fully dense silicon carbide is one of several ceramics which exhibits exceptionally high dynamic strength. Hugoniot elastic limits in the range of 13 to 16 GPa have been measured for this ceramic [Grady and Kipp, 1993].

Data for several different silicon carbide ceramics are provided in this report. The first of these was a hot-pressed material provided by Eagle Picher Industries. This ceramic has a nominal grain size of 7 μm. The material is about 1% porous. The near spherical pores reside on the grain boundaries.

Further silicon carbide ceramics tested under shock compression for this report were prepared and provided by Cercom Incorporated. The first material is the commercially available baseline SiC-B ceramic produced by this company. The material is a near-full-density hot-pressed ceramic with a nominal grain size of 4 μm. the second material (indentified by Cercom as Type-N) is an improvement of the baseline SiC-B ceramic in which a wet milling procedure is used to achieve a high homogeneity in the chemistry and microstructure. Again the nominal grain size for this improved ceramic is about 4 μm. The third material (Type-C) is yet a further improvement in which the nominal grain size of the ceramic is reduced to approximately 1 μm.

The final material tested was a reaction-bonded Si/SiC ceramic prepared by Cercom Incorporated for the U.S. Army Research Laboratory. Briefly, the ceramic is prepared by infiltrating liquid silicon into a compact of silicon carbide and colloidal graphite. Samples of the same material were also subjected to further sintering by microwave processing. Several shock compression tests were also performed on the microwave sintered material.

Tests SC1 and SC2 on Eagle Picher silicon carbide were among the first several shock compression experiments performed within the present compilation of wave-profile data [Kipp and Grady, 1989]. Tests SC3 and SC4 were performed to broaden the stress range of the wave-profile data on the Eagle Picher material, and SC5 provides data over a more complex loading, release, and reload path. The remaining shock-wave experiments were performed on the various improved-microstructure silicon carbide ceramics developed by Cercom Incorporated as mentioned above.

Shot Number:	SC1	**Impact Velocity:**	1.542 km/s
Test Material:	Silicon Carbide		
Supplier:	Eagle Picher Industries	**Velocity Per Fringe:**	430.92 m/s

	Material	Thickness (mm)	Diameter (mm)	Density (kg/m^3)
Sample	Silicon Carbide	8.939	55.0	3177
Window	Lithium Fluoride	25.4	50.8	2640
Impactor	Silicon Carbide	3.987	55.0	3177
Backer	Polyurethane Foam	6.0	87.5	320

Comments:

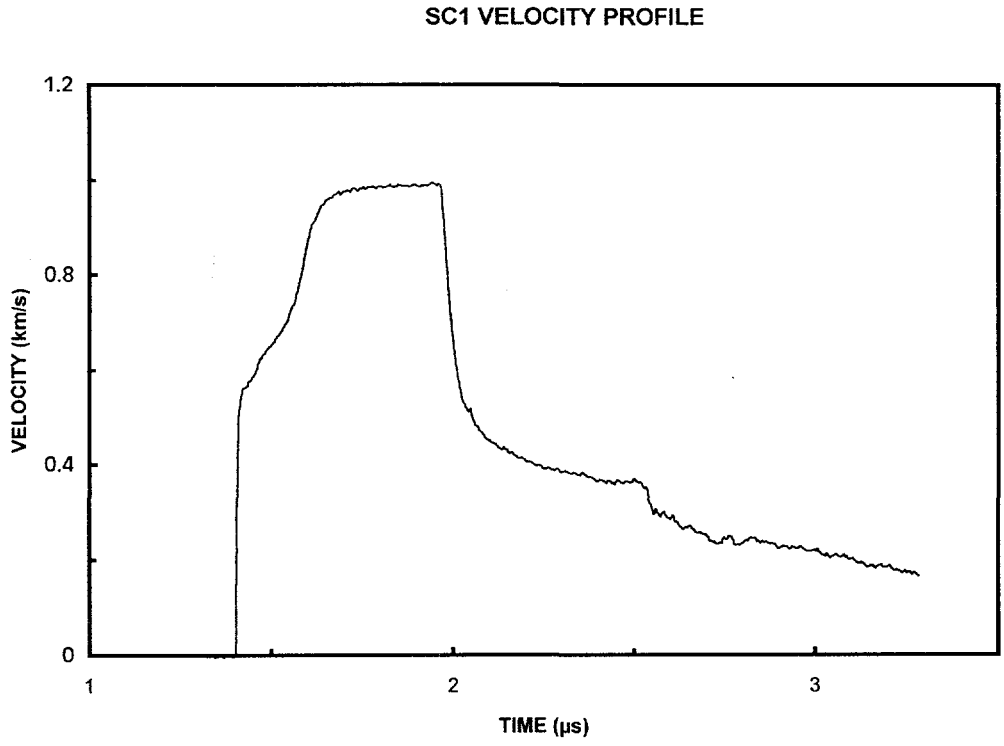

Shot Number:	SC2	**Impact Velocity:**	2.100 km/s
Test Material:	Silicon Carbide		
Supplier:	Eagle Picher Industries	**Velocity Per Fringe:**	430.92 m/s

	Material	Thickness (mm)	Diameter (mm)	Density (kg/m^3)
Sample	Silicon Carbide	8.940	55.0	3177
Window	Lithium Fluoride	25.4	50.8	2640
Impactor	Silicon Carbide	3.995	55.0	3177
Backer	Polyurethane Foam	6.0	87.5	640

Comments:

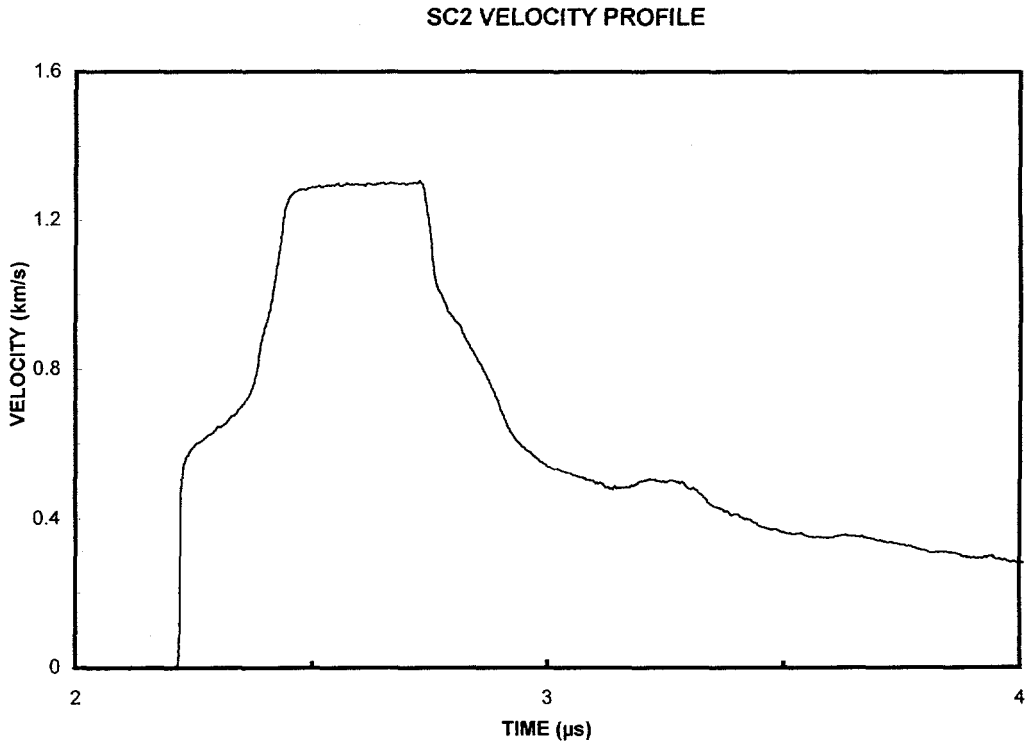

Shot Number:	SC3	**Impact Velocity:**	2.118 km/s
Test Material:	Silicon Carbide		
Supplier:	Eagle Picher Industries	**Velocity Per Fringe:**	681.52 m/s

	Material	Thickness (mm)	Diameter (mm)	Density (kg/m^3)
Sample	Silicon Carbide	8.956	52.5	3177
Window	Lithium Fluoride	25.4	50.8	2640
Impactor	Tantalum	1.516	87.5	16652
Backer	Polyurethane Foam	6.0	87.5	640

Comments:

SC3 VELOCITY PROFILE

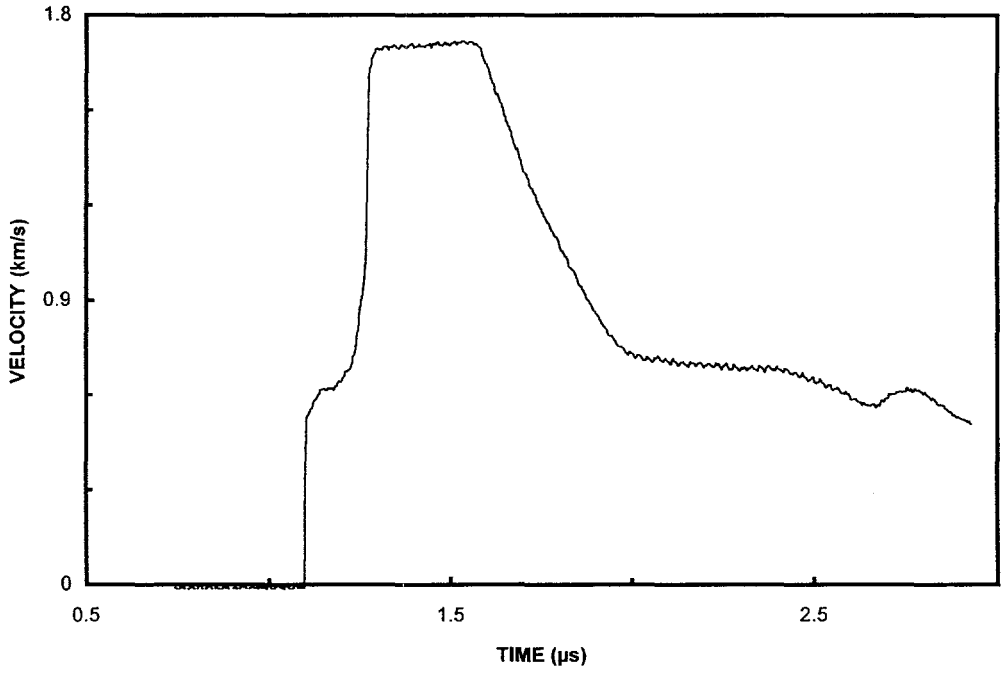

Shot Number:	SC4	**Impact Velocity:**	0.612 km/s
Test Material:	Silicon Carbide		
Supplier:	Eagle Picher Industries	**Velocity Per Fringe:**	128.07 m/s

	Material	Thickness (mm)	Diameter (mm)	Density (kg/m^3)
Sample	Silicon Carbide	9.841	50.0	3177
Window	Lithium Fluoride	25.4	50.8	2640
Impactor	Silicon Carbide	4.958	50.0	3177
Backer	Polyurethane Foam	6.0	87.5	320

Comments:

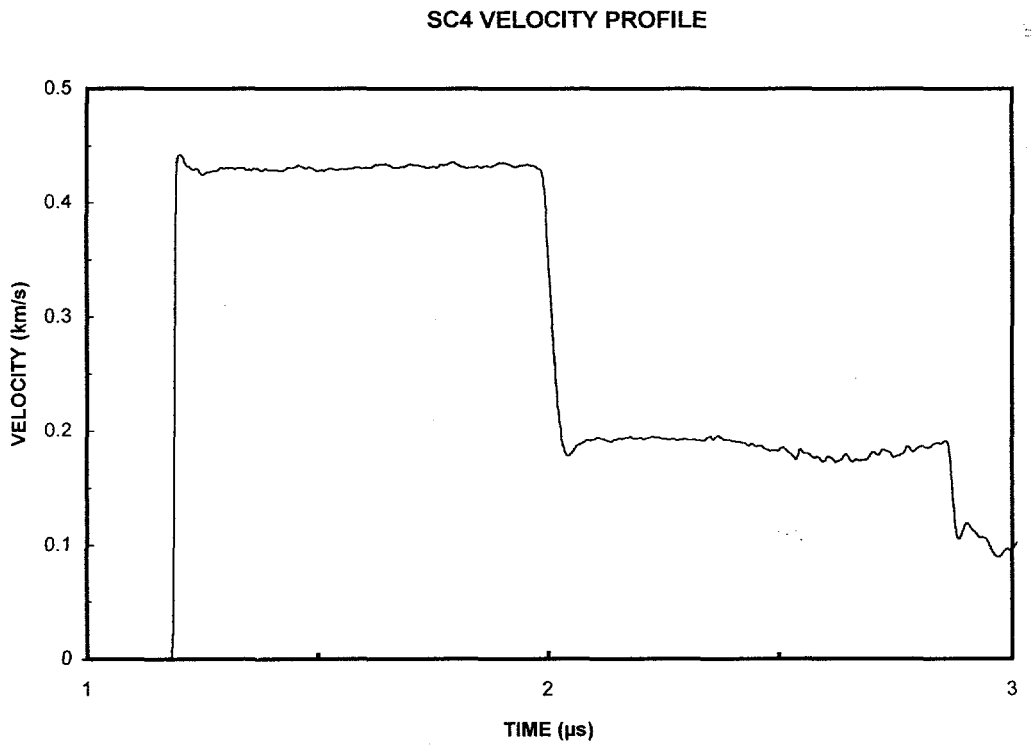

Shot Number:	SC5	**Impact Velocity:**	2.206 km/s
Test Material:	Silicon Carbide		
Supplier:	Eagle Picher Industries	**Velocity Per Fringe:**	430.92 m/s

	Material	Thickness (mm)	Diameter (mm)	Density (kg/m^3)
Sample	Silicon Carbide	4.963	76.14	3177
Window	Lithium Fluoride	25.4	50.7	2640
Impactor	Lithium Fluoride	3.297	50.8	2640
Backer	Tantalum	1.510	87.5	16501

Comments:

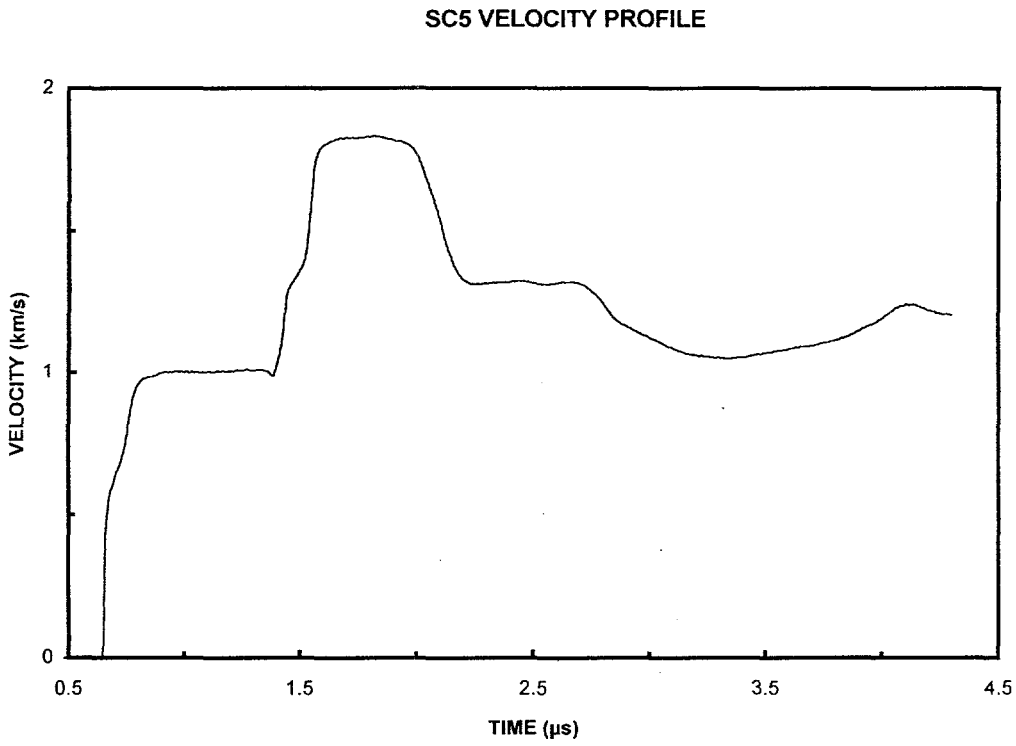

Shot Number:	SC6	**Impact Velocity:**	2.385 km/s
Test Material:	Silicon Carbide		
Supplier:	Cercom	**Velocity Per Fringe:**	551.61 m/s

	Material	Thickness (mm)	Diameter (mm)	Density (kg/m^3)
Sample	Silicon Carbide	8.995	50.85	3216
Window	Lithium Fluoride	25.4	50.8	2640
Impactor	Silicon Carbide	4.527	50.8	3215
Backer	Polyurethane Foam	8.0	87.5	640

Comments: *Type-C silicon carbide*

SC6 VELOCITY PROFILE

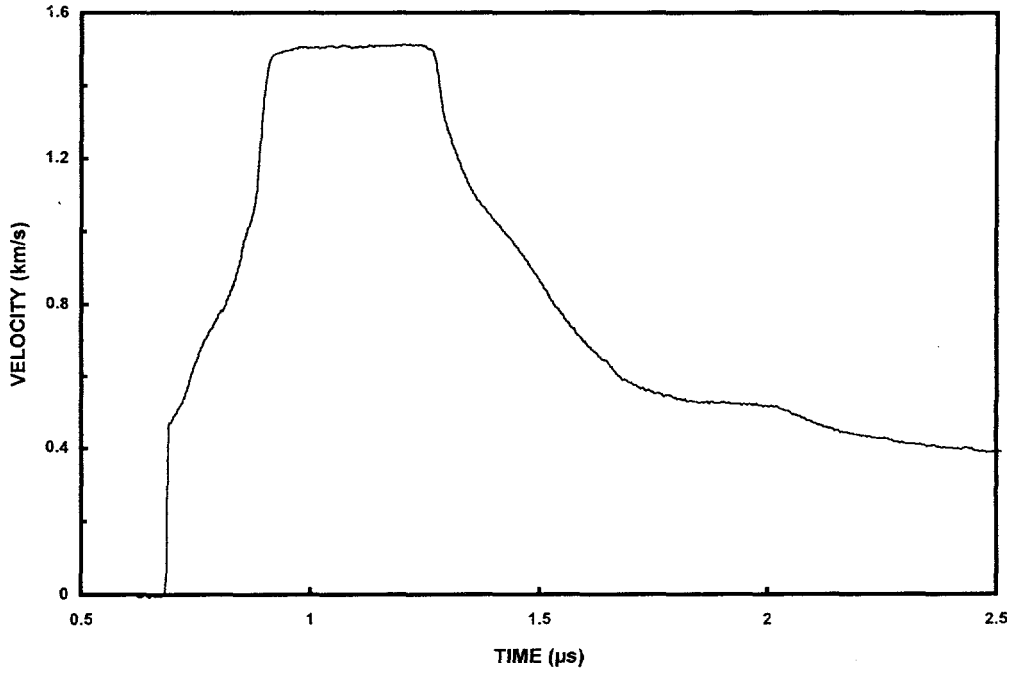

Shot Number:	SC7	**Impact Velocity:**	0.535 km/s
Test Material:	Silicon Carbide		
Supplier:	Cercom	**Velocity Per Fringe:**	94.76 m/s

	Material	Thickness (mm)	Diameter (mm)	Density (kg/m^3)
Sample	Silicon Carbide	4.035	17.975	3221
Window	Lithium Fluoride	9.196	37.95	2640
Impactor	Aluminum 6061-T6	0.990	38.083	2703
Backer	PMMA	6.35	87.5	1186

Comments: Baseline SiC-B silicon carbide

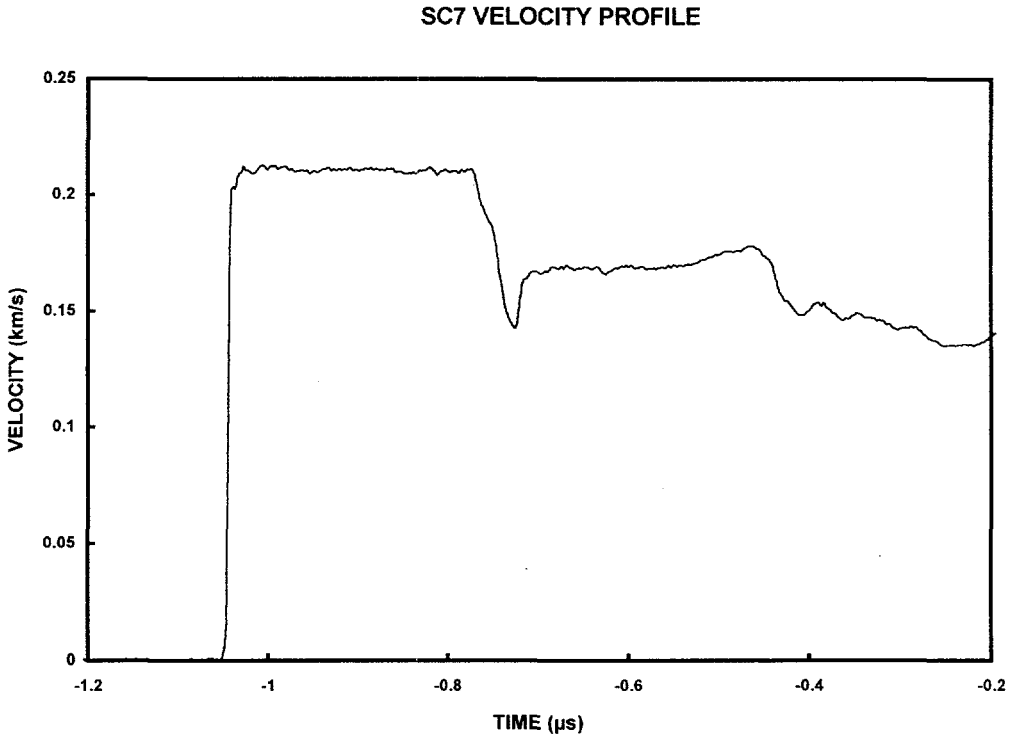

Shot Number:	SC8	**Impact Velocity:**	0.489 km/s
Test Material:	Silicon Carbide		
Supplier:	Cercom	**Velocity Per Fringe:**	94.76 m/s

	Material	Thickness (mm)	Diameter (mm)	Density (kg/m^3)
Sample	Silicon Carbide	4.025	17.866	3244
Window	Lithium Fluoride	9.20	37.98	2640
Impactor	Magnesium	0.60	38.0	1740
Backer	PMMA	6.35	87.5	1186

Comments: Type-C silicon carbide

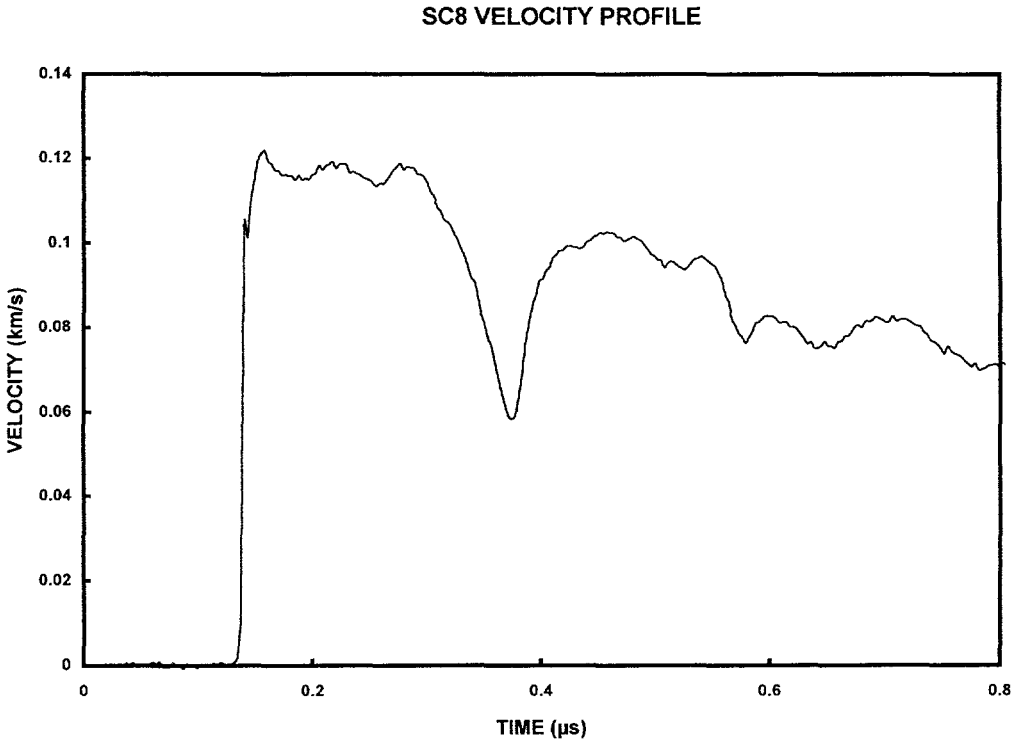

Shot Number:	SC9	**Impact Velocity:**	0.485 km/s
Test Material:	Silicon Carbide		
Supplier:	Cercom	**Velocity Per Fringe:**	121.34 m/s

	Material	Thickness (mm)	Diameter (mm)	Density (kg/m^3)
Sample	Silicon Carbide	4.512	29.471	3227
Window	PMMA	24.2	50.7	1186
Impactor	Magnesium	0.5974	27.0	1739
Backer	Polyurethane Foam	8.04	87.5	640

Comments: Type-N silicon carbide

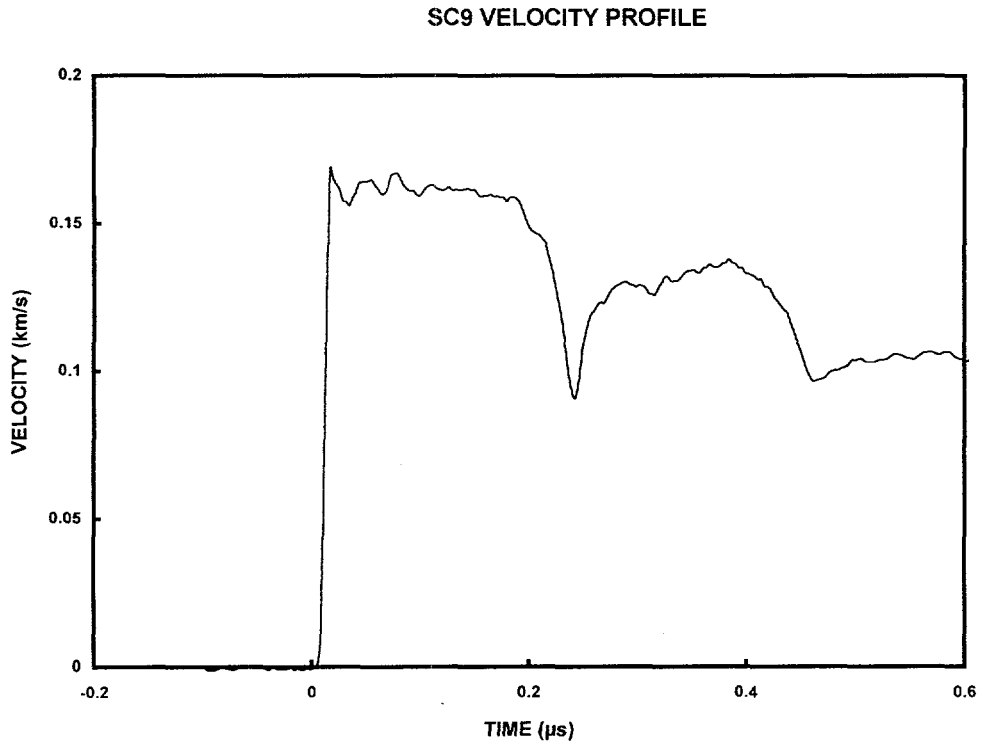

Shot Number:	SC10	**Impact Velocity:**	0.485 km/s
Test Material:	Silicon Carbide		
Supplier:	Cercom	**Velocity Per Fringe:**	121.34 m/s

	Material	Thickness (mm)	Diameter (mm)	Density (kg/m^3)
Sample	Silicon Carbide	4.527	50.7	3226
Window	PMMA	24.2	50.7	1186
Impactor	Aluminum 6061-T6	1.042	50.7	2703
Backer	Polyurethane Foam	8.03	87.5	640

Comments: Type-C silicon carbide

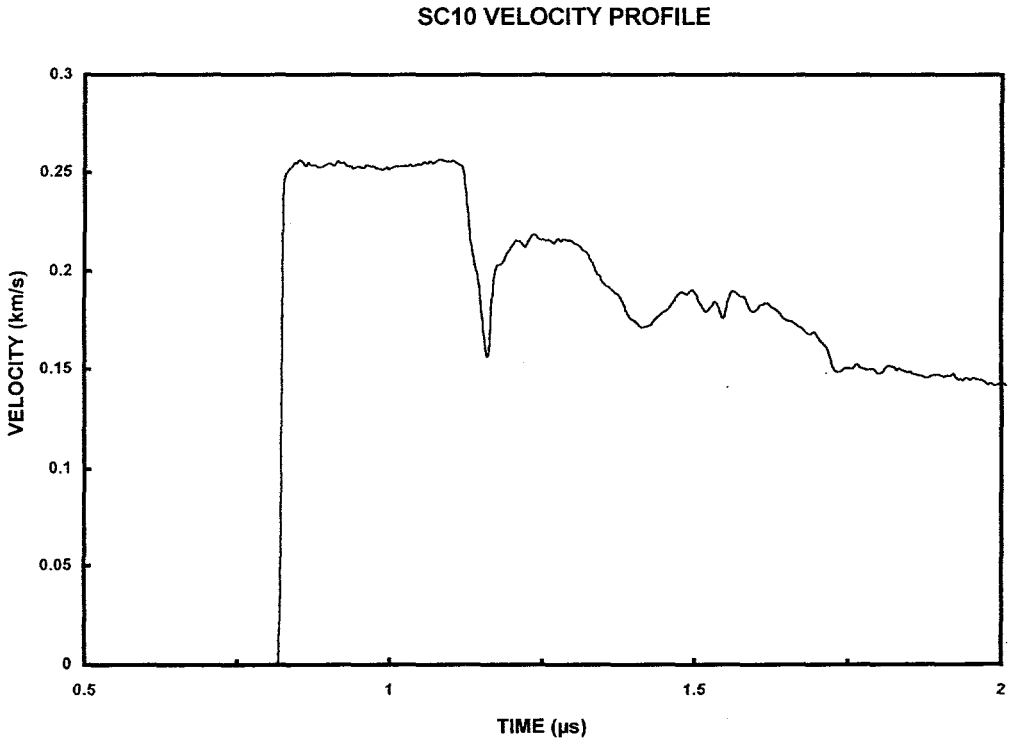

Shot Number:	SC11	**Impact Velocity:**	1.611 km/s
Test Material:	Silicon Carbide		
Supplier:	Cercom	**Velocity Per Fringe:**	375.10 m/s

	Material	Thickness (mm)	Diameter (mm)	Density (kg/m^3)
Sample	Silicon Carbide	5.986	32.0	3145
Window	Lithium Fluoride	19.2	25.4	2640
Impactor	Silicon Carbide	2.996	32.0	3135
Backer	Polyurethane Foam	6.26	87.5	320

Comments: Reaction-bonded and microwave-sintered silicon carbide

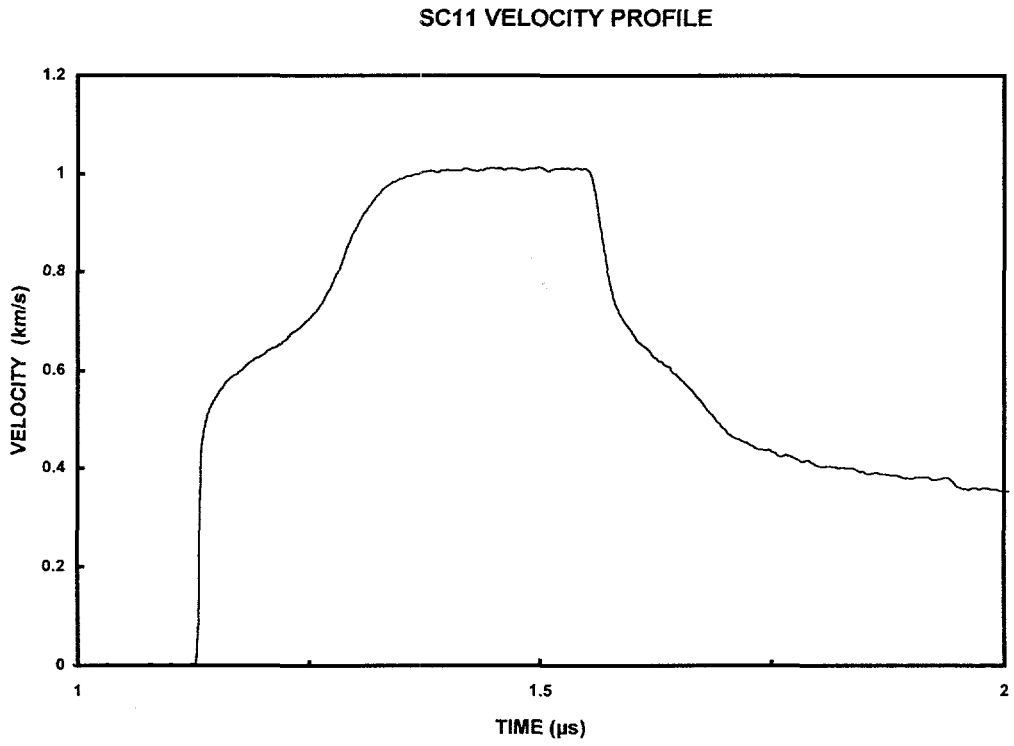

Shot Number:	SC12	**Impact Velocity:**	2.386 km/s
Test Material:	Silicon Carbide		
Supplier:	Cercom	**Velocity Per Fringe:**	551.60 ms

	Material	Thickness (mm)	Diameter (mm)	Density (kg/m^3)
Sample	Silicon Carbide	5.992	32.2	3111
Window	Lithium Fluoride	19.2	25.4	2640
Impactor	Silicon Carbide	2.986	32.0	3132
Backer	Polyurethane Foam	8.04	87.5	320

Comments: Reaction-bonded and microwave-sintered silicon carbide

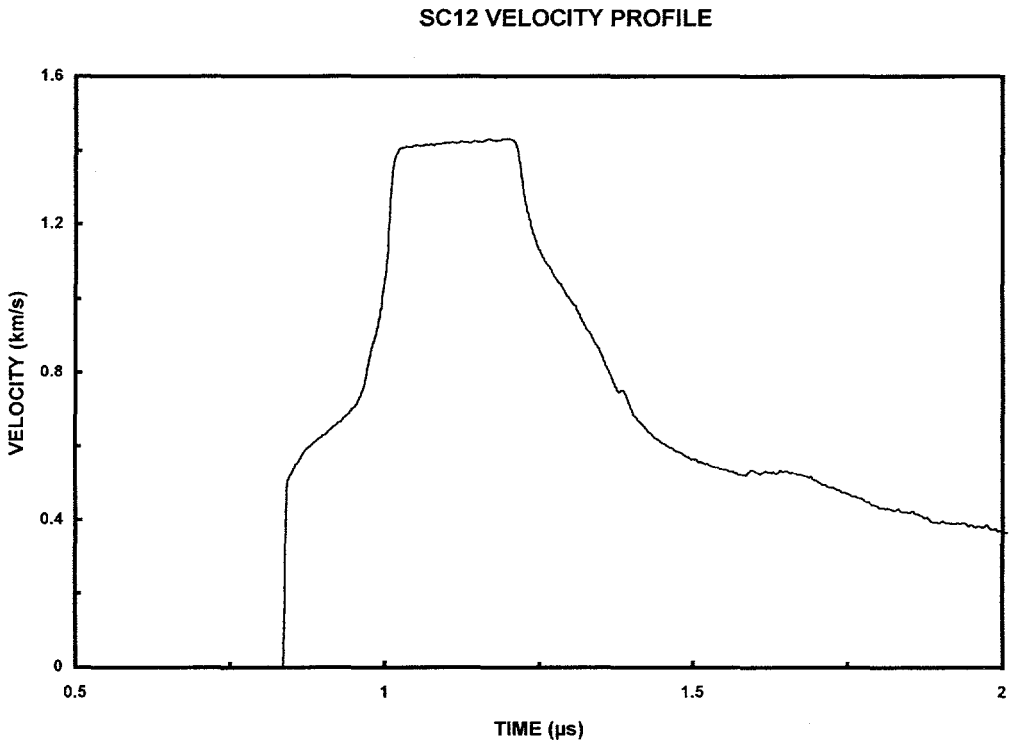

Shot Number:	SC13	**Impact Velocity:**	1.607 km/s
Test Material:	Silicon Carbide		
Supplier:		**Velocity Per Fringe:**	375.10 m/s

	Material	Thickness (mm)	Diameter (mm)	Density (kg/m^3)
Sample	Silicon Carbide	5.954	32.0	3111
Window	Lithium Fluoride	19.13	25.3	2640
Impactor	Silicon Carbide	3.011	32.0	3138
Backer	Polyurethane Foam	6.29	87.5	320

Comments: Reaction-bonded silicon carbide

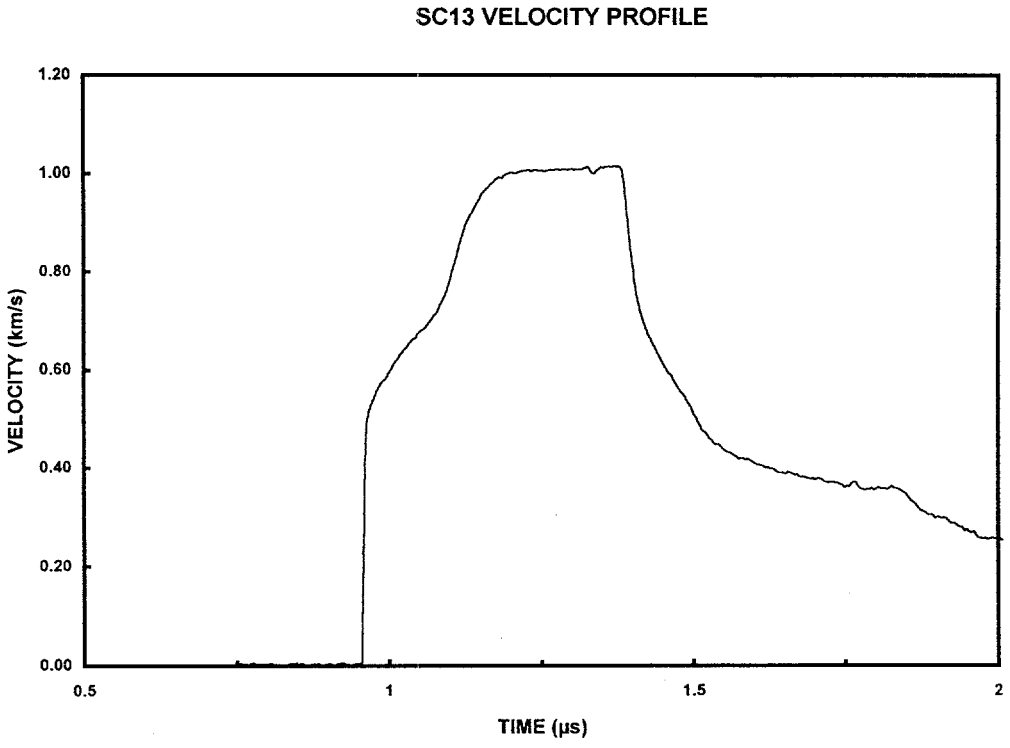

Shot Number:	SC14	**Impact Velocity:**	2.257 km/s
Test Material:	Silicon Carbide		
Supplier:		**Velocity Per Fringe:**	551.60 m/s

	Material	Thickness (mm)	Diameter (mm)	Density (kg/m^3)
Sample	Silicon Carbide	5.961	31.9	3139
Window	Lithium Fluoride	19.0	25.2	2640
Impactor	Silicon Carbide	2.981	32.0	3131
Backer	Polyurethane Foam	8.06	87.5	320

Comments: Reaction-bonded silicon carbide

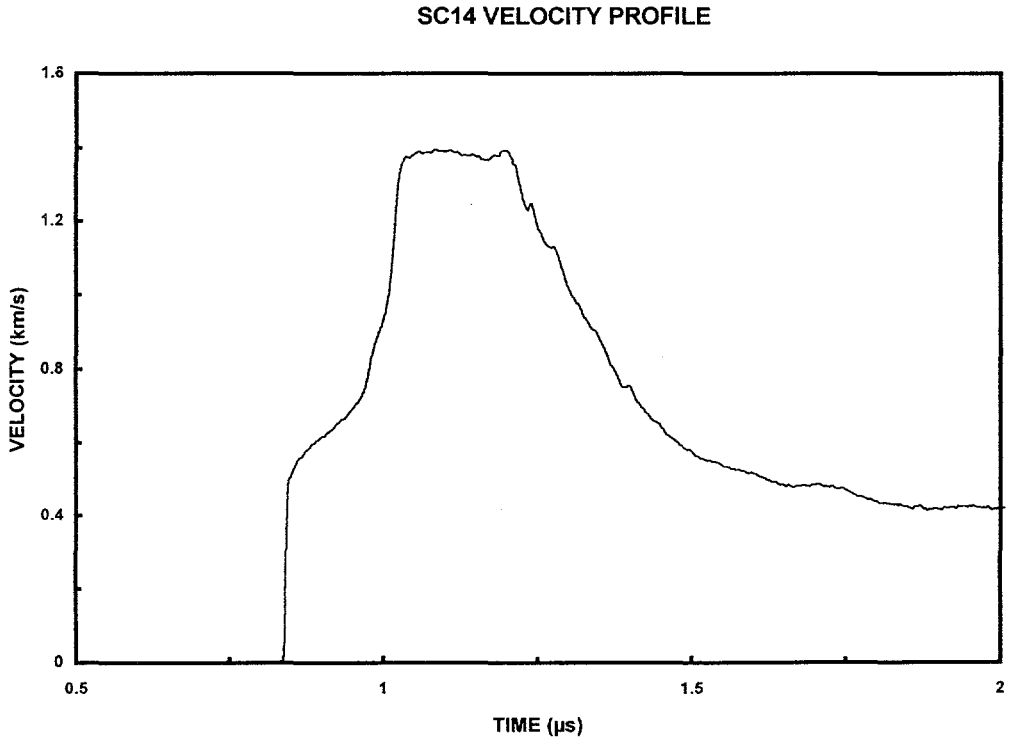

Shot Number:	SC15	**Impact Velocity:**	1.566 km/s
Test Material:	Silicon Carbide		
Supplier:	Cercom	**Velocity Per Fringe:**	375.10 m/s

	Material	Thickness (mm)	Diameter (mm)	Density (kg/m^3)
Sample	Silicon Carbide	9.014	50.8	3220
Window	Lithium Fluoride	25.4	50.8	2640
Impactor	Silicon Carbide	4.490	50.8	3220
Backer	Polyurethane Foam	8.0	87.3	311

Comments: Baseline SiC-B silicon carbide

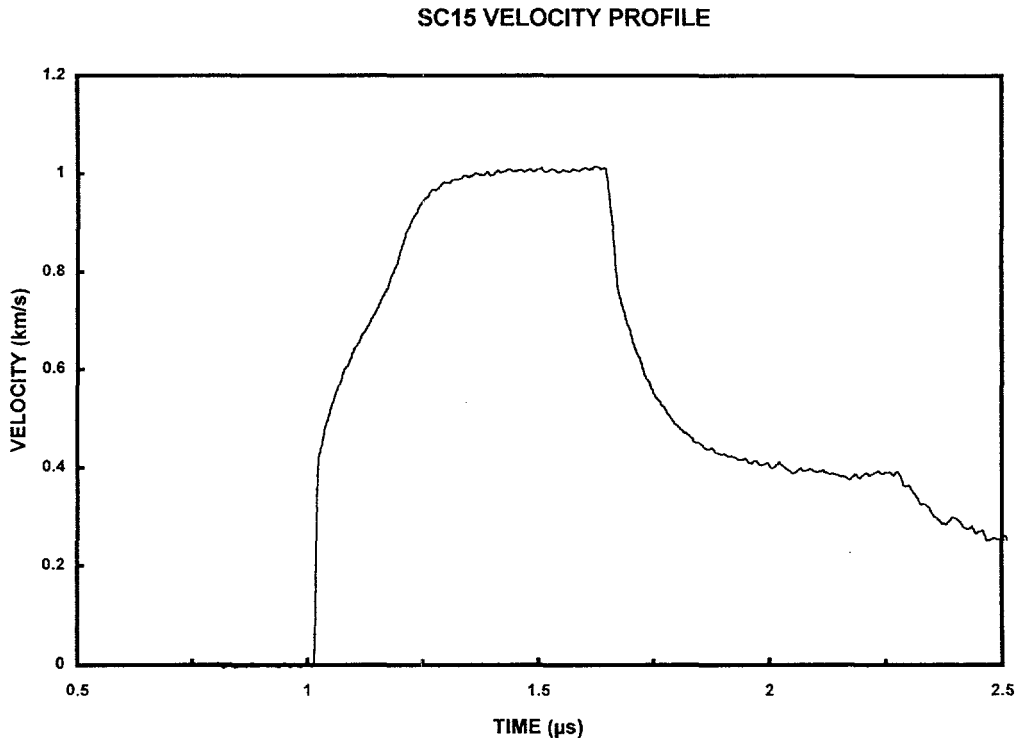

Shot Number:	SC16	**Impact Velocity:**	2.259 km/s
Test Material:	Silicon Carbide		
Supplier:	Cercom	**Velocity Per Fringe:**	551.61 m/s

	Material	Thickness (mm)	Diameter (mm)	Density (kg/m^3)
Sample	Silicon Carbide	8.993	50.8	3220
Window	Lithium Fluoride	25.4	50.8	2640
Impactor	Silicon Carbide	4.516	50.8	3220
Backer	Polyurethane Foam	8.0	87.5	557

Comments: Baseline SiC-B silicon carbide

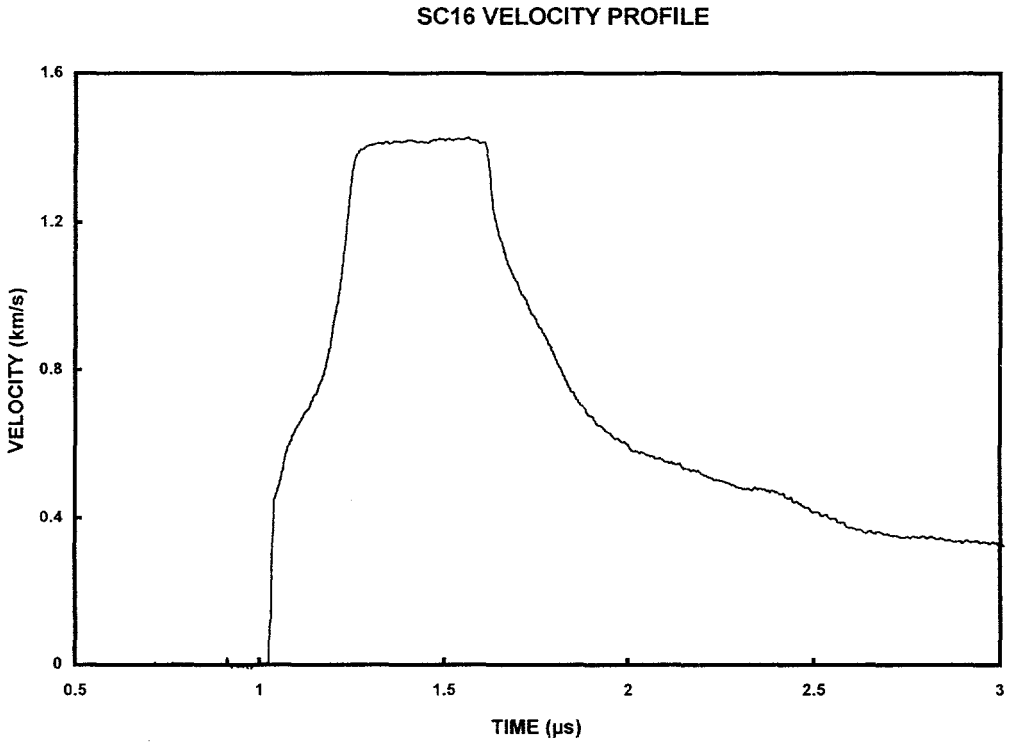

Shot Number:	SC17	**Impact Velocity:**	1.596 km/s
Test Material:	Silicon Carbide		
Supplier:	Cercom	**Velocity Per Fringe:**	375.10 m/s

	Material	Thickness (mm)	Diameter (mm)	Density (kg/m^3)
Sample	Silicon Carbide	9.012	50.8	3220
Window	Lithium Fluoride	25.4	50.8	2640
Impactor	Silicon Carbide	4.503	50.8	3230
Backer	Polyurethane Foam	8.0	87.5	328

Comments: Type-N silicon carbide

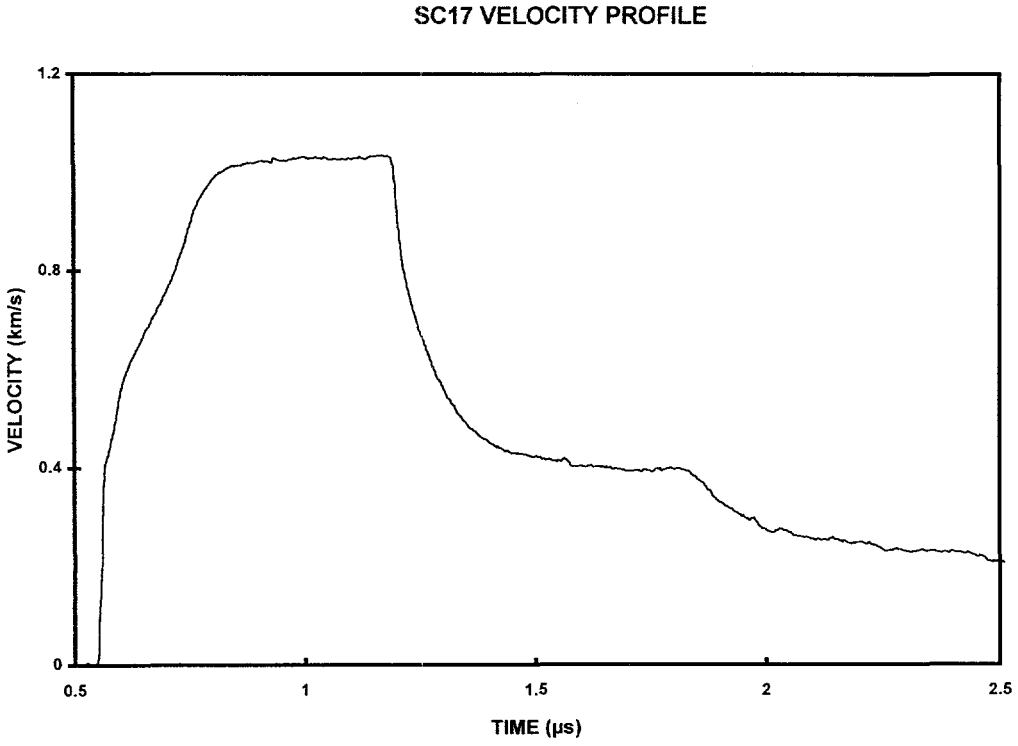

Shot Number:	SC18	**Impact Velocity:**	2.352 km/s
Test Material:	Silicon Carbide		
Supplier:	Cercom	**Velocity Per Fringe:**	551.61 m/s

	Material	Thickness (mm)	Diameter (mm)	Density (kg/m^3)
Sample	Silicon Carbide	8.998	50.8	3230
Window	Lithium Fluoride	25.4	50.8	2640
Impactor	Silicon Carbide	4.504	50.8	3220
Backer	Polyurethane Foam	8.0	87.5	625

Comments: Type-N silicon carbide

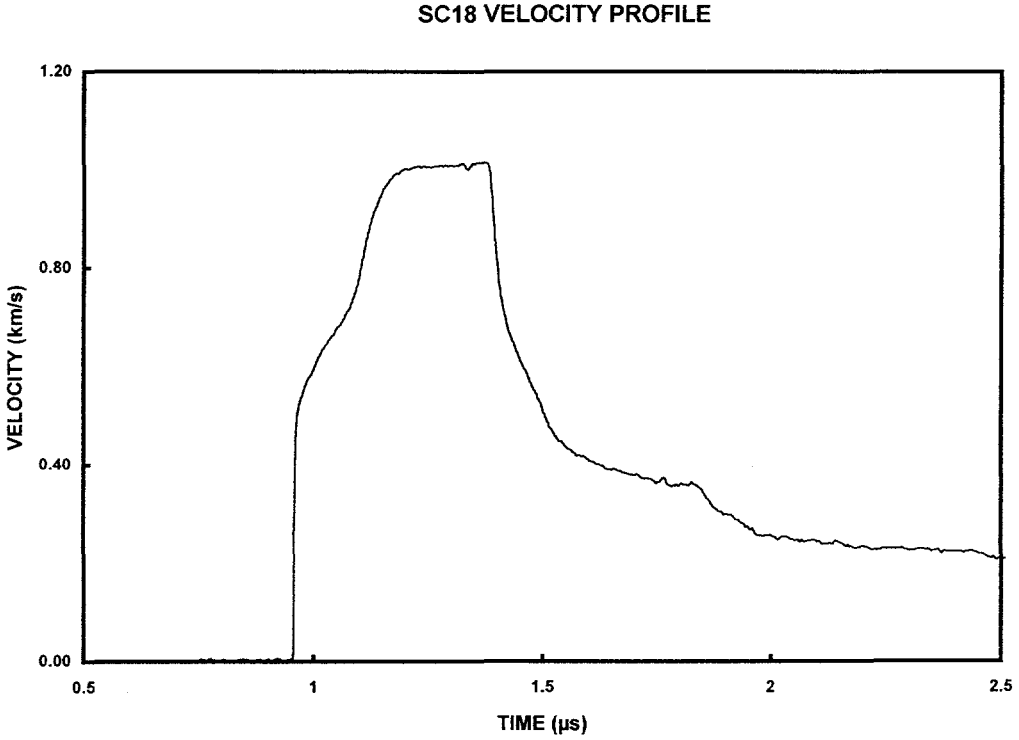

Shot Number:	SC19	**Impact Velocity:**	1.605 km/s
Test Material:	Silicon Carbide		
Supplier:	Cercom	**Velocity Per Fringe:**	375.10 m/s

	Material	Thickness (mm)	Diameter (mm)	Density (kg/m^3)
Sample	Silicon Carbide	9.013	50.8	3220
Window	Lithium Fluoride	25.4	50.8	2640
Impactor	Silicon Carbide	4.506	50.8	3220
Backer	Polyurethane Foam	8.0	87.3	318

Comments: Type-C silicon carbide

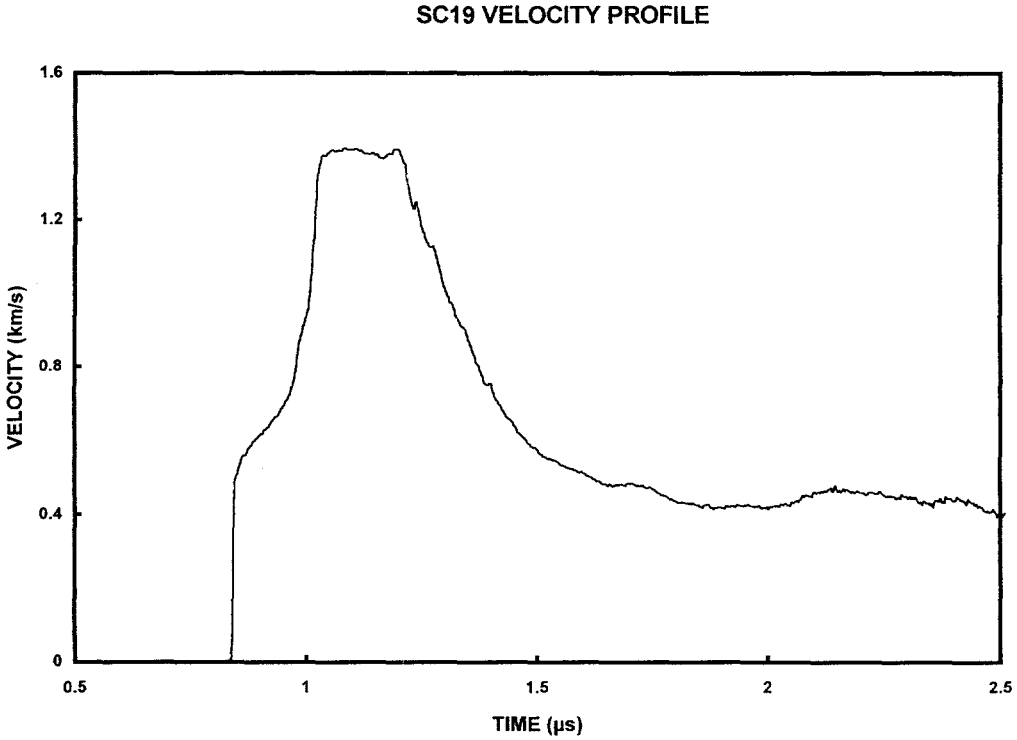

7. Silicon Nitride Ceramics

Silicon nitride is a low density ceramic with excellent mechanical strength and thermal shock properties at high temperatures. Impact-shock compression data for this ceramic is relatively sparse. Yamakawa, et al. (1993) and Mashimo (1993) report shock-Hugoniot and Hugoniot elastic-limit data for several materials, varying in initial grain size and porosity. In that report, Hugoniot elastic-limit values ranged from about 10 to 20 GPa, with higher values corresponding to reduced porosity and grain size. The materials tested had relatively high binder content (8 wt%) of Al_2O_3 and Y_2O_3. Nahme, et al. (1994) have conducted shock-profile measurements with VISAR diagnostics on two different silicon nitride ceramics–a near full-density ceramic (3150 kg/m^3) and a porous ceramic (2280 kg/m^3). Nahme's report contains Hugoniot elastic-limit and spall data along with features of the measured shock-profiles.

The silicon nitride material from which the wave profiles of this report were measured is a sintered, near-full-density ceramic produced and provided by Kyocera Industrial Ceramics Corporation, and it is identified as their product SN-220. This material is less than 0.3wt% tungsten, oxygen, and yttria with a reported grain size of 0.4 - 0.7 μm. The nominal reference density for this product is 3152 kg/m^3. Measured longitudinal and shear-elastic wave speeds are 10.31 km/s and 5.81 km/s, respectively.

Tests SN1, SN2, and SN4 show an abrupt drop in particle velocity early in the compressive wave which was never explained, but it is believed to be an experimental problem. Test SN7, which was a repeat of SN1, did not show this feature. Tests SN1 through SN5 reveal shock properties at increasing impact amplitudes. Test SN5 shows unusual properties, including a reduced shock velocity and what appears to be a rarefaction shock. This test suggests a possible phase transformation within the vicinity of the maximum stress achieved.

Tests SN6, SN7, and SN8 were performed at the same impact velocities on samples that were 15, 10, and 5 mm in thickness, respectively. These data nicely reveal wave evolution properties of this ceramic.

Shot Number:	SN1	**Impact Velocity:**	1.057 km/s
Test Material:	Silicon Nitride		
Supplier:	Kyocera Corporation	**Velocity Per Fringe:**	430.92 m/s

	Material	Thickness (mm)	Diameter (mm)	Density (kg/m^3)
Sample	Silicon Nitride	10.013	76.2	3156
Window	Lithium Fluoride	25.6	50.8	2640
Impactor	Silicon Nitride	5.005	87.5	3156
Backer	Polyurethane Foam	12.8	87.5	316

Comments: The abrupt drop in particle velocity at approximately 1.7 μs is not understood–possibly an experimental difficulty.

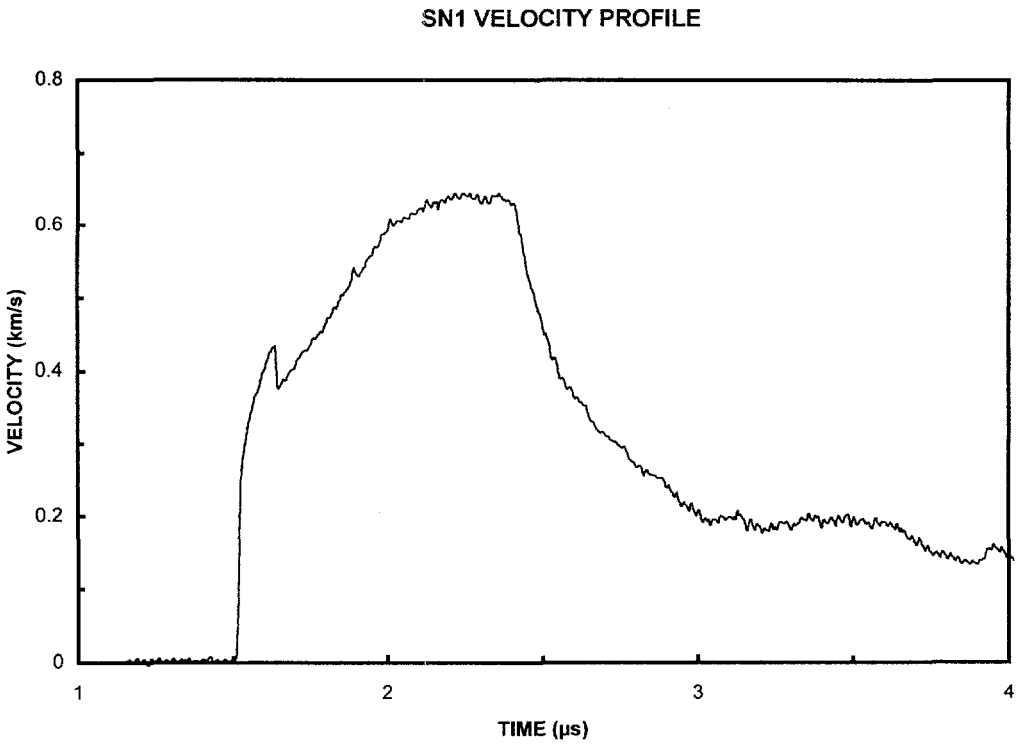

Shot Number:	SN2	**Impact Velocity:**	1.478 km/s
Test Material:	Silicon Nitride		
Supplier:	Kyocera Corporation	**Velocity Per Fringe:**	430.92 m/s

	Material	Thickness (mm)	Diameter (mm)	Density (kg/m^3)
Sample	Silicon Nitride	10.026	76.2	3158
Window	Lithium Fluoride	25.6	50.8	2640
Impactor	Silicon Nitride	5.003	87.5	3158
Backer	Polyurethane Foam	12.7	87.5	312

Comments:

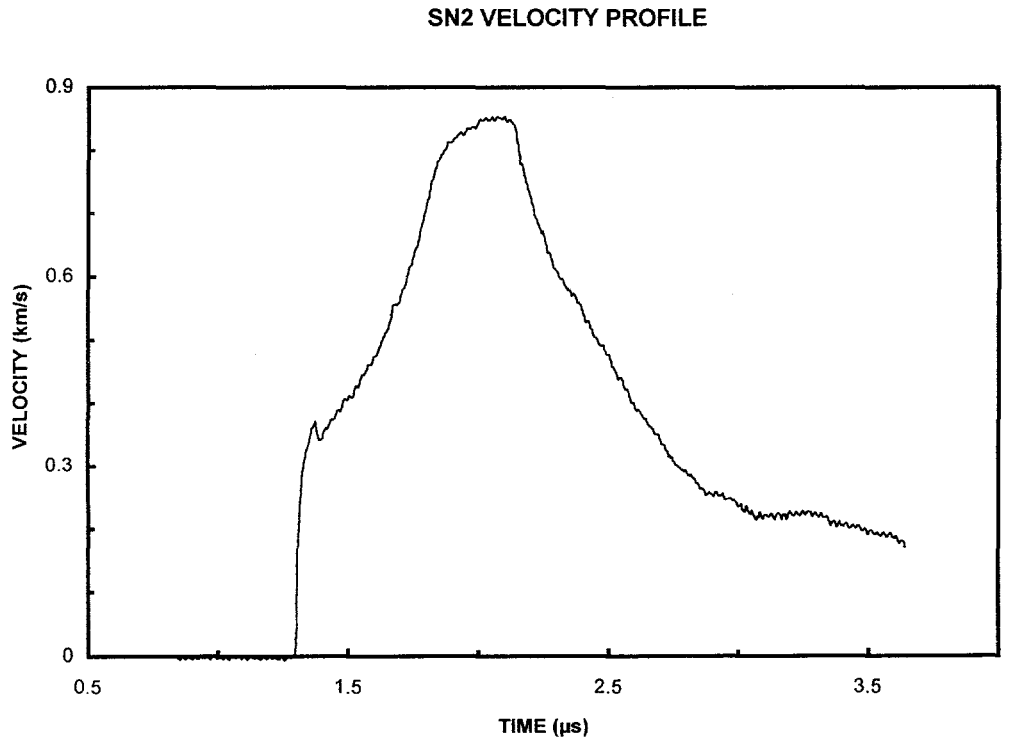

Shot Number:	SN3	**Impact Velocity:**	2.080 km/s
Test Material:	Silicon Nitride		
Supplier:	Kyocera Corporation	**Velocity Per Fringe:**	430.92 m/s

	Material	Thickness (mm)	Diameter (mm)	Density (kg/m^3)
Sample	Silicon Nitride	10.011	76.2	3156
Window	Lithium Fluoride	25.6	50.8	2640
Impactor	Silicon Nitride	5.004	87.5	3156
Backer	Polyurethane Foam	12.7	87.5	312

Comments:

SN3 VELOCITY PROFILE

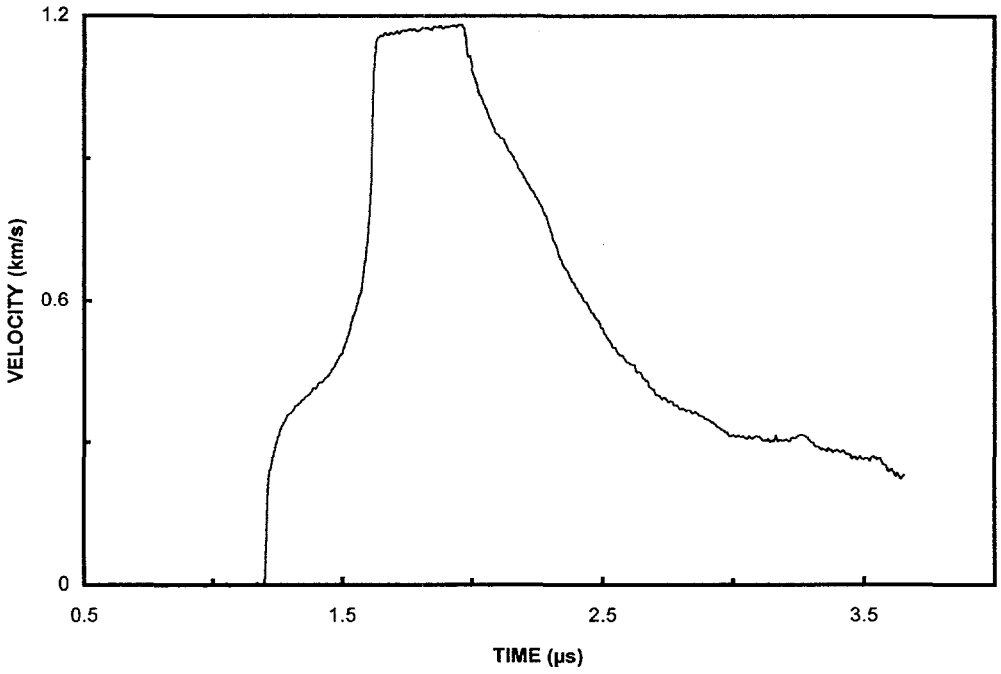

Shot Number:	SN4	**Impact Velocity:**	2.487 km/s
Test Material:	Silicon Nitride		
Supplier:	Kyocera Corporation	**Velocity Per Fringe:**	430.92 m/s

	Material	Thickness (mm)	Diameter (mm)	Density (kg/m^3)
Sample	Silicon Nitride	10.023	76.2	3156
Window	Lithium Fluoride	25.4	50.7	2640
Impactor	Silicon Nitride	5.000	87.5	3156
Backer	Polyurethane Foam	8.0	87.5	623

Comments:

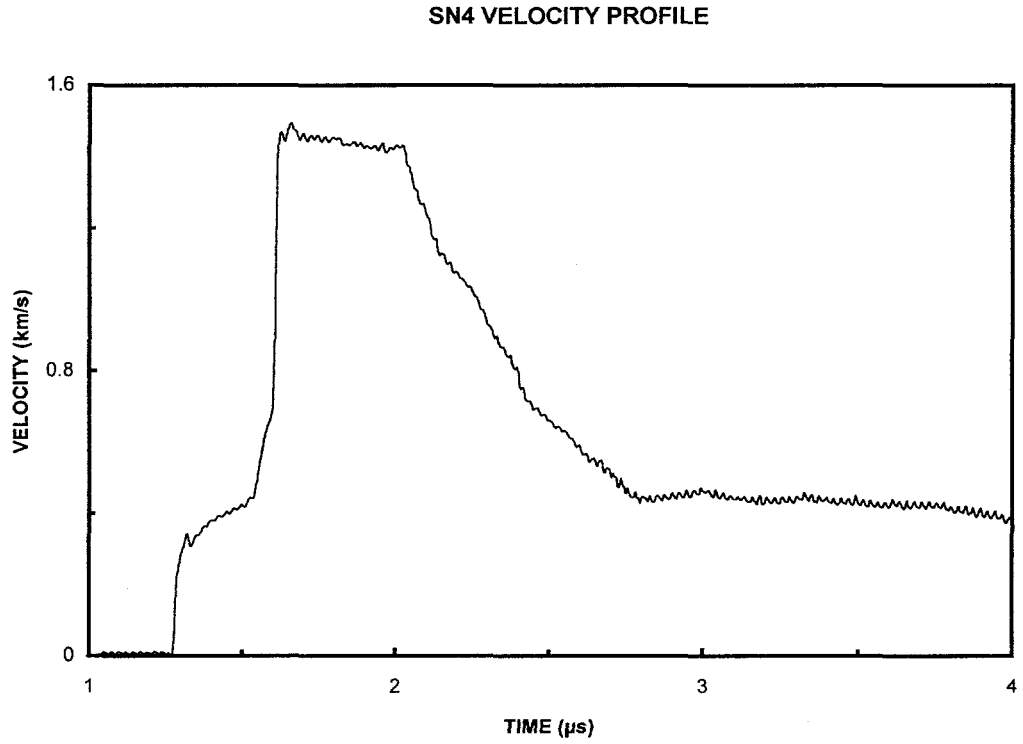

Shot Number:	SN5	**Impact Velocity:**	2.284 km/s
Test Material:	Silicon Nitride		
Supplier:	Kyocera Corporation	**Velocity Per Fringe:**	768.59 km/s

	Material	Thickness (mm)	Diameter (mm)	Density (kg/m^3)
Sample	Silicon Nitride	10.023	76.2	3156
Window	Lithium Fluoride	25.4	50.8	2640
Impactor	Tantalum	1.520	87.6	16658
Backer	PMMA	5.904	87.5	1182

Comments: Possible rarefaction shock

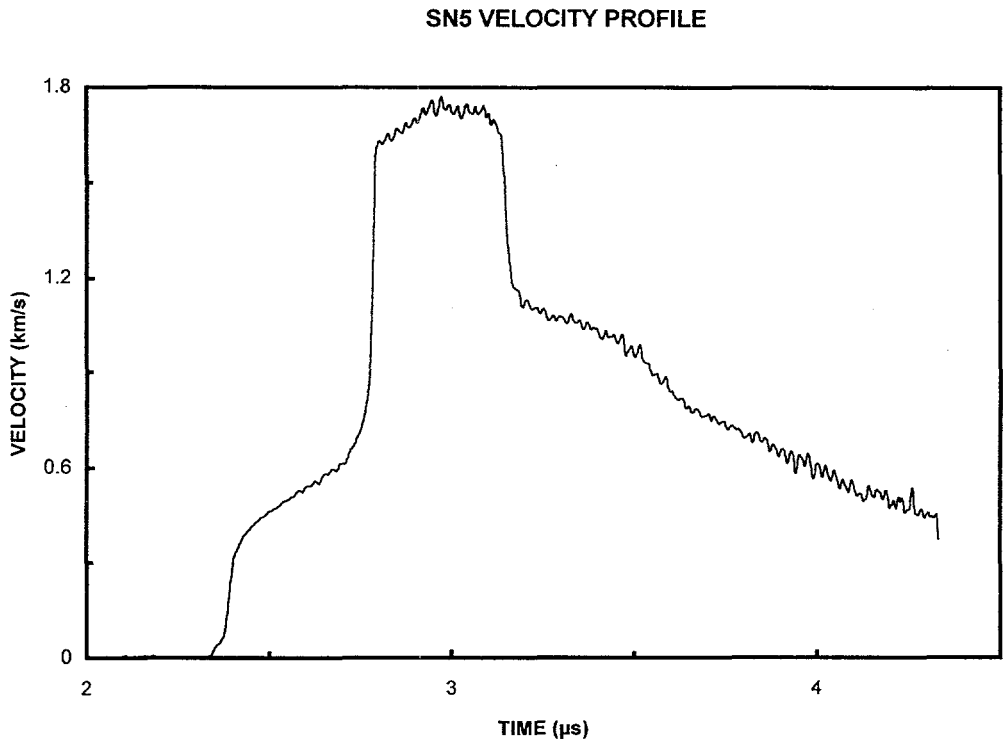

Shot Number:	SN6	**Impact Velocity:**	1.047 km/s
Test Material:	Silicon Nitride		
Supplier:	Kyocera Corporation	**Velocity Per Fringe:**	352.95 m/s

	Material	Thickness (mm)	Diameter (mm)	Density (kg/m^3)
Sample	Silicon Nitride	15.007	50.7	3126
Window	Lithium Fluoride	25.4	50.8	2640
Impactor	Silicon Nitride	4.984	50.8	3126
Backer	Polyurethane Foam	6.3	87.5	320

Comments:

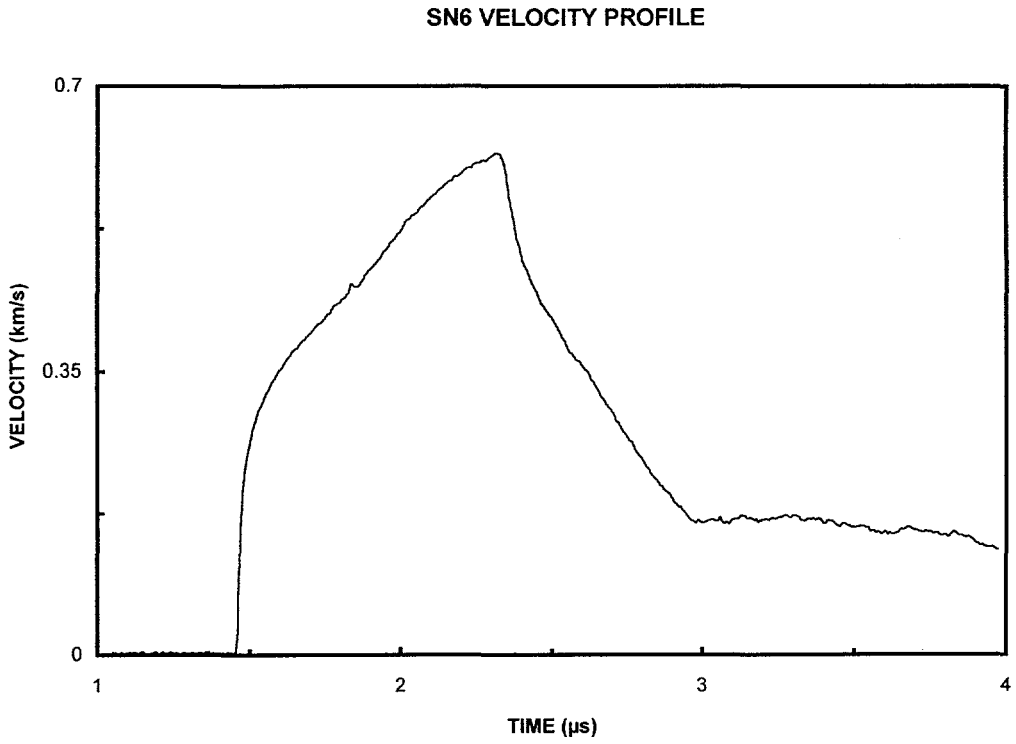

Shot Number:	SN7	**Impact Velocity:**	1.059 km/s
Test Material:	Silicon Nitride		
Supplier:	Kyocera Corporation	**Velocity Per Fringe:**	352.95 m/s

	Material	Thickness (mm)	Diameter (mm)	Density (kg/m^3)
Sample	Silicon Nitride	10.016	50.8	3126
Window	Lithium Flouride	25.4	38.1	2640
Impactor	Silicon Nitride	5.039	50.8	3126
Backer	Polyurethane Foam	6.3	87.5	320

Comments:

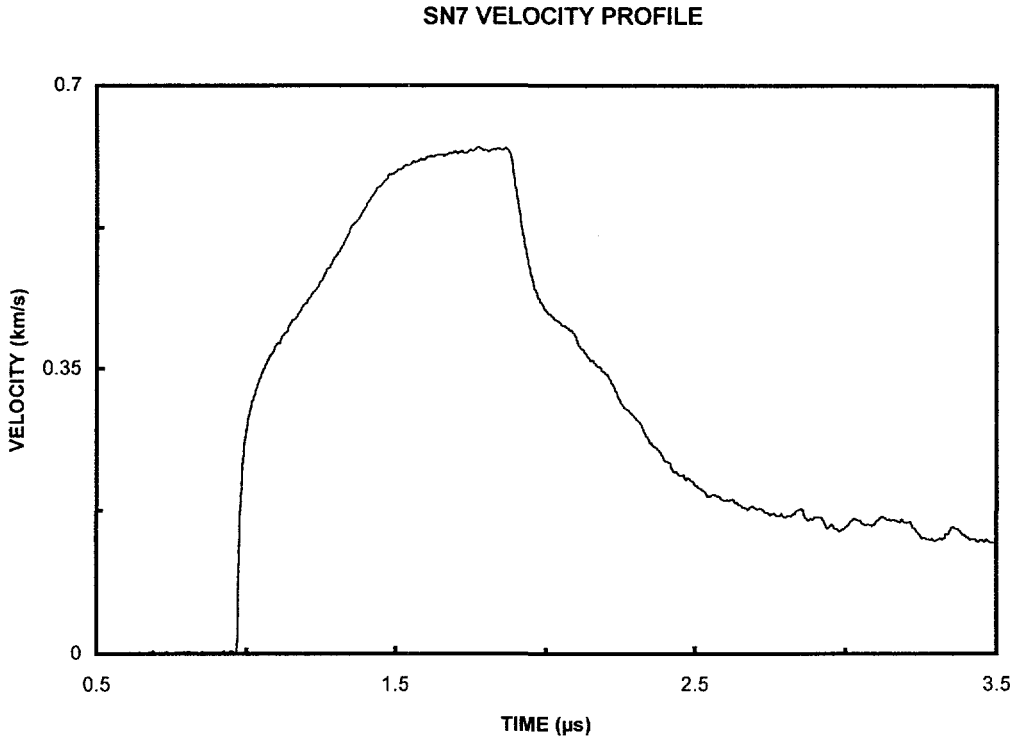

Shot Number:	SN8	**Impact Velocity:**	1.049 km/s
Test Material:	Silicon Nitride		
Supplier:	Kyocera Corporation	**Velocity Per Fringe:**	430.92 m/s

	Material	Thickness (mm)	Diameter (mm)	Density (kg/m^3)
Sample	Silicon Nitride	5.013	76.2	3130
Window	Lithium Fluoride	25.6	50.8	2640
Impactor	Silicon Nitride	5.008	87.5	3130
Backer	Polyurethane Foam	7.8	87.5	319

Comments:

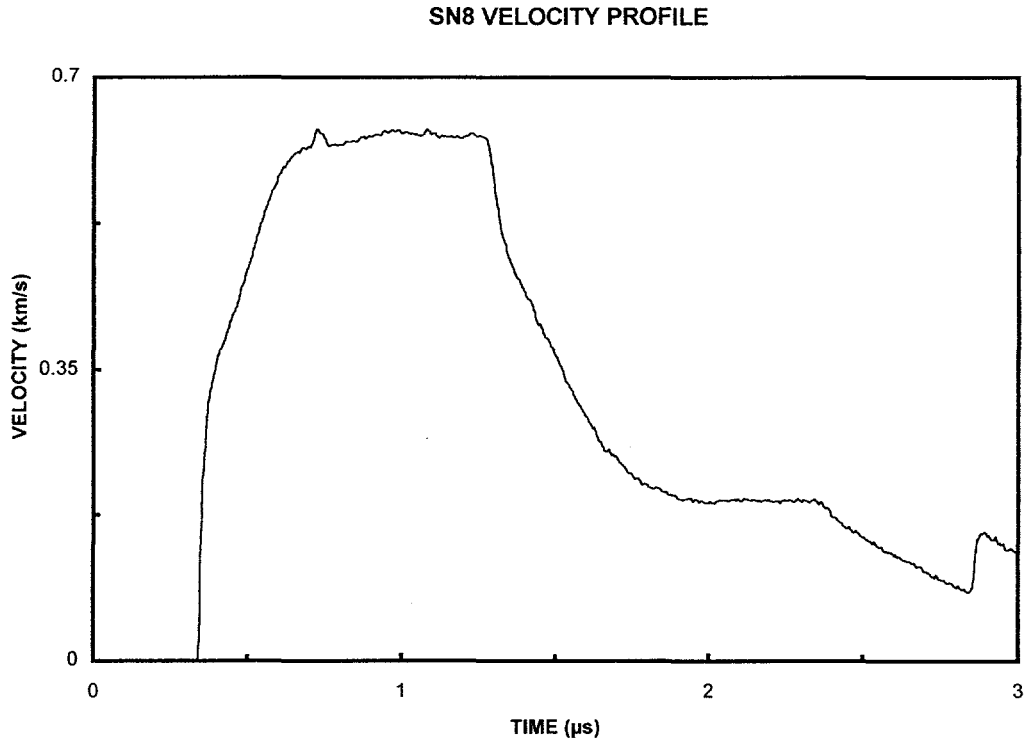

8. Titanium Diboride Ceramics

Titanium diboride is a hexagonal crystal of the AlB_2 type which, in the polycrystalline ceramic form, exhibits some unusual shock properties. Extensive Hugoniot data for titanium diboride was reported in the study of Gust, et al. (1973). A two-yield process has been reported in the compressive-wave features of titanium diboride [Kipp and Grady, 1989]. Although the possibility of a phase-transition that causes one or the other of the compressive features to occur cannot be ruled out [Grady, 1992a,b], more recent studies lean toward a mechanical explanation for these behaviors [Dandekar and Benfanti, 1993]. Both dislocation and microfracture features were observed in shock-recovered samples of titanium diboride [Vanderwalker and Croft, 1988; Vanderwalker, 1989; Winkler and Stilp, 1992; Grady and Wise, 1993].

Titanium diboride ceramics from several suppliers were tested for this report. This testing of different materials–supplied by separate manufacturers–offered a valuable perspective of the dependence of the shock features in titanium diboride, as related to their differing chemistries and microstructures. The first material tested was supplied and produced by Eagle Picher Industries. This material has a nominal grain size of about 12 μm, and both SEM analysis and density measurements indicate several percent of porosity for this ceramic. Cercom Incorporated provided and produced the second titanium diboride ceramic tested. Density for this second material is slightly higher, and the nominal grain size is about 30 μm. Another titanium diboride ceramic that was tested was a hot-pressed material produced by Ceradyne Incorporated, and it is the same material tested by Dandekar and Benfanti (1993). Lastly, one shock-compression experiment was performed on the titanium diboride ceramic that Winkler and Stilp (1992) studied.

The first two shock profile experiments on titanium diboride ceramic were performed on the Eagle Picher material (TB1 and TB19), and they were first reported in Kipp and Grady (1989). One further experiment on the Eagle Picher material (TB10) achieved a significantly higher shock pressure using a tantalum impact plate.

A variety of wave-profile experiments were performed on the Cercom titanium diboride (TB2 through TB9 with TB11, TB17, TB18, TB20, and TB21). In particular, tests TB2 and TB3 were performed at the same impact velocity on different thicknesses of ceramic samples, and they provided data on wave evolution with propagation distance. Tests TB4, TB9, TB11, TB20, and TB21 achieve shock amplitudes above the first compression-softening anomally but below the second. Several of the tests, including TB4, TB7, TB8, TB9, and TB11, were configured to provide spall strength data. Test TB8 was clearly the least successful of these efforts.

The ceramic samples in tests TB17 and TB18 were machined so that shock propagation was orthogonal to the cylindrical axis of the received samples. These samples were found to exhibit substantial elastic anisotropy, with longitudinal velocities along the axis of 10.79 km/s and across the axis of 11.83 km/s. These tests were conducted to investigate for corresponding strength anisotropy.

Tests TB12 through TB15 provide high pressure compression and release profiles on the Ceradyne ceramic, complementing the data reported by Dandekar and Benfanti (1993). Test TB16 was performed on a titanium diboride ceramic provided by the Ernst-Mach Institute, and it was specifically peformed to demonstrate a three-wave structure in the ceramic that was studied by Winkler and Stilp (1992). These latter data are discussed further in Grady and Wise (1993).

Shot Number:	TB1	**Impact Velocity:**	2.113 km/s
Test Material:	Titanium Diboride		
Supplier:	Eagle Picher Industries	**Velocity Per Fringe:**	430.92 m/s

	Material	Thickness (mm)	Diameter (mm)	Density (kg/m^3)
Sample	Titanium Diboride	10.747	69.2	4452
Window	Lithium Fluoride	25.4	50.8	2640
Impactor	Titanium Diboride	3.337	69.2	4452
Backer	Polyurethane Foam	6.0	87.5	640

Comments:

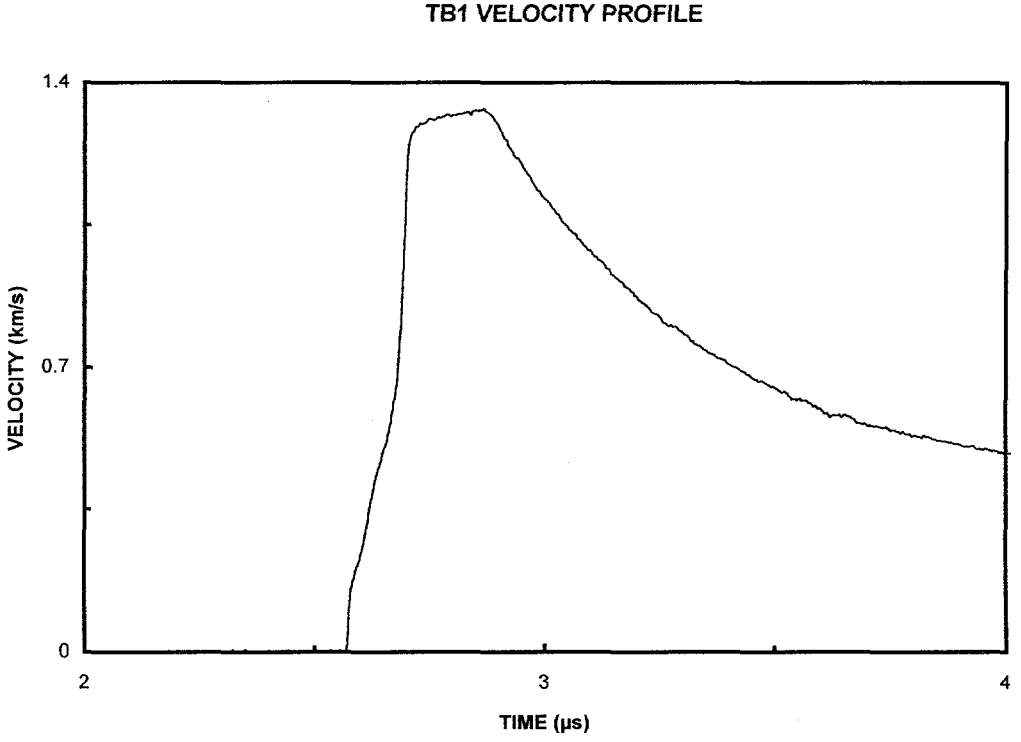

Shot Number:	TB2	**Impact Velocity:**	1.503 km/s
Test Material:	Titanium Diboride		
Supplier:	Cercom	**Velocity Per Fringe:**	430.92 m/s

	Material	Thickness (mm)	Diameter (mm)	Density (kg/m^3)
Sample	Titanium Diboride	5.011	76.2	4509
Window	Lithium Fluoride	25.4	50.8	2640
Impactor	Titanium Diboride	2.501	76.2	4509
Backer	Polyurethane Foam	6.0	87.5	320

Comments: Tests TB2 and TB3 were performed at the same impact velocity, but they had different sample thicknesses and they show evolution of the compressive wave.

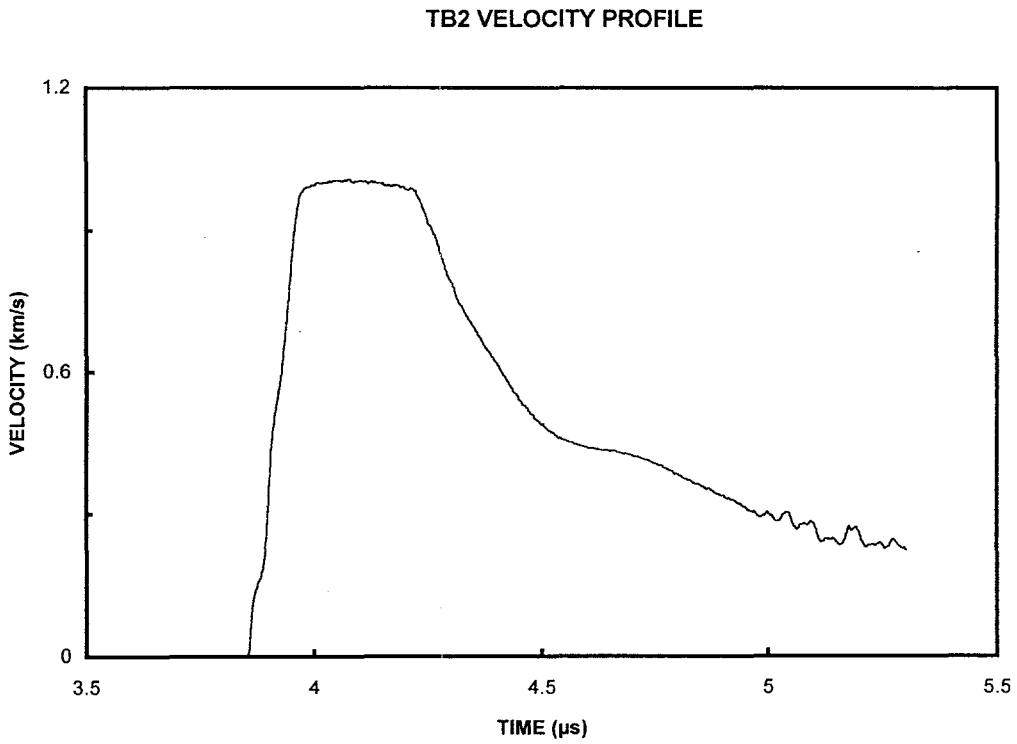

Shot Number:	TB3	**Impact Velocity:**	1.503 km/s
Test Material:	Titanium Diboride		
Supplier:	Cercom	**Velocity Per Fringe:**	430.92 m/s

	Material	Thickness (mm)	Diameter (mm)	Density (kg/m^3)
Sample	Titanium Diboride	10.097	76.2	4509
Window	Lithium Fluoride	25.4	50.8	2640
Impactor	Titanium Diboride	5.146	76.2	4509
Backer	Polyurethane Foam	6.0	87.5	320

Comments:

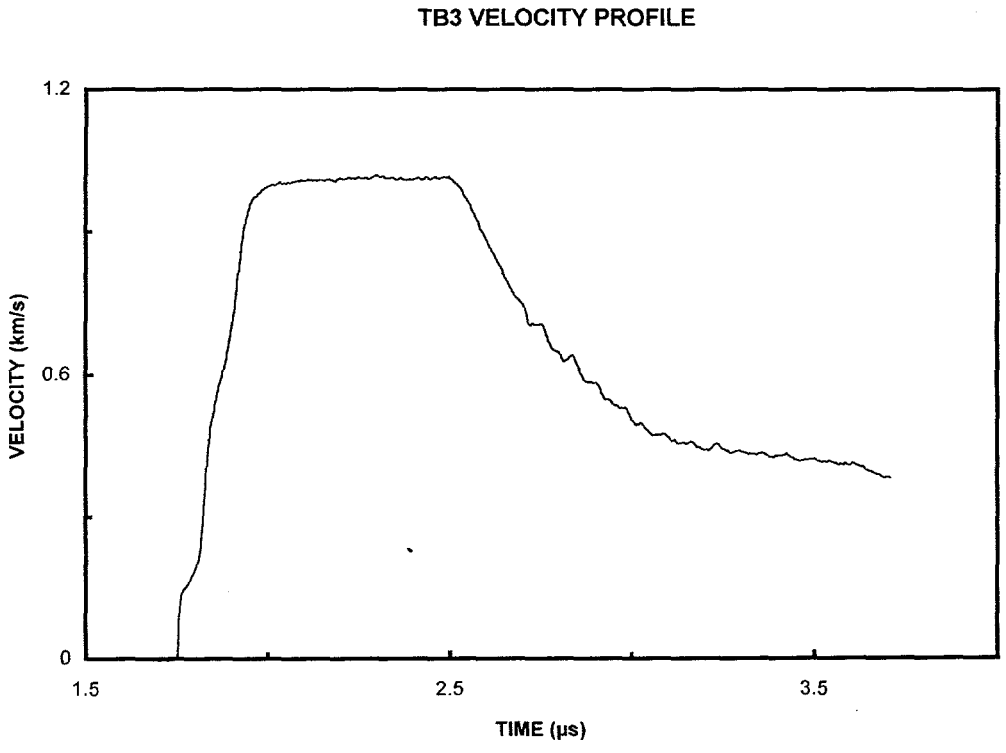

Shot Number:	TB4	**Impact Velocity:**	0.367 km/s
Test Material:	Titanium Diboride		
Supplier:	Cercom	**Velocity Per Fringe:**	121.34 m/s

	Material	Thickness (mm)	Diameter (mm)	Density (kg/m^3)
Sample	Titanium Diboride	10.091	76.2	4509
Window	PMMA	25.4	50.8	1186
Impactor	Titanium Diboride	4.899	76.2	4509
Backer	Polyurethane Foam	6.0	87.5	320

Comments: Spall experiment

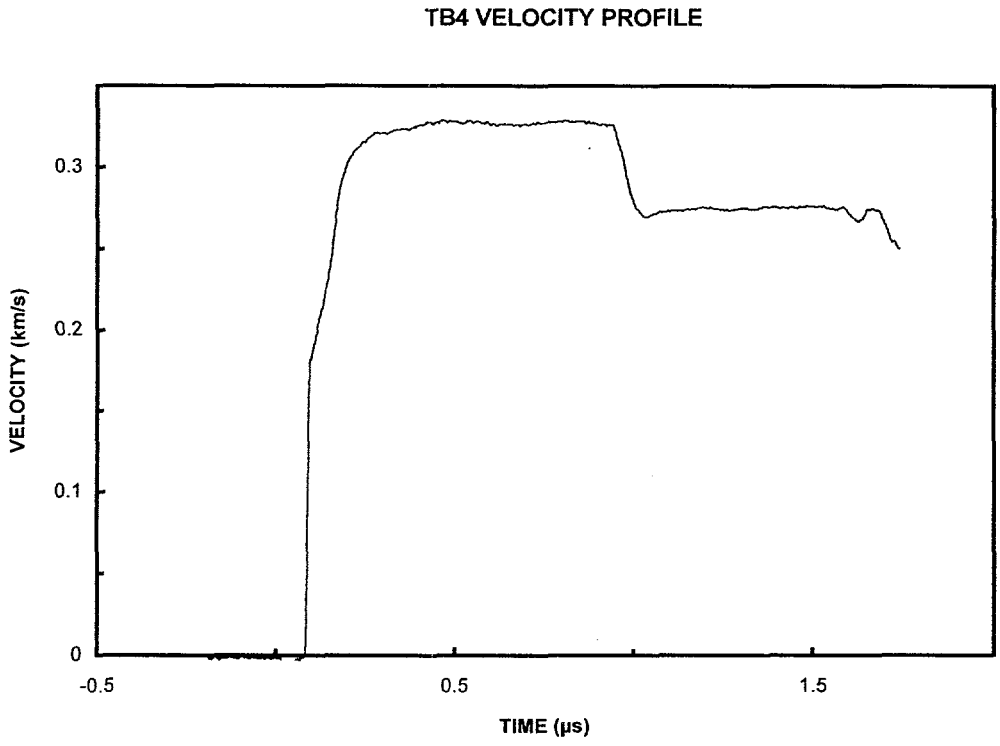

Shot Number:	TB5	**Impact Velocity:**	1.112 km/s
Test Material:	Titanium Diboride		
Supplier:	Cercom	**Velocity Per Fringe:**	430.92 m/s

	Material	Thickness (mm)	Diameter (mm)	Density (kg/m^3)
Sample	Titanium Diboride	10.193	76.2	4509
Window	Lithium Fluoride	25.4	50.8	2640
Impactor	Titanium Diboride	5.100	76.2	4509
Backer	Polyurethane Foam	6.0	87.5	320

Comments:

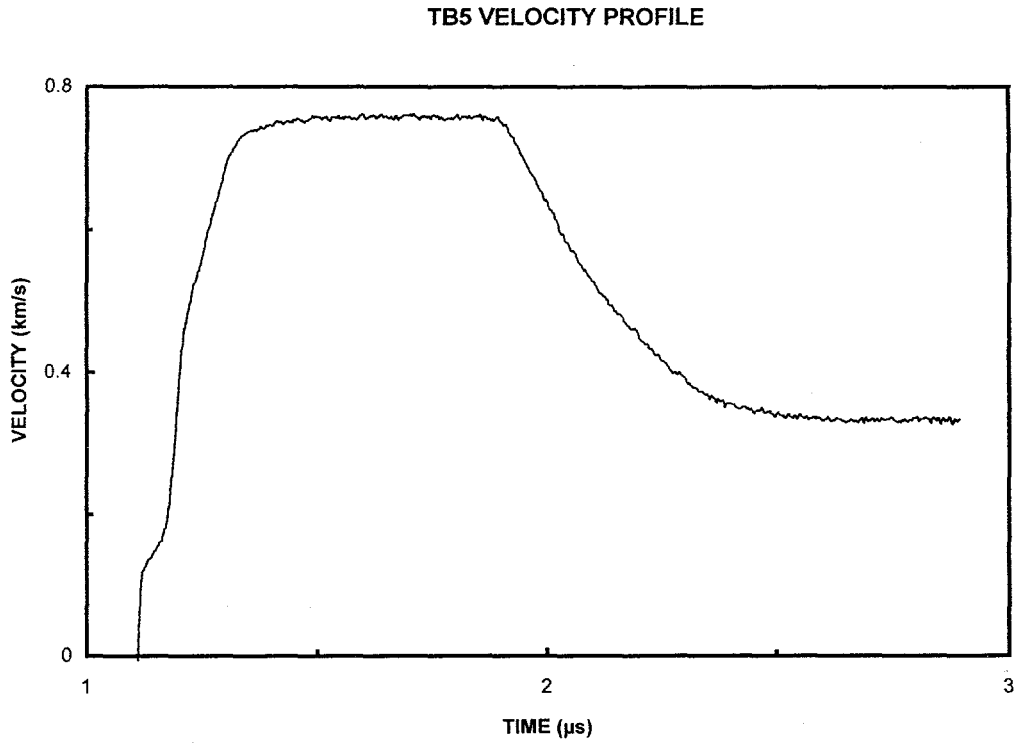

Shot Number:	TB6	**Impact Velocity:**	2.293 km/s
Test Material:	Titanium Diboride		
Supplier:	Cercom	**Velocity Per Fringe:**	430.92 m/s

	Material	Thickness (mm)	Diameter (mm)	Density (kg/m^3)
Sample	Titanium Diboride	10.165	76.2	4509
Window	Lithium Fluoride	25.4	50.8	2640
Impactor	Titanium Diboride	5.161	76.2	4509
Backer	Polyurethane Foam	6.0	87.5	640

Comments:

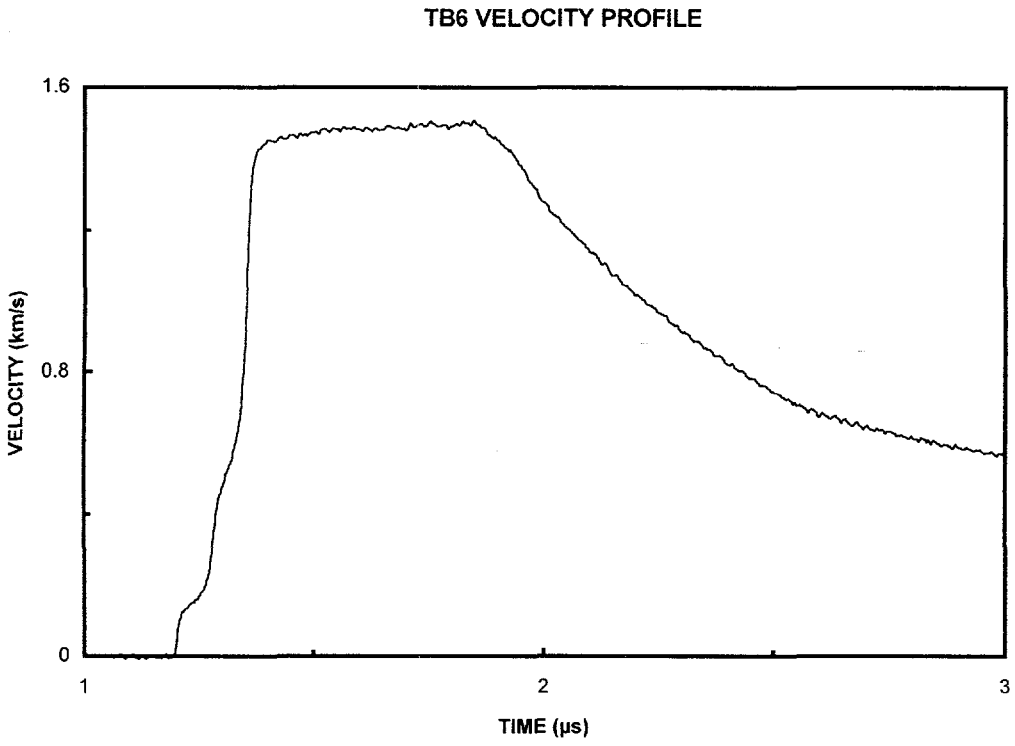

Shot Number:	TB7	**Impact Velocity:**	0.741 km/s
Test Material:	Titanium Diboride		
Supplier:	Cercom	**Velocity Per Fringe:**	121.34 m/s

	Material	Thickness (mm)	Diameter (mm)	Density (kg/m^3)
Sample	Titanium Diboride	10.088	76.2	4509
Window	PMMA	25.4	50.8	1186
Impactor	PMMA	2.018	87.5	1186
Backer	Polyurethane Foam	6.0	87.5	160

Comments: Spall experiment

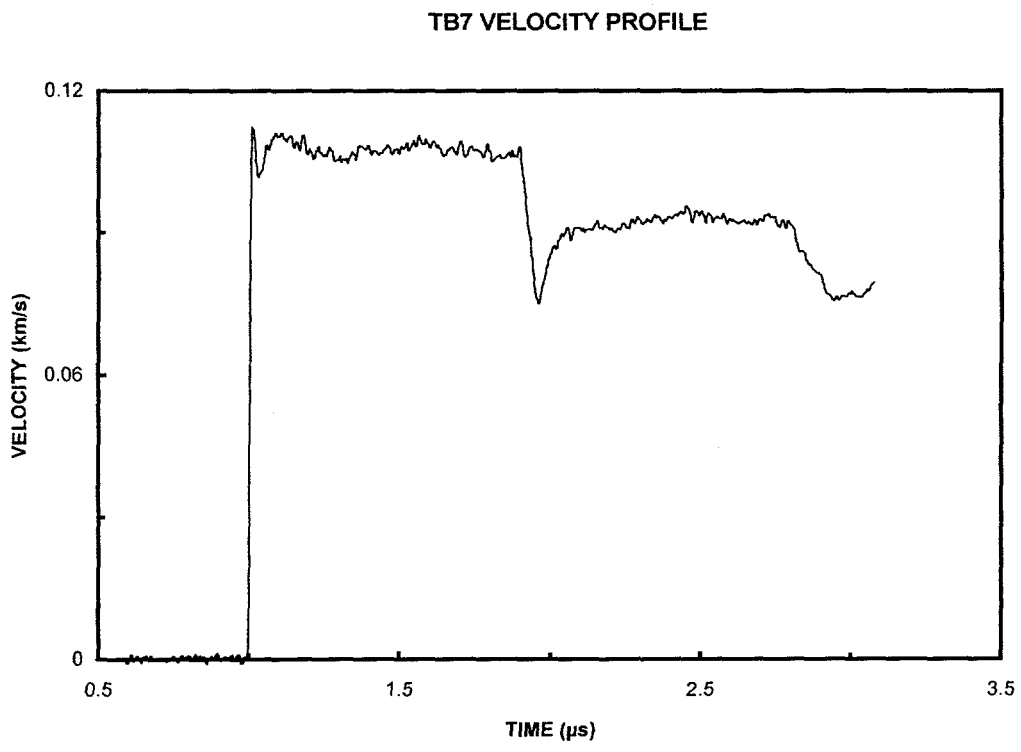

Shot Number:	TB8	**Impact Velocity:**	1.155 km/s
Test Material:	Titanium Diboride		
Supplier:	Cercom	**Velocity Per Fringe:**	121.34 m/s

	Material	Thickness (mm)	Diameter (mm)	Density (kg/m^3)
Sample	Titanium Diboride	10.347	76.2	4509
Window	PMMA	24.1	50.8	1186
Impactor	PMMA	2.000	87.5	1186
Backer	Polyurethane Foam	8.0	87.5	160

Comments: The wave profile resulting from this experiment is not understood.

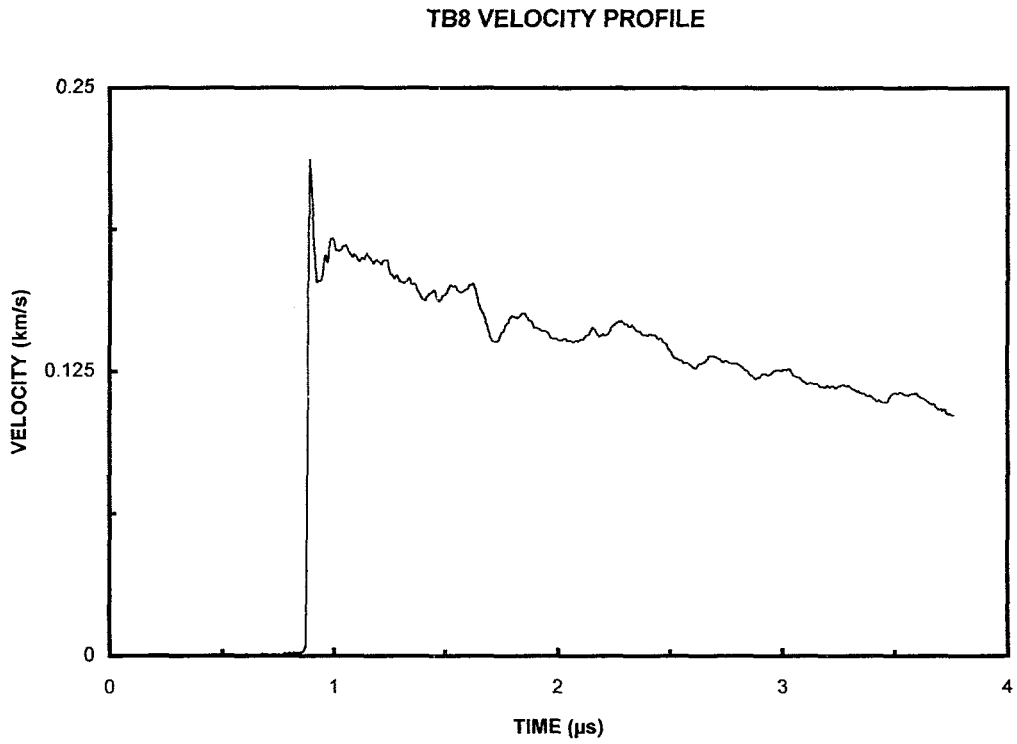

Shot Number:	TB9	**Impact Velocity:**	1.439 km/s
Test Material:	Titanium Diboride		
Supplier:	Cercom	**Velocity Per Fringe:**	121.34 ms

	Material	Thickness (mm)	Diameter (mm)	Density (kg/m^3)
Sample	Titanium Diboride	10.246	10.246	4509
Window	PMMA	24.21	50.8	1186
Impactor	PMMA	2.002	87.5	1186
Backer	Polyurethane Foam	8.0	87.5	160

Comments: Spall experiment

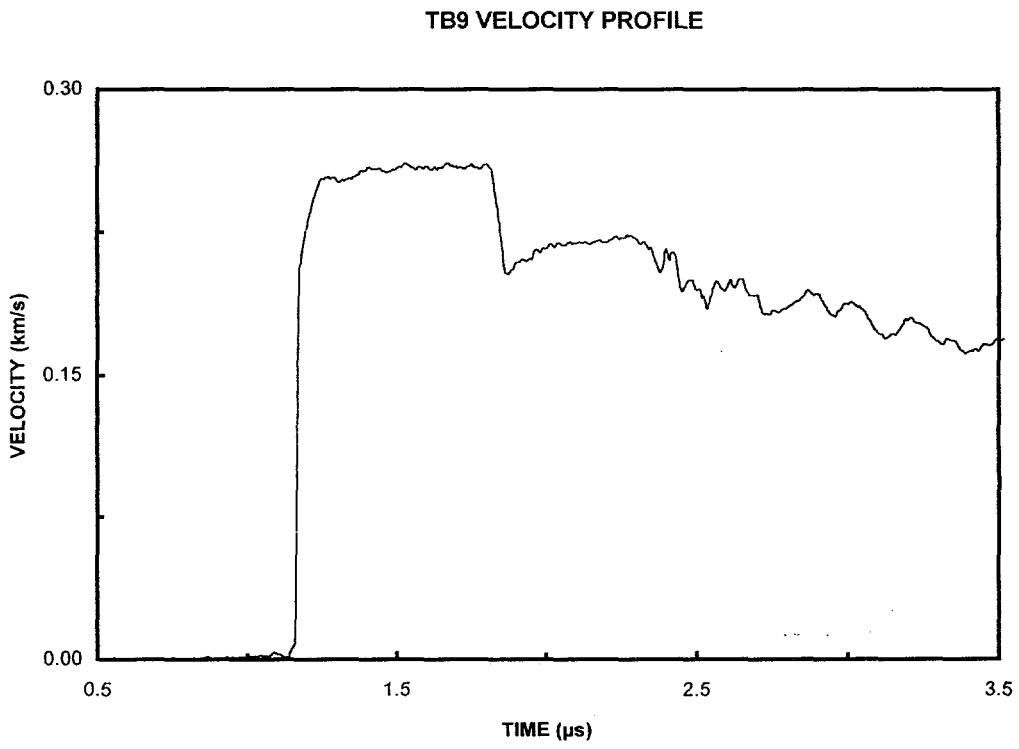

Shot Number:	TB10	**Impact Velocity:**	2.253 km/s
Test Material:	Titanium Diboride		
Supplier:	Eagle Picher Industries	**Velocity Per Fringe:**	681.52 m/s

	Material	Thickness (mm)	Diameter (mm)	Density (kg/m^3)
Sample	Titanium Diboride	10.055	76.2	4452
Window	Lithium Fluoride	25.4	50.8	2640
Impactor	Tantalum	1.506	87.5	16771
Backer	Polyurethane Foam	6.0	87.5	640

Comments:

TB10 VELOCITY PROFILE

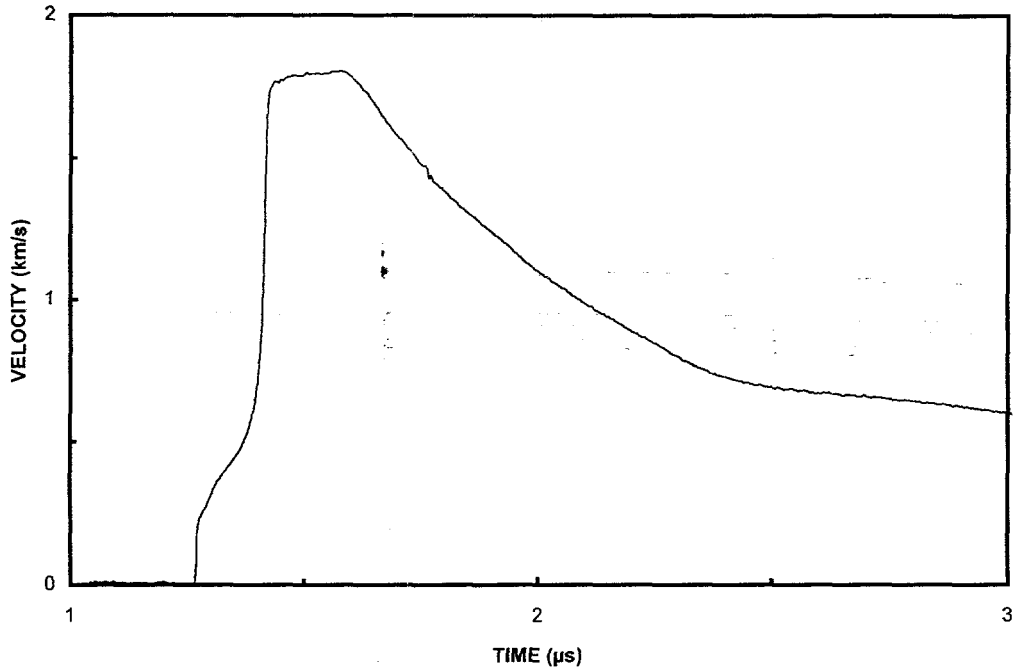

Shot Number:	TB11	**Impact Velocity:**	1.708 km/s
Test Material:	Titanium Diboride		
Supplier:	Cercom	**Velocity Per Fringe:**	94.76 m/s

	Material	Thickness (mm)	Diameter (mm)	Density (kg/m^3)
Sample	Titanium Diboride	10.126	76.2	4509
Window	Lithium Fluoride	25.4	50.8	2640
Impactor	PMMA	2.001	87.5	1186
Backer	Polyurethane Foam	7.9	87.5	139

Comments:

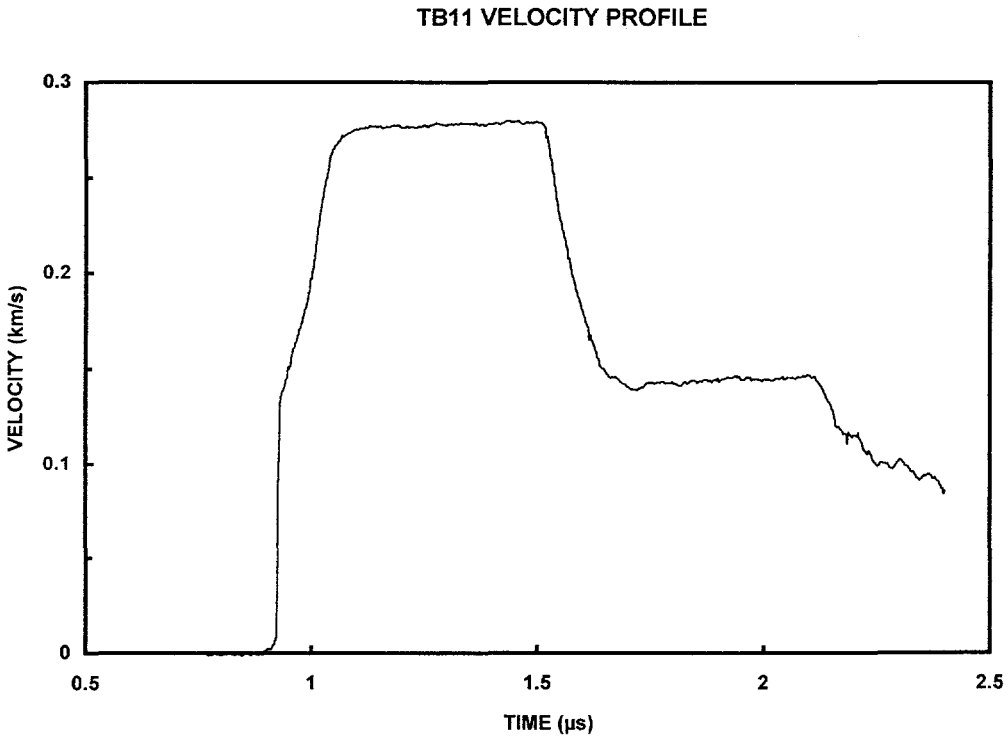

Shot Number:	TB12	**Impact Velocity:**	1.073 km/s
Test Material:	Titanium Diboride		
Supplier:	Ceradyne	**Velocity Per Fringe:**	551.36 m/s

	Material	Thickness (mm)	Diameter (mm)	Density (kg/m^3)
Sample	Titanium Diboride	9.039	63.5	4490
Window	Lithium Fluoride	18.9	38.3	2640
Impactor	Titanium Diboride	5.012	63.5	4490
Backer	Polyurethane Foam	7.9	87.5	394

Comments:

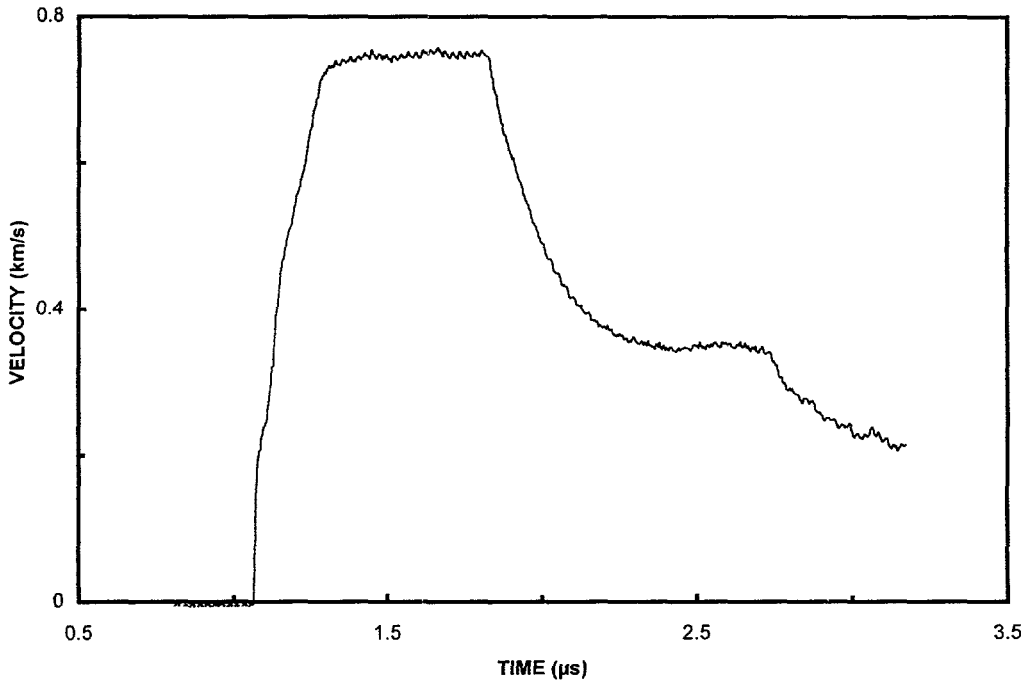

Shot Number:	TB13	**Impact Velocity:**	1.805 km/s
Test Material:	Titanium Diboride		
Supplier:	Ceradyne	**Velocity Per Fringe:**	681.52 m/s

	Material	Thickness (mm)	Diameter (mm)	Density (kg/m^3)
Sample	Titanium Diboride	9.028	63.5	4490
Window	Lithium Fluoride	18.9	38.1	2640
Impactor	Titanium Diboride	5.008	63.5	4490
Backer	Polyurethane Foam	7.9	87.5	419

Comments:

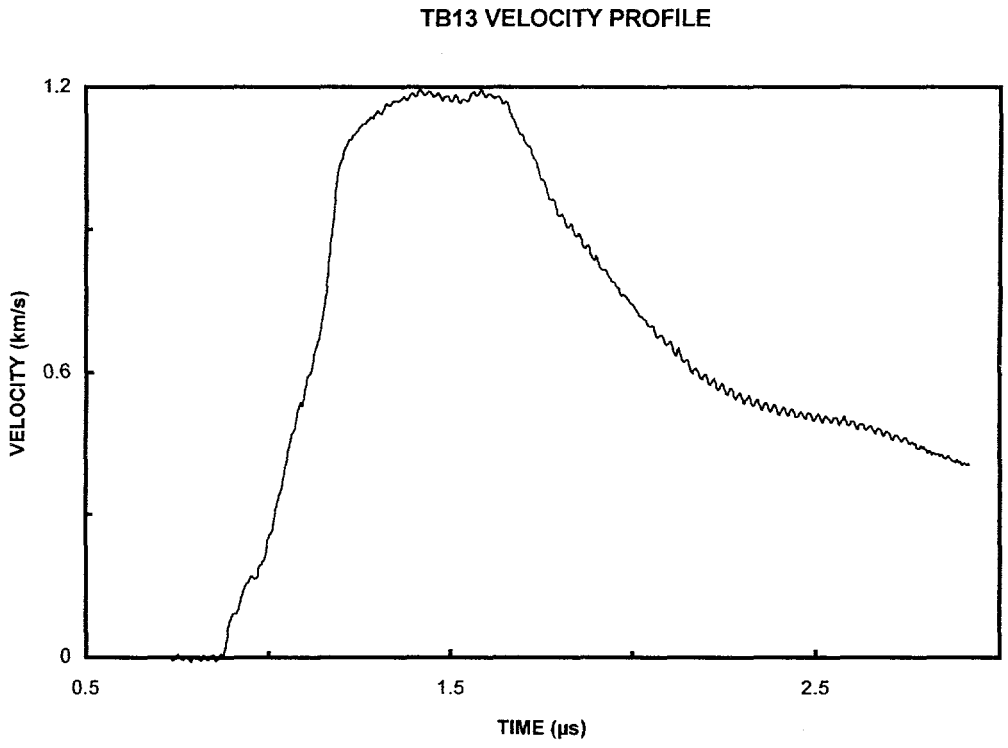

Shot Number:	TB14	**Impact Velocity:**	1.972 km/s
Test Material:	Titanium Diboride		
Supplier:	Ceradyne	**Velocity Per Fringe:**	681.52 m/s

	Material	Thickness (mm)	Diameter (mm)	Density (kg/m^3)
Sample	Titanium Diboride	9.031	63.5	4490
Window	Lithium Fluoride	19.024	38.1	2640
Impactor	Tantalum	1.507	87.5	16534
Backer	PMMA	6.340	87.5	1187

Comments:

TB14 VELOCITY PROFILE

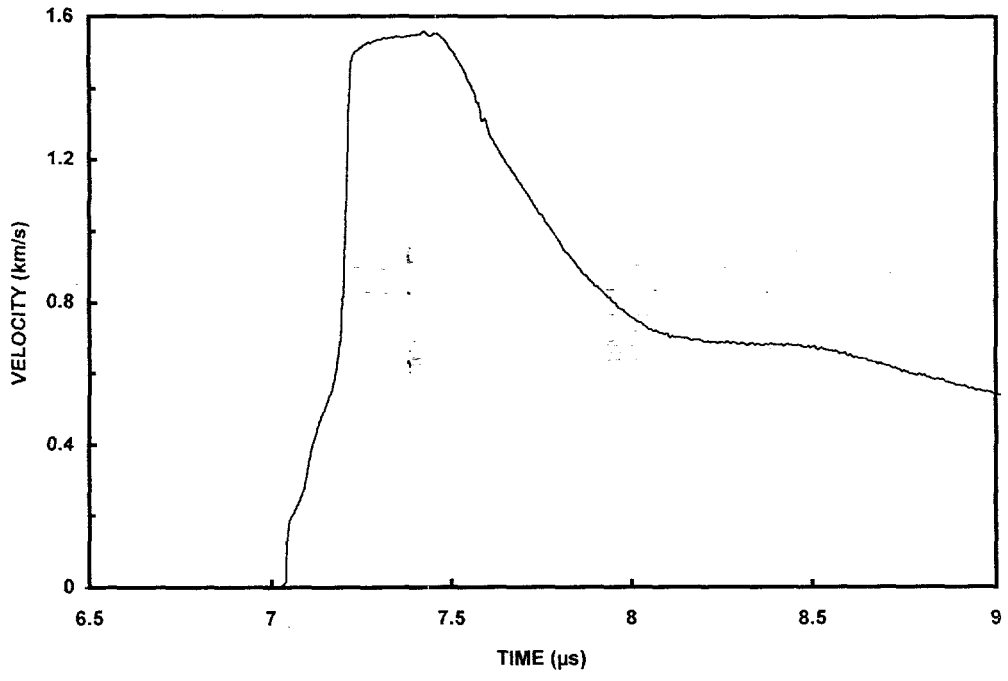

Shot Number:	TB15	**Impact Velocity:**	2.221 km/s
Test Material:	Titanium Diboride		
Supplier:	Ceradyne	**Velocity Per Fringe:**	681.52 m/s

	Material	Thickness (mm)	Diameter (mm)	Density (kg/m^3)
Sample	Titanium Diboride	9.036	63.5	4490
Window	Lithium Fluoride	19.12	38.1	2640
Impactor	Tungsten	1.51	87.5	19200
Backer	PMMA	6.34	87.5	1186

Comments:

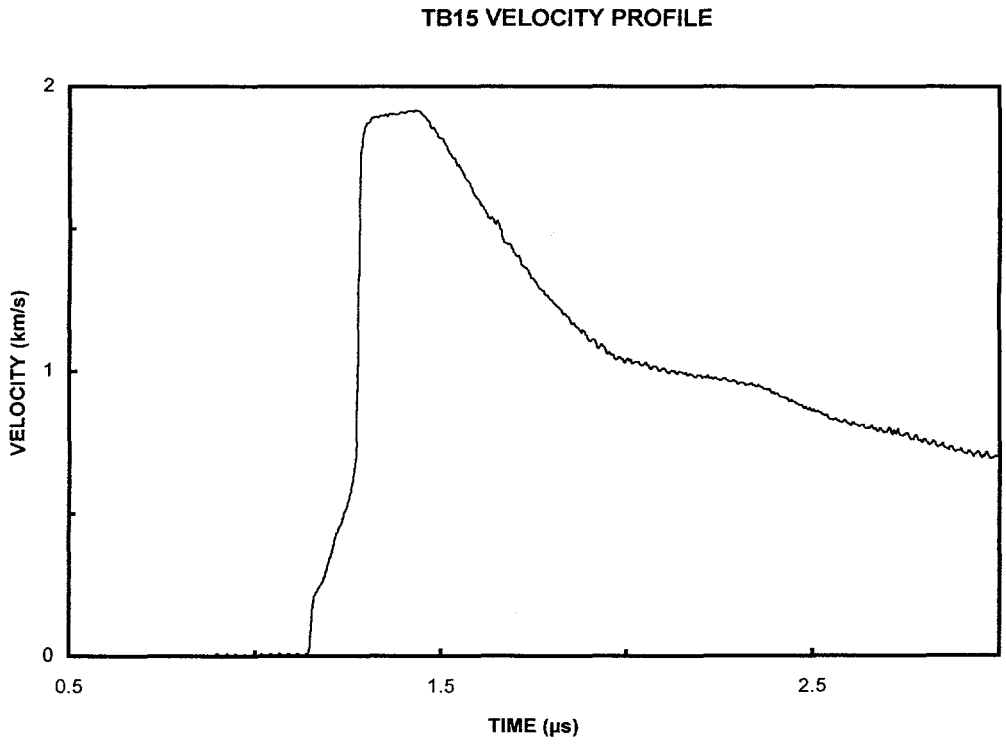

Shot Number:	TB16	**Impact Velocity:**	1.458 km/s
Test Material:	Titanium Diboride		
Supplier:	Ernst-Mach Institute	**Velocity Per Fringe:**	681.52 m/s

	Material	Thickness (mm)	Diameter (mm)	Density (kg/m^3)
Sample	Titanium Diboride	4.521	20.7	4380
Window	Lithium Fluoride	19.2	19.0	2640
Impactor	Copper OFHC	9.424	87.4	8930
Backer	n/a			

Comments:

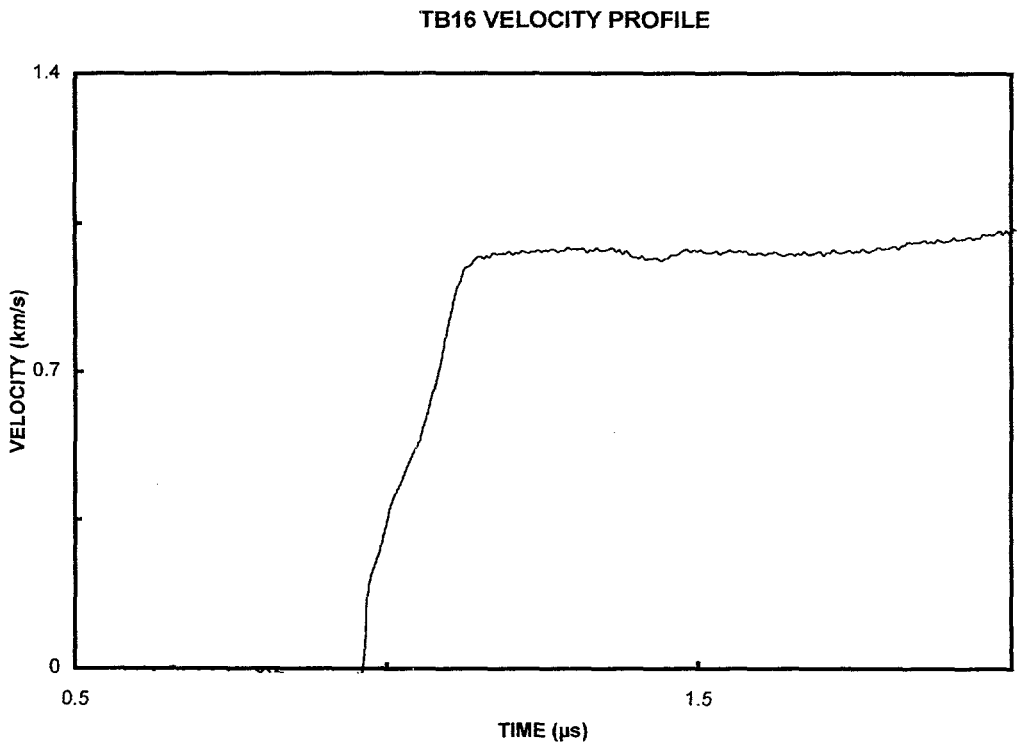

Shot Number:	TB17	**Impact Velocity:**	1.469 km/s
Test Material:	Titanium Diboride		
Supplier:	Cercom	**Velocity Per Fringe:**	430.92 m/s

	Material	Thickness (mm)	Diameter (mm)	Density (kg/m^3)
Sample	Titanium Diboride	5.016	40.0	4509
Window	Lithium Fluoride	19.0	25.4	2640
Impactor	Titanium Diboride	2.985	40.0	4509
Backer	Polyurethane Foam	8.0	87.5	420

Comments: Tests TB17 and TB18 were prepared and shock-loaded perpendicular to the cylindrical axis of the received sample

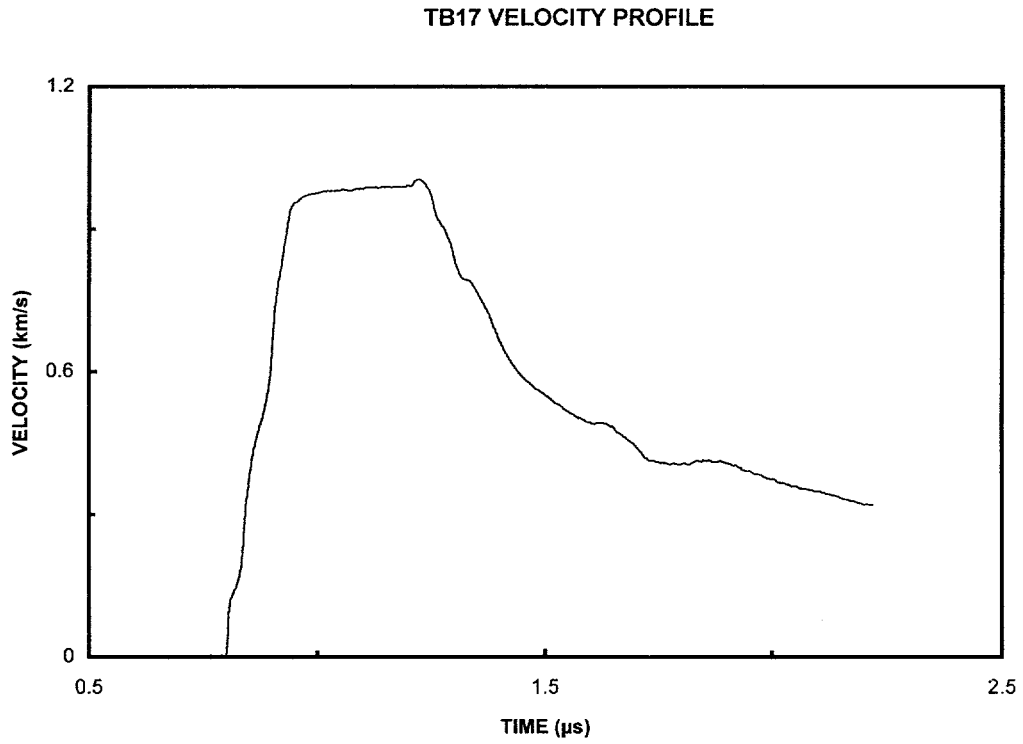

Shot Number:	TB18	**Impact Velocity:**	1.110 km/s
Test Material:	Titanium Diboride		
Supplier:	Cercom	**Velocity Per Fringe:**	430.92 m/s

	Material	Thickness (mm)	Diameter (mm)	Density (kg/m^3)
Sample	Titanium Diboride	4.906	40.1	4509
Window	Lithium Fluoride	18.9	25.4	2640
Impactor	Titanium Diboride	3.000	40.0	4509
Backer	Polyurethane Foam	8.0	87.5	390

Comments:

TB18 VELOCITY PROFILE

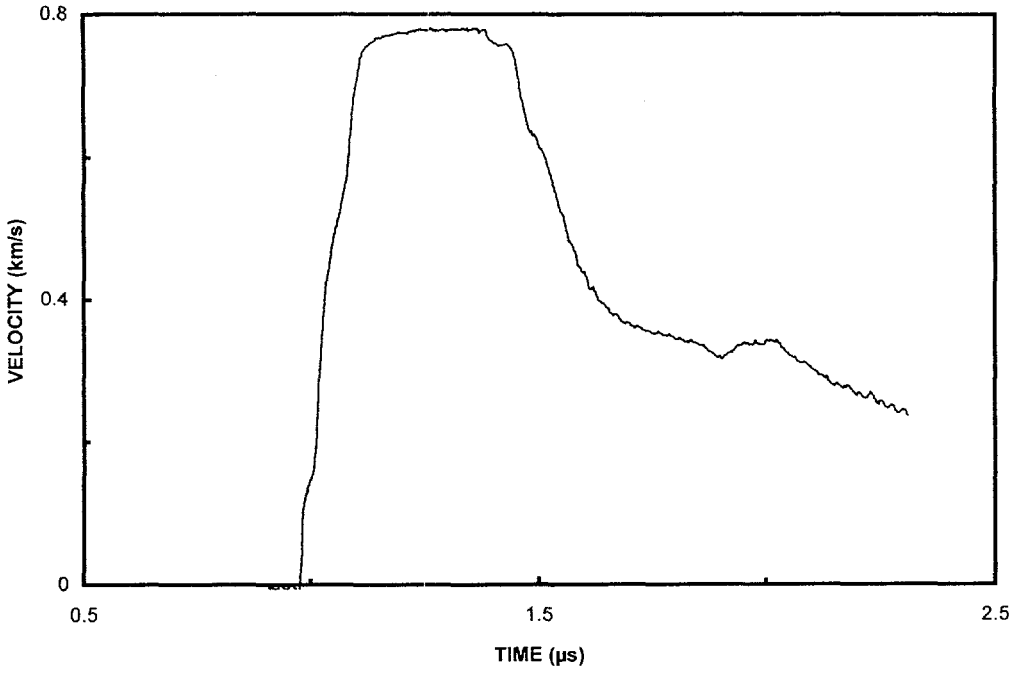

Shot Number:	TB19	**Impact Velocity:**	1.515 km/s
Test Material:	Titanium Diboride		
Supplier:	Eagle Picher	**Velocity Per Fringe:**	430.92 m/s

	Material	Thickness (mm)	Diameter (mm)	Density (kg/m^3)
Sample	Titanium Diboride	10.804	69.2	4452
Window	Lithium Fluoride	25.4	50.8	2640
Impactor	Titanium Diboride	3.972	69.2	4452
Backer	Polyurethane Foam	6.0	87.5	320

Comments:

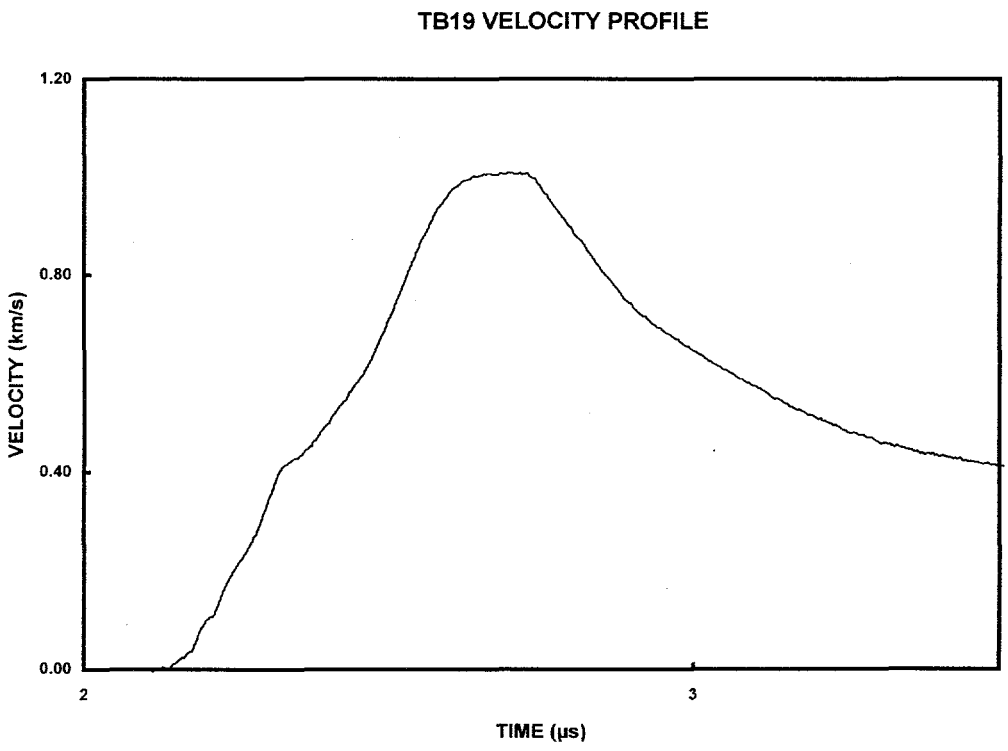

Shot Number:	TB20	**Impact Velocity:**	0.604 km/s
Test Material:	Titanium Diboride		
Supplier:	Cercom	**Velocity Per Fringe:**	197.44 m/s

	Material	Thickness (mm)	Diameter (mm)	Density (kg/m^3)
Sample	Titanium Diboride	5.356	76.2	4509
Window	Lithium Fluoride	25.4	50.8	2640
Impactor	Titanium Diboride	5.514	76.3	4509
Backer	Polyurethane Foam	6.3	87.5	330

Comments:

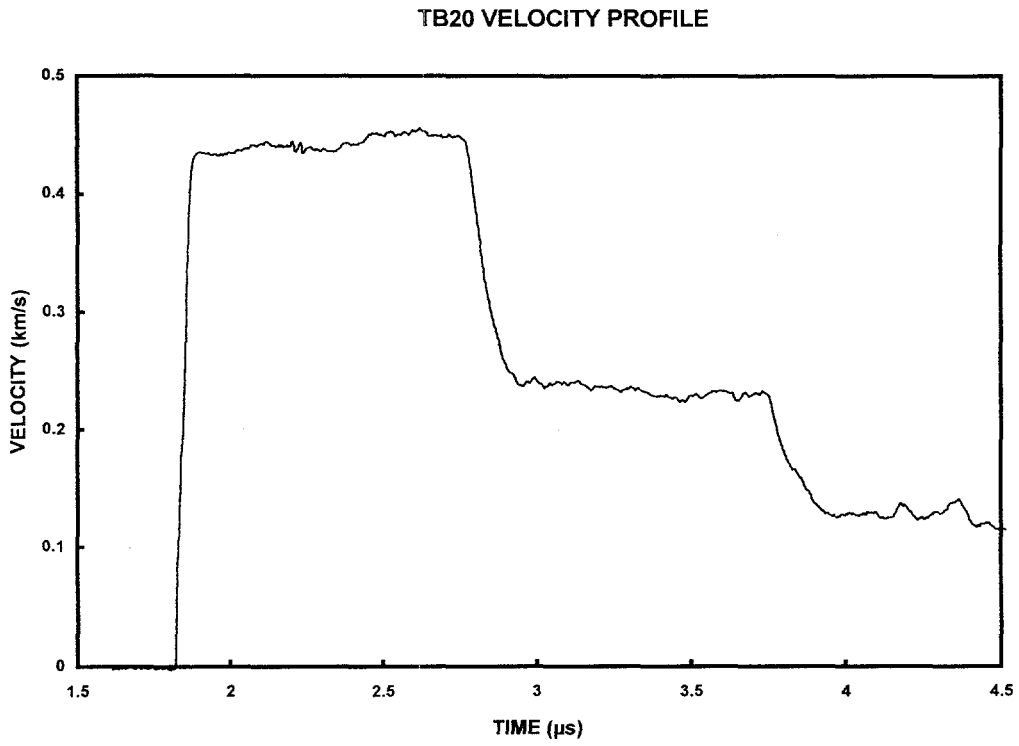

Shot Number:	TB21	**Impact Velocity:**	0.552 km/s
Test Material:	Titanium Diboride		
Supplier:	Cercom	**Velocity Per Fringe:**	155.23 m/s

	Material	Thickness (mm)	Diameter (mm)	Density (kg/m^3)
Sample	Titanium Diboride	10.352	76.3	4509
Window	Lithium Fluoride	25.4	50.8	2640
Impactor	Titanium Diboride	5.377	76.2	4509
Backer	Polyurethane Foam	6.4	87.5	340

Comments:

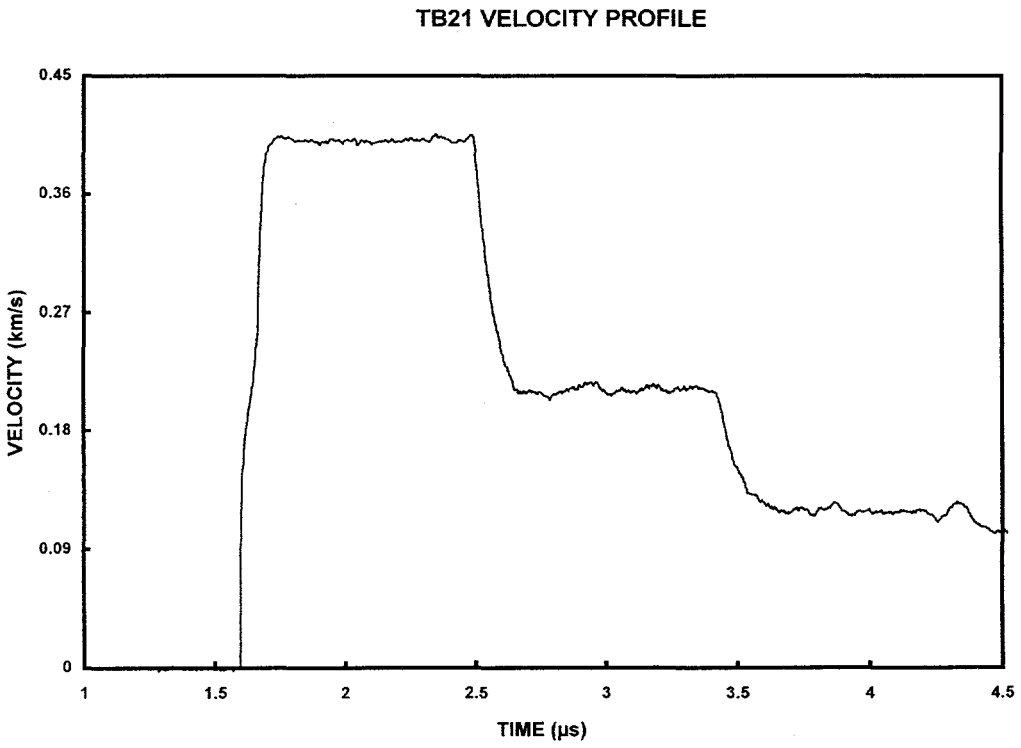

9. Tungsten Carbide Ceramics

Tungsten carbide is a high-density ceramic, typically prepared by liquid-phase sintering. It usually contains a few percent-by-weight metal content. Relatively little shock-wave data exists for this material. Early Hugoniot data for WC-5wt%Co was generated by McQueen (1968) and McQueen, et al. (1970), and it has been adequately tabulated in the LANL Shock Hugoniot Compendium [Marsh, 1980]. Also, several compression-wave profiles for tungsten carbide–using the free-surface capacitor technique–were measured by Taylor and Hopson, and this data is published in the LANL Shock Wave Profile Compendium [Morris, 1980]. Gust (1980) indicates shock Hugoniot experiments were performed at Lawrence Livermore National Laboratories; however, only a Hugoniot elastic limit is provided in this reference. Steinberg (1991) has assimilated the above data and has provided partial material property parameters in the framework of the Steinberg-Guinan model. Velocity-interferometry wave-profile and spall data which are included in this report are reported in Grady (1995).

One material tested in this study is K-68 Kennametal, reported to have a metal content of 5.7wt%Co and 1.9wt%Ta, along with minor amounts of other metals. A second tungsten carbide ceramic was extracted from 14.5mm AP(BS-41) rounds provided by Los Alamos National Laboratory. Test samples for this second material were less than 11mm in diameter, providing a challenge to the impact-test and VISAR-diagnostics technology. This material contained a 3-4wt%Ni along with minor amounts of other metals. A final tungsten carbide ceramic was prepared by Cercom Incorporated. This ceramic was a hot-pressed, nearly 100% tungsten carbide (WC), with an average grain size of 0.9 μm.

Tests WC1 and WC2 were performed on the Kennametal material, and they focused on the compression-profile and Hugoniot properties at shock-wave amplitudes, which were high relative to the Hugoniot elastic limit. Hugoniot states were slightly stiffer, but comparable to, the earlier data [McQueen, 1968; McQueen, et al., 1968].

Tests WC3 through WC6 were performed on the AP (BS-41) tungsten carbide. Only lower amplitude compression properties were investigated in tests WC3 and WC4. Spall strength properties were the focus of tests WC5 and WC6. One further test, WC7, was performed on the Kennametal ceramic, to determine comparable spall strength characteristics of this material. Pullback waves provided tensile strengths of 2.5 - 3.5 GPa for these materials. The motion anomaly in the compression profiles of WC4, WC5, and WC6 are believed to be due to an experimental problem.

Tests WC8, WC9, and WC10 examine the shock compression and spall properties of the monolithic tungsten carbide ceramic provided by Cercom. Spall strengths of this ceramic were about half of the earlier liquid-phase, sintered tungsten carbides.

Shot Number:	WC1	**Impact Velocity:**	1.141 km/s
Test Material:	Tungsten Carbide		
Supplier:	Kennametal	**Velocity Per Fringe:**	551.36 m/s

	Material	Thickness (mm)	Diameter (mm)	Density (kg/m^3)
Sample	Tungsten Carbide	6.566	63.7	14930
Window	Lithium Fluoride	25.4	50.8	2640
Impactor	Tungsten carbide	3.370	63.1	14930
Backer	PMMA	5.82	87.5	1186

Comments:

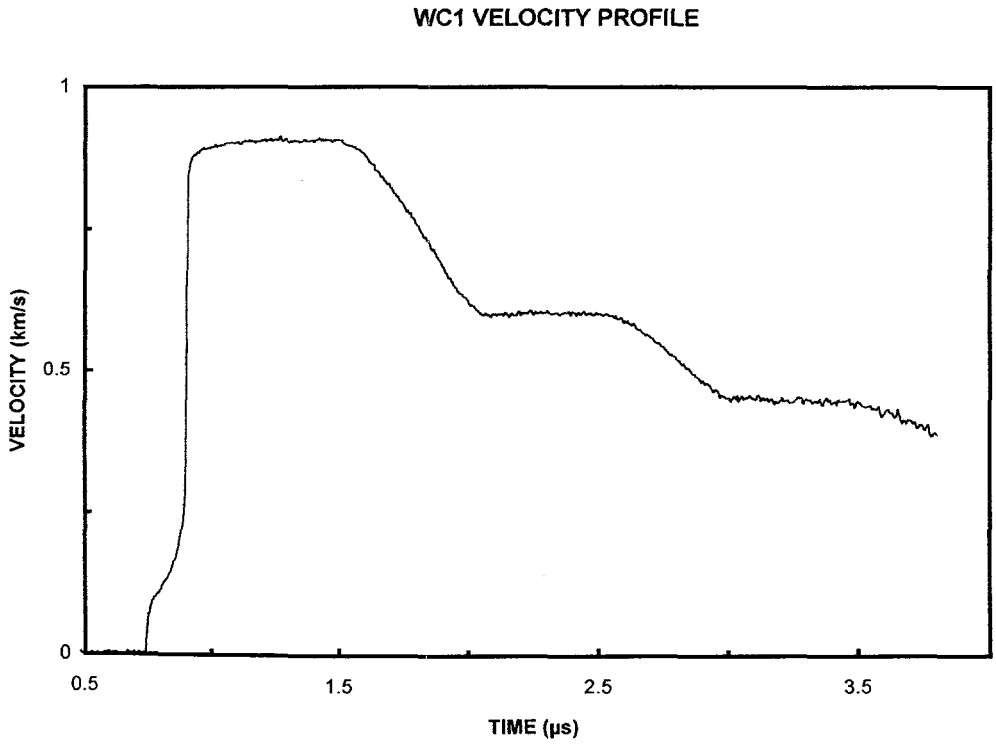

Shot Number:	WC2	**Impact Velocity:**	1.566 km/s
Test Material:	Tungsten Carbide		
Supplier:	Kennametal	**Velocity Per Fringe:**	551.36 m/s

	Material	Thickness (mm)	Diameter (mm)	Density (kg/m^3)
Sample	Tungsten Carbide	6.542	63.7	14930
Window	Lithium Fluoride	25.4	50.8	2640
Impactor	Tungsten carbide	3.363	63.0	14930
Backer	PMMA	5.91	87.5	1183

Comments:

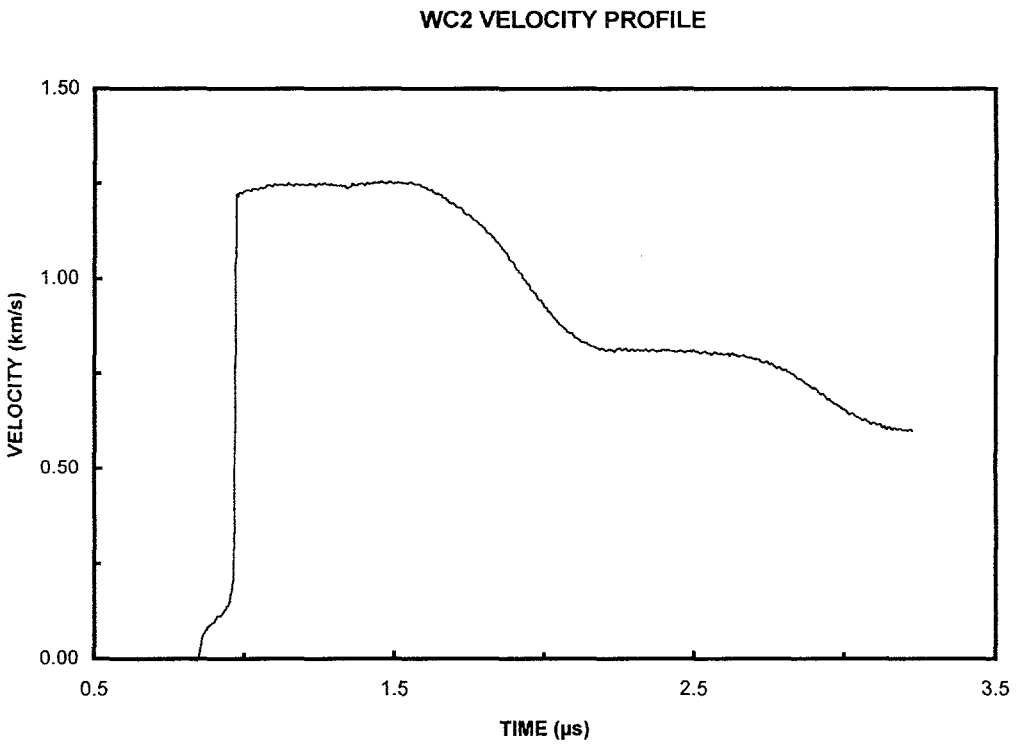

Shot Number:	WC3	**Impact Velocity:**	1.039 km/s
Test Material:	Tungsten Carbide		
Supplier:	LANL	**Velocity Per Fringe:**	197.44 m/s

	Material	Thickness (mm)	Diameter (mm)	Density (kg/m^3)
Sample	Tungsten Carbide	2.985	10.9	14910
Window	Lithium Fluoride	9.542	19.0	2640
Impactor	Aluminum 6061-T6	12.87	87.5	2703
Backer	n/a			

Comments: Material for this experiment was provided by Los Alamos National Laboratories (LANL).

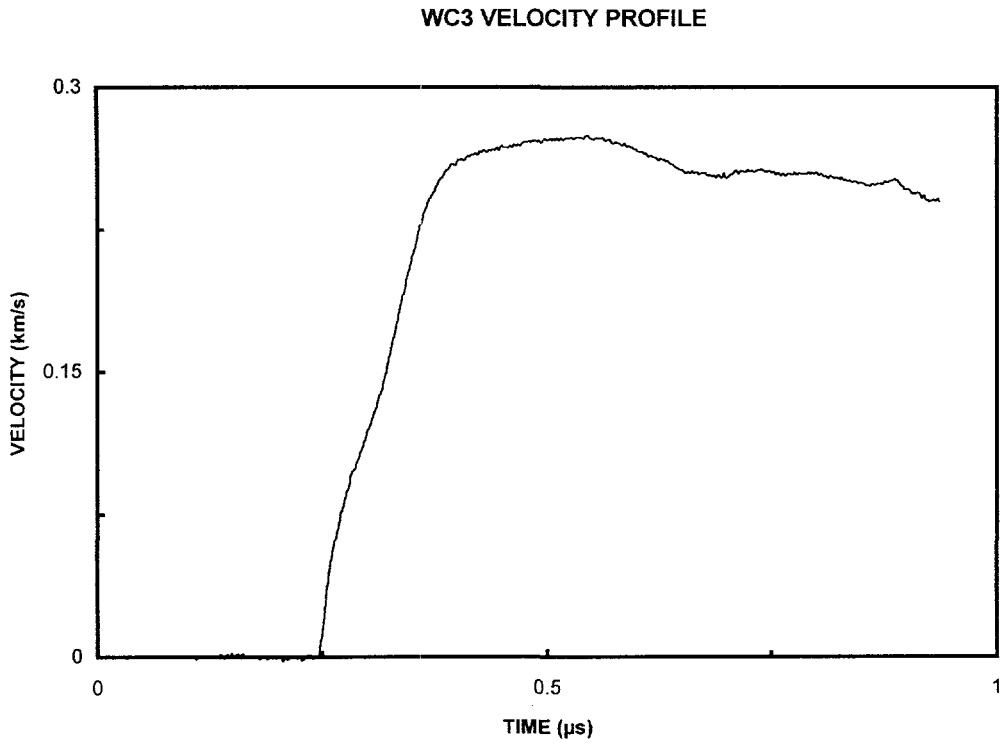

Shot Number:	WC4	**Impact Velocity:**	0.687 km/s
Test Material:	Tungsten Carbide		
Supplier:	LANL	**Velocity Per Fringe:**	197.44 m/s

	Material	**Thickness (mm)**	**Diameter (mm)**	**Density (kg/m^3)**
Sample	Tungsten Carbide	2.994	10.8	14910
Window	Lithium Fluoride	9.45	19.0	2640
Impactor	Aluminum 6061-T6	12.51	87.5	2703
Backer	n/a			

Comments: The abrupt velocity drop at approximately 0.4 μs is not understood–possibly an experimental difficulty.

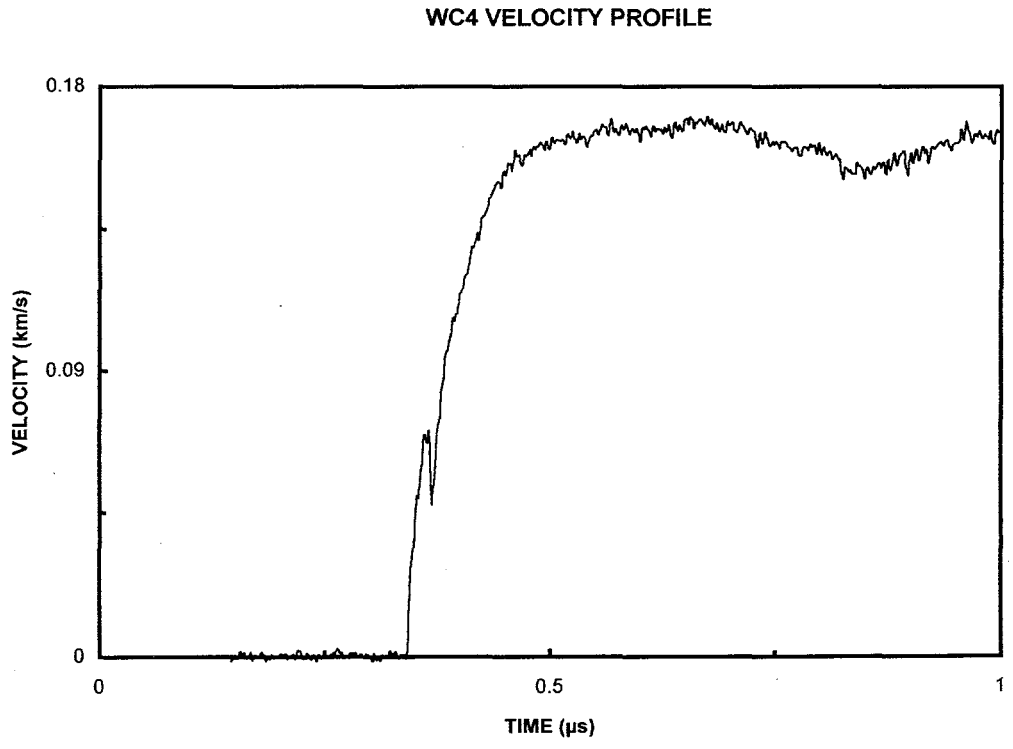

Shot Number:	WC5	**Impact Velocity:**	0.361 km/s
Test Material:	Tungsten Carbide		
Supplier:	LANL	**Velocity Per Fringe:**	94.76 m/s

	Material	Thickness (mm)	Diameter (mm)	Density (kg/m^3)
Sample	Tungsten Carbide	2.986	10.8	14910
Window	Lithium Fluoride	9.47	19.0	2640
Impactor	Aluminum 6061-T6	1.047	50.8	2703
Backer	PMMA	5.85	87.5	1186

Comments: Spall experiment

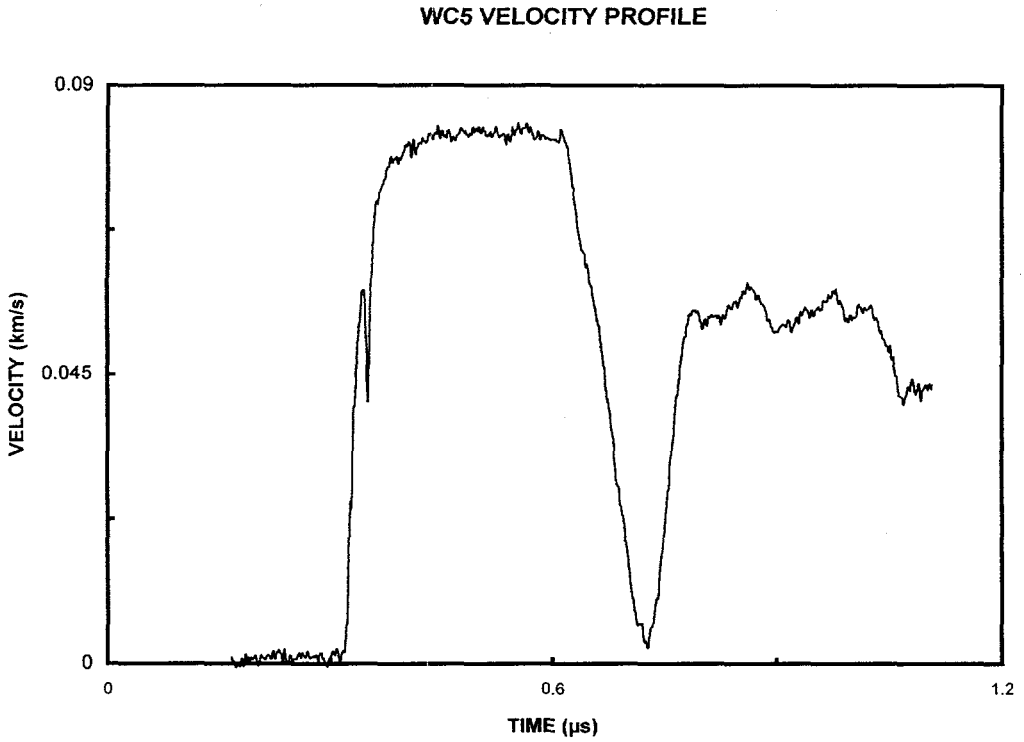

Shot Number:	WC6	**Impact Velocity:**	0.446 km/s
Test Material:	Tungsten Carbide		
Supplier:	LANL	**Velocity Per Fringe:**	94.76 ms

	Material	Thickness (mm)	Diameter (mm)	Density (kg/m^3)
Sample	Tungsten Carbide	2.980	10.831	14910
Window	Lithium Fluoride	9.54	19.0	2640
Impactor	Aluminum 6061-T6	1.038	50.7	2703
Backer	PMMA	5.91	87.5	1186

Comments: Spall experiment

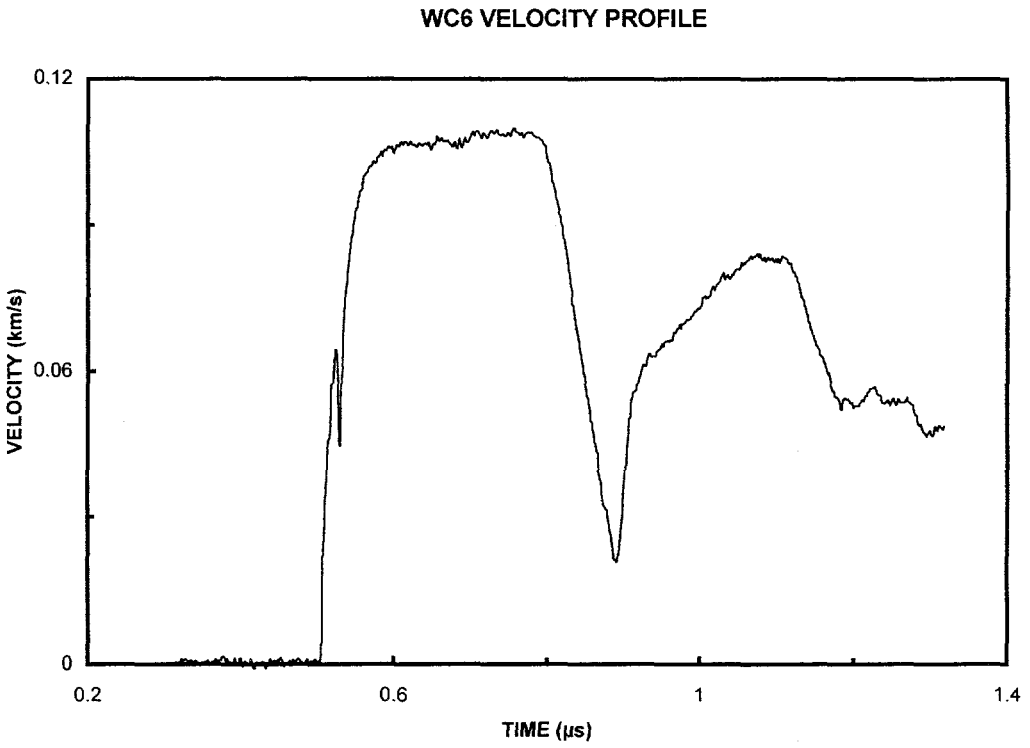

Shot Number:	WC7	**Impact Velocity:**	0.405 km/s
Test Material:	Tungsten Carbide		
Supplier:	Kennametal	**Velocity Per Fringe:**	108.85 m/s

	Material	Thickness (mm)	Diameter (mm)	Density (kg/m^3)
Sample	Tungsten Carbide	3.357	63.5	14930
Window	Lithium Fluoride	25.4	38.0	2640
Impactor	Aluminum 6061-T6	1.030	50.7	2703
Backer	PMMA	5.90	87.5	1186

Comments: Spall experiment

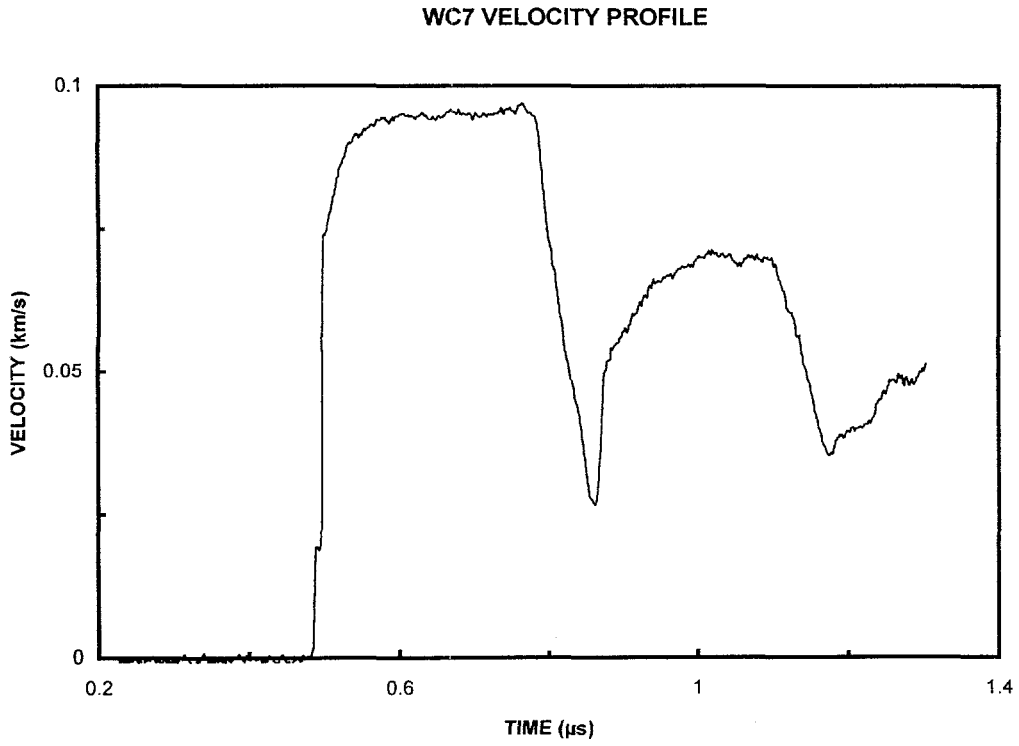

Shot Number:	WC8	**Impact Velocity:**	1.660 km/s
Test Material:	Tungsten Carbide		
Supplier:	Cercom	**Velocity Per Fringe:**	551.36 m/s

	Material	Thickness (mm)	Diameter (mm)	Density (kg/m^3)
Sample	Tungsten Carbide	6.178	50.2	15560
Window	Lithium Fluoride	19.0	50.8	2640
Impactor	Tungsten Carbide	6.200	50.1	15560
Backer	PMMA	5.82	87.5	1186

Comments:

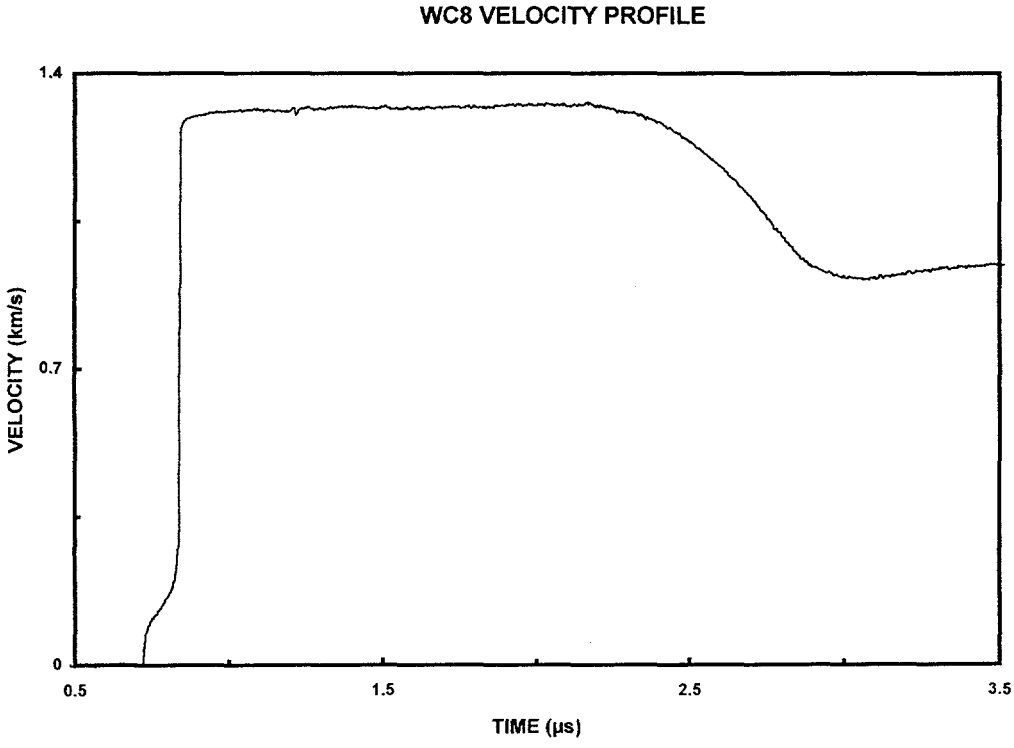

Shot Number:	WC9	**Impact Velocity:**	0.362 km/s
Test Material:	Tungsten Carbide		
Supplier:	Cercom	**Velocity Per Fringe:**	155.23 m/s

	Material	Thickness (mm)	Diameter (mm)	Density (kg/m^3)
Sample	Tungsten Carbide	6.192	50.2	15560
Window	Lithium Fluoride	19.0	50.8	2640
Impactor	Aluminum 6061-T6	1.507	50.7	2703
Backer	PMMA	5.90	87.5	1186

Comments: Spall experiment

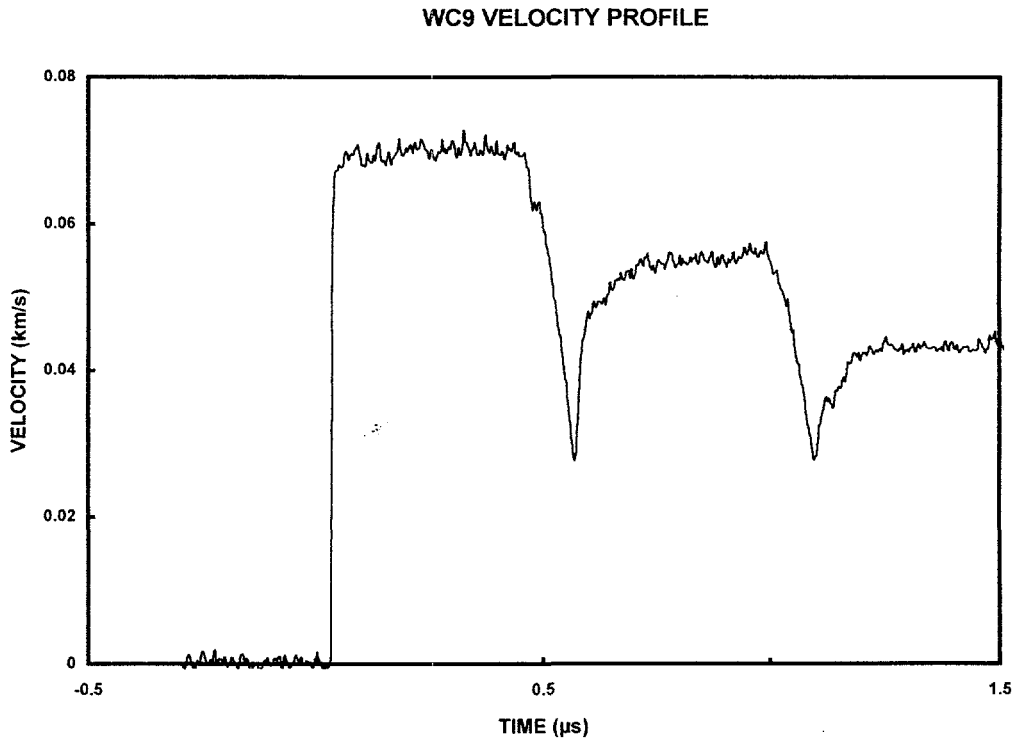

Shot Number:	WC10	**Impact Velocity:**	0.454 km/s
Test Material:	Tungsten Carbide		
Supplier:	Cercom	**Velocity Per Fringe:**	108.85 m/s

	Material	Thickness (mm)	Diameter (mm)	Density (kg/m^3)
Sample	Tungsten Carbide	6.190	50.0	15560
Window	Lithium Fluoride	18.9	50.7	2640
Impactor	Aluminum 6061-T6	1.500	50.8	2703
Backer	PMMA	5.90	87.5	1186

Comments: Spall experiment

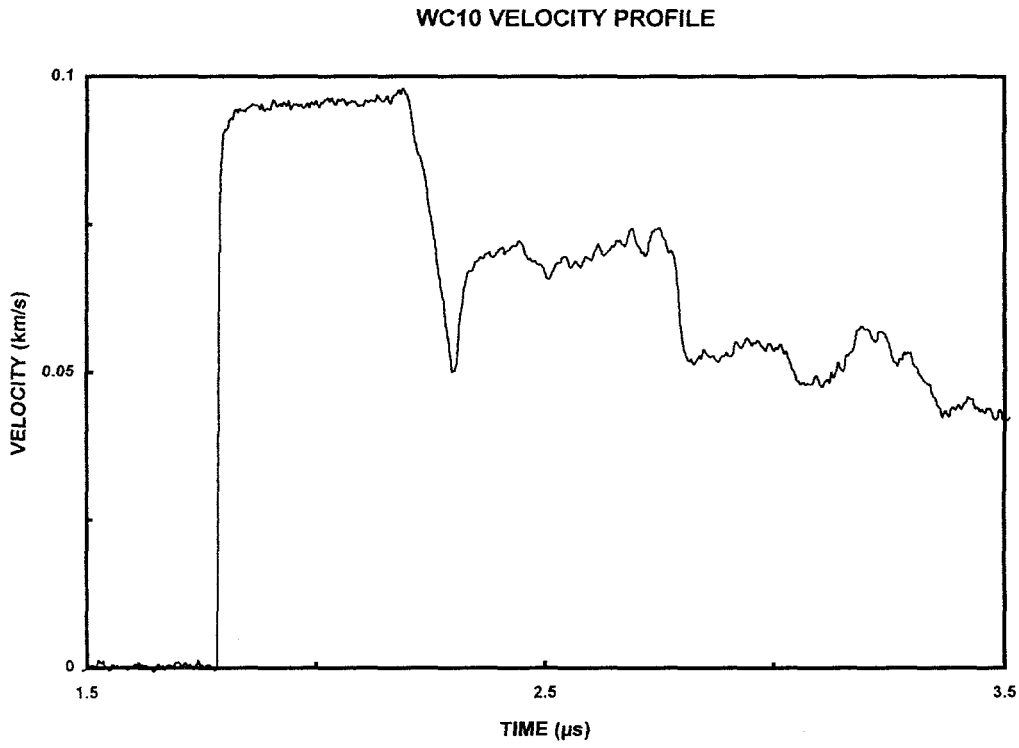

10. Zirconium Dioxide Ceramics

Zirconia ceramics have shown fascinating mechanical properties due to careful engineering of their chemistry and microstructure. Zirconium dioxide, in its pure form, exists in the stable monoclinic crystal structure. Through doping with other oxides (such as calcia, magnesia, or yttria in the several percent range), zirconium dioxide can be stabilized in either the cubic or the tetragonal structure. It is the latter structure which leads to the large fracture toughness (transformation toughening) properties exhibited by this ceramic.

The shock-compression properties of zirconia are also unusual. The shock properties of zirconium dioxide in both its pure form and its stabilized form (produced with oxide additives), have been extensively investigated [Mashimo, 1988; Mashimo, 1993 and references therein].

One material, an yttria-stabilized, tetragonal zirconia, has been observed to exhibit remarkable dynamic strength characteristics. In fact, Hugoniot measurements on this material, using inclined-mirror diagnostics, suggest a Hugoniot elastic limit in excess of 30 GPa [Mashimo, 1988], although streak photographs of the inclined mirror hint at possible structure in the profile of the precursor wave.

More recent shock-wave studies indicate a precursor amplitude at 13-17 GPa, raising questions concerning the dynamic strength reported in earlier works [Grady and Mashimo, 1992].

The principal material investigated in this study is Y_2O_3 (3 mol %), stabilized zirconium dioxide consisting of almost 100% tetragonal phase. The stabilized tetragonal zirconia has frequently been called partially stabilized zirconia in previous literature. This material was prepared by the hot, isostatic press method, and it was provided by Sumitomo Electric Industries. This zirconia is the same material investigated in an earlier shock-wave equation-of-state study [Mashimo, 1988]. A total of six shock compression and release experiments were performed on this material. In two of the tests (ZO3 and ZO4), a sample density of 5954 kg/m^3 was determined. Ultrasonic longitudinal and shear wave speeds for this material are 6.87 and 3.63 km/s, respectively. The remaining four experiments (ZO5 through ZO8) were performed on samples from a later batch, having a higher density of 6028 kg/m^3 and longitudinal and shear velocities of 7.11 and 3.72 km/s, respectively. The slight difference in densities between the two materials led to measurable and revealing differences in the shock-wave properties. Spall experiments performed in the tests ZO7 and ZO8 demonstrated unique dynamic tensile strength properties, possibly related to the transformation toughened nature of this material.

In addition, two further experiments (ZO1 and ZO2) were performed on a 10.5 mol %, yttria-stabilized, zironium dioxide from a different source. This material was nearly 100% cubic phase, with a density of 5602 kg/m^3. This material was approximately 4-6% porous, with pore volume distributed principally as intragranular, near-spherical, voids. Grain size was 7-15 μm, and longitudinal and shear velocities for this material were 6.61 and 3.54 km/s, respectively. The material was supplied by McDonald Refractories, Beaver Falls, Pennsylvania.

Shot Number:	ZO1	**Impact Velocity:**	1.556 km/s
Test Material:	Zirconium Dioxide		
Supplier:	McDonald	**Velocity Per Fringe:**	430.92 m/s

	Material	Thickness (mm)	Diameter (mm)	Density (kg/m^3)
Sample	Zirconium Dioxide	6.635	53.0	5602
Window	Lithium Fluoride	25.4	50.8	2640
Impactor	Zirconium Dioxide	3.313	53.0	5602
Backer	Polyurethane Foam	6.0	87.5	320

Comments: Tests Z01 and Z02 were performed on cubic zirconia

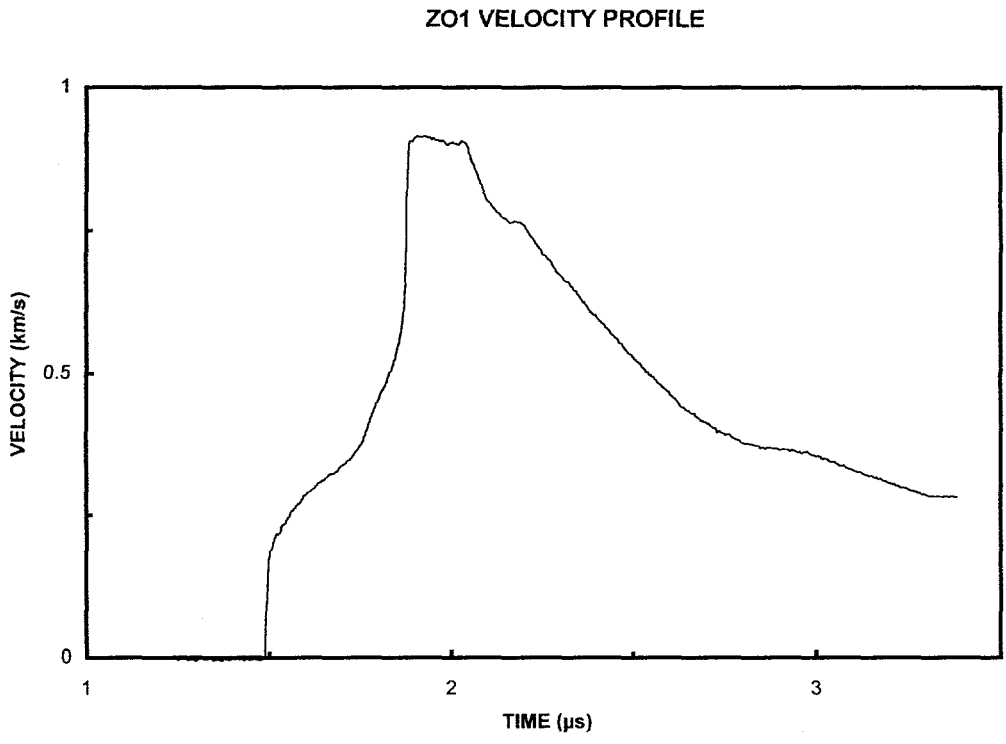

Shot Number:	ZO2	**Impact Velocity:**	2.075 km/s
Test Material:	Zirconium Dioxide		
Supplier:	McDonald	**Velocity Per Fringe:**	430.92 m/s

	Material	Thickness (mm)	Diameter (mm)	Density (kg/m^3)
Sample	Zirconium Dioxide	6.624	53.0	5602
Window	Lithium Fluoride	25.4	50.8	2640
Impactor	Zirconium Dioxide	3.247	53.0	5602
Backer	Polyurethane Foam	6.0	87.5	640

Comments:

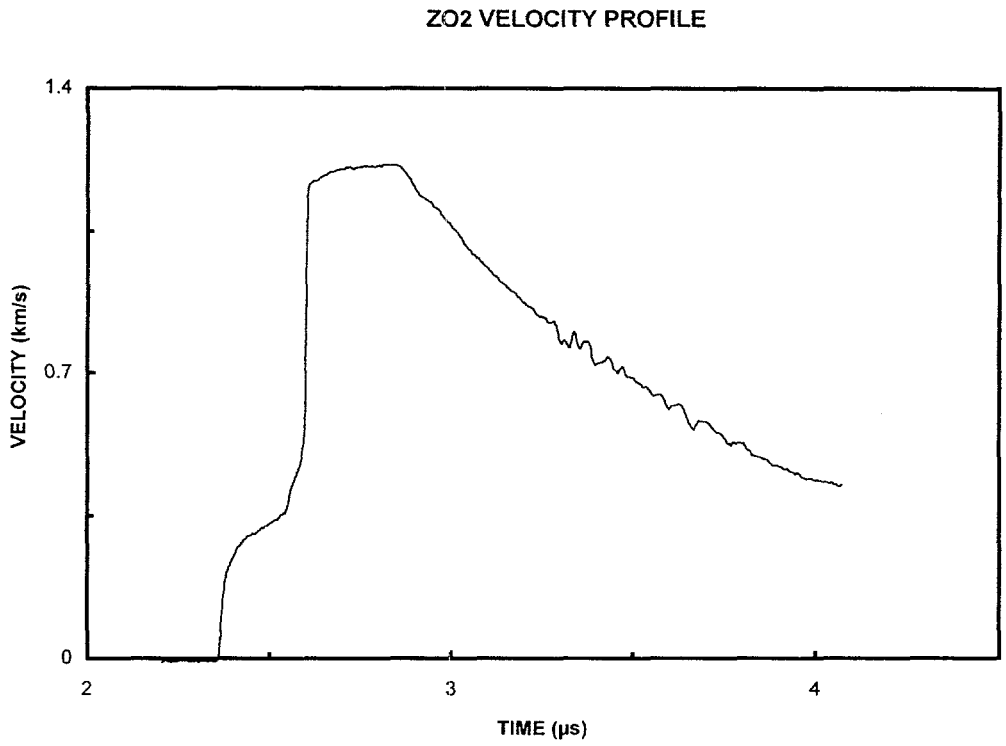

Shot Number:	ZO3	**Impact Velocity:**	1.749 km/s
Test Material:	Zirconium Dioxide		
Supplier:	Sumitomo Industries	**Velocity Per Fringe:**	551.36 m/s

	Material	Thickness (mm)	Diameter (mm)	Density (kg/m^3)
Sample	Zirconium Dioxide	4.102	30.3	5954
Window	Lithium Fluoride	19.0	25.4	2640
Impactor	Zirconium Dioxide	2.506	30.3	5954
Backer	Polyurethane Foam	3.0	87.5	640

Comments: Tests Z03 through Z08 were performed on tetragonal zirconia

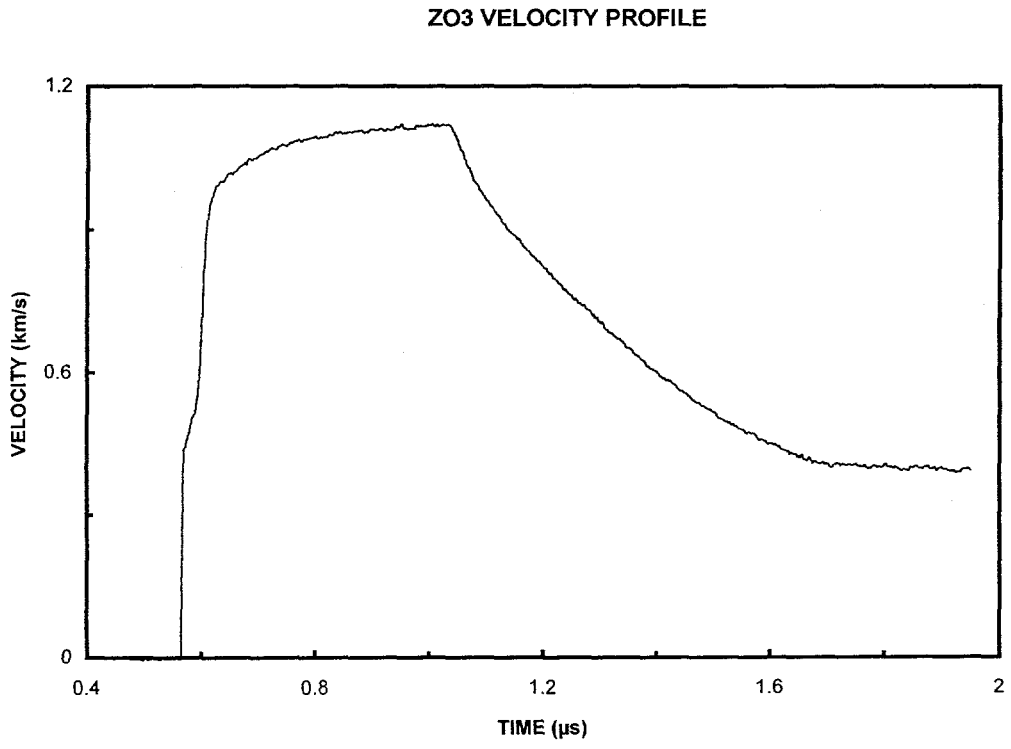

Shot Number:	ZO4	**Impact Velocity:**	2.308 km/s
Test Material:	Zirconium Dioxide		
Supplier:	Sumitomo Industries	**Velocity Per Fringe:**	551.36 m/s

	Material	Thickness (mm)	Diameter (mm)	Density (kg/m^3)
Sample	Zirconium Dioxide	4.088	30.3	5954
Window	Lithium Fluoride	19.0	25.4	2640
Impactor	Zirconium Dioxide	2.509	30.3	5954
Backer	Polyurethane Foam	3.0	87.5	640

Comments: Noise on release portion portion at wave is electronic

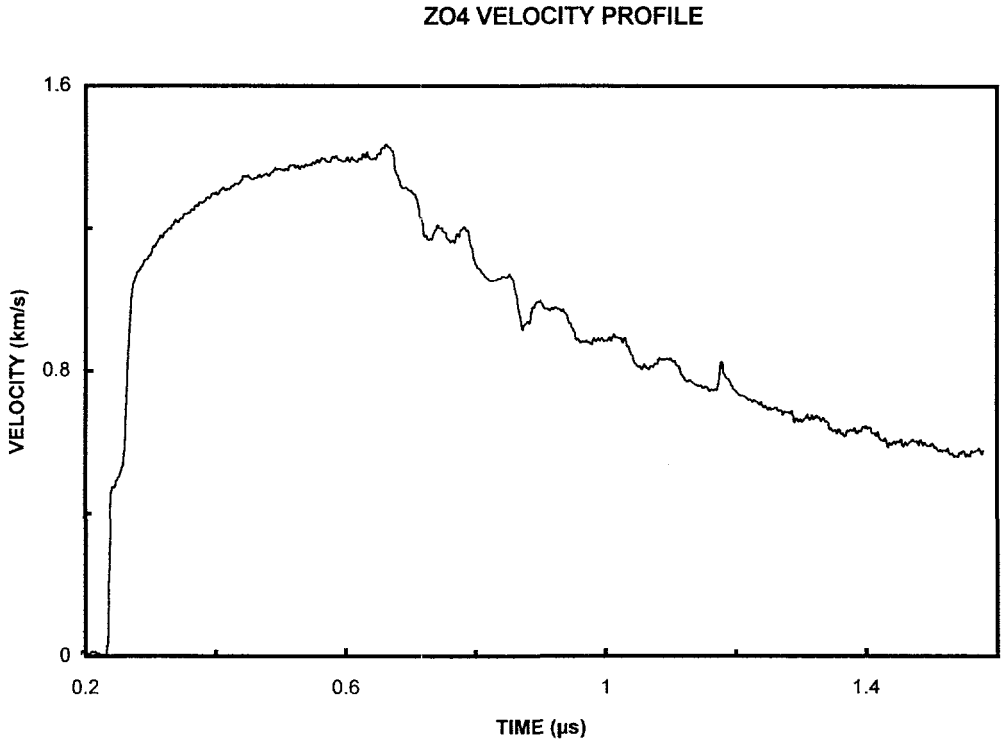

Shot Number:	ZO5	**Impact Velocity:**	2.270 km/s
Test Material:	Zirconium Dioxide		
Supplier:	Sumitomo Industries	**Velocity Per Fringe:**	681.52 m/s

	Material	Thickness (mm)	Diameter (mm)	Density (kg/m^3)
Sample	Zirconium Dioxide	3.958	29.9	6028
Window	Lithium Fluoride	19.0	25.4	2640
Impactor	Tantalum	1.316	73.7	16600
Backer	PMMA	6.0	87.5	1186

Comments:

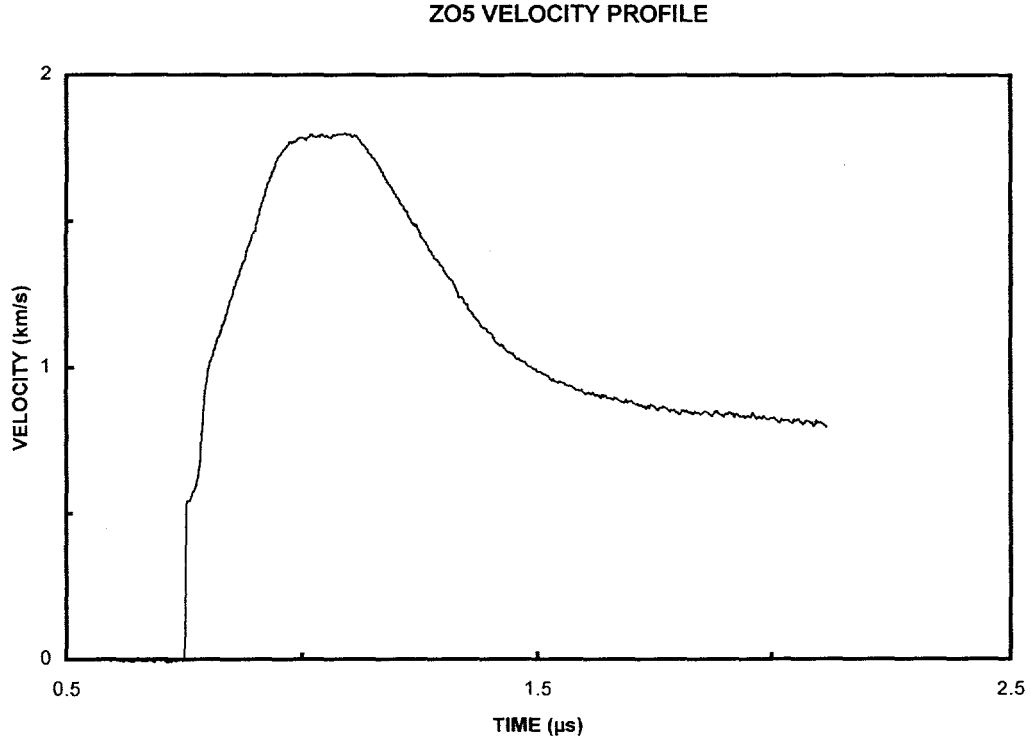

Shot Number:	ZO6	**Impact Velocity:**	1.100 km/s
Test Material:	Zirconium Dioxide		
Supplier:	Sumitomo Industries	**Velocity Per Fringe:**	430.92 m/s

	Material	Thickness (mm)	Diameter (mm)	Density (kg/m^3)
Sample	Zirconium Dioxide	3.955	29.9	6028
Window	Lithium Fluoride	19.0	25.4	2640
Impactor	Tantalum	1.308	73.7	16600
Backer	PMMA	6.0	87.5	1186

Comments:

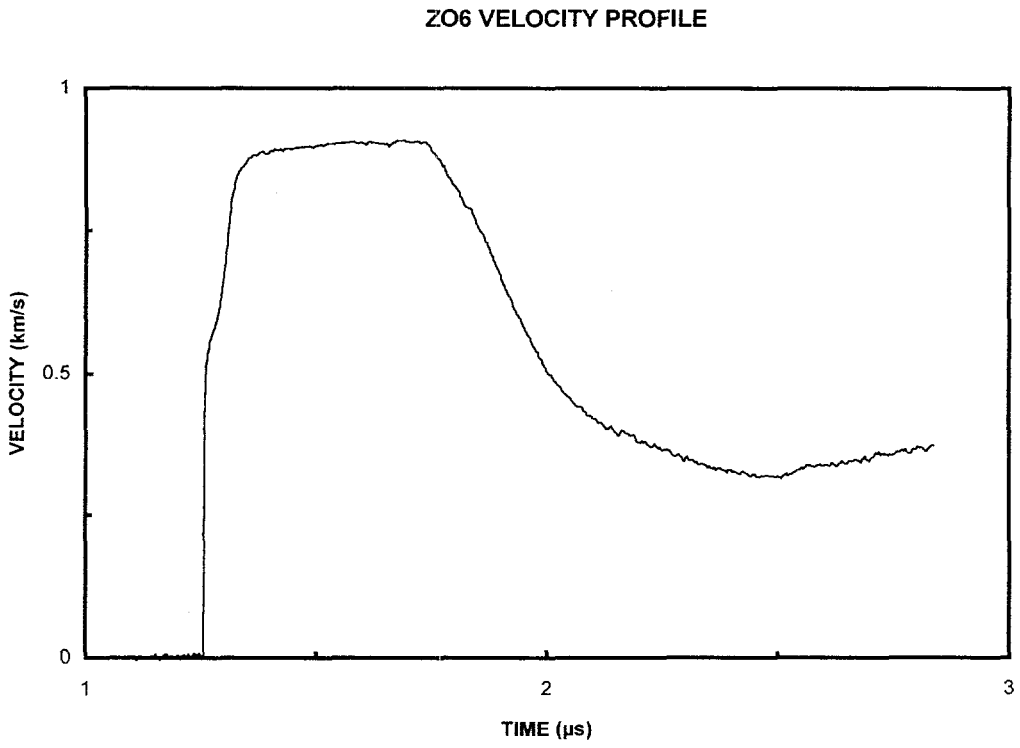

Shot Number:	ZO7	**Impact Velocity:**	0.519 km/s
Test Material:	Zirconium Dioxide		
Supplier:	Sumitomo Industries	**Velocity Per Fringe:**	128.07 m/s

	Material	Thickness (mm)	Diameter (mm)	Density (kg/m^3)
Sample	Zirconium Dioxide	4.953	29.9	6028
Window	Lithium Fluoride	19.0	19.0	2640
Impactor	Zirconium Dioxide	2.408	29.9	6028
Backer	Polyurethane Foam	5.0	87.5	320

Comments:

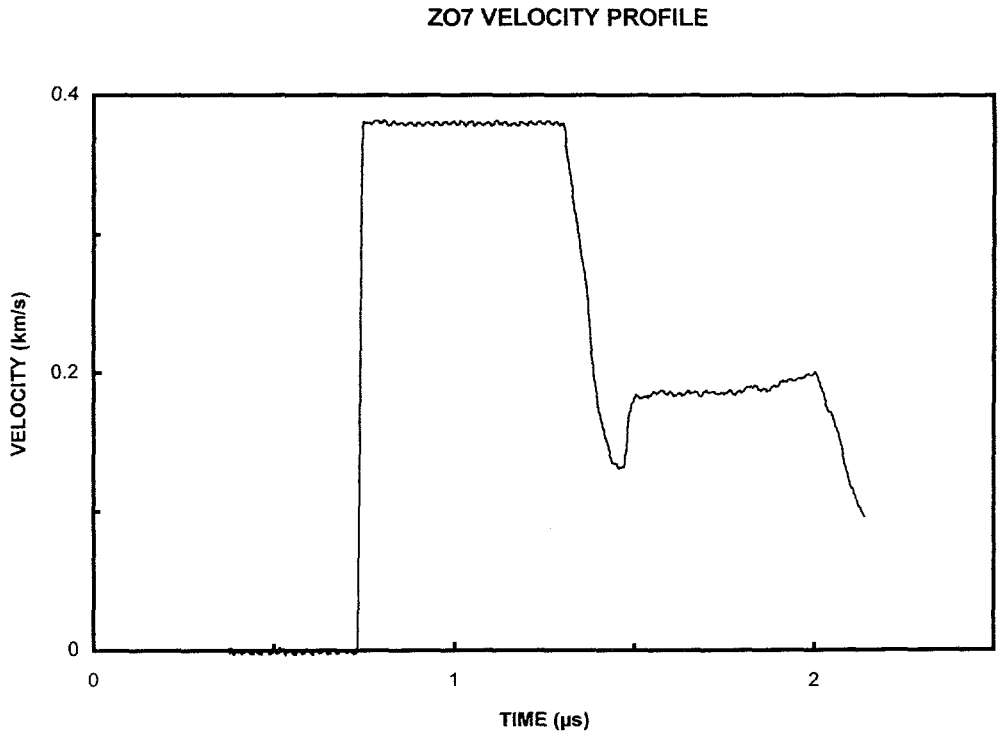

Shot Number:	ZO8	**Impact Velocity:**	0.564 km/s
Test Material:	Zirconium Dioxide		
Supplier:	Sumitomo Industries	**Velocity Per Fringe:**	128.07 m/s

	Material	Thickness (mm)	Diameter (mm)	Density (kg/m^3)
Sample	Zirconium Dioxide	4.938	29.9	6028
Window	Lithium Fluoride	19.0	19.0	2640
Impactor	Zirconium Dioxide	2.398	29.9	6028
Backer	Polyurethane Foam	5.0	87.5	320

Comments:

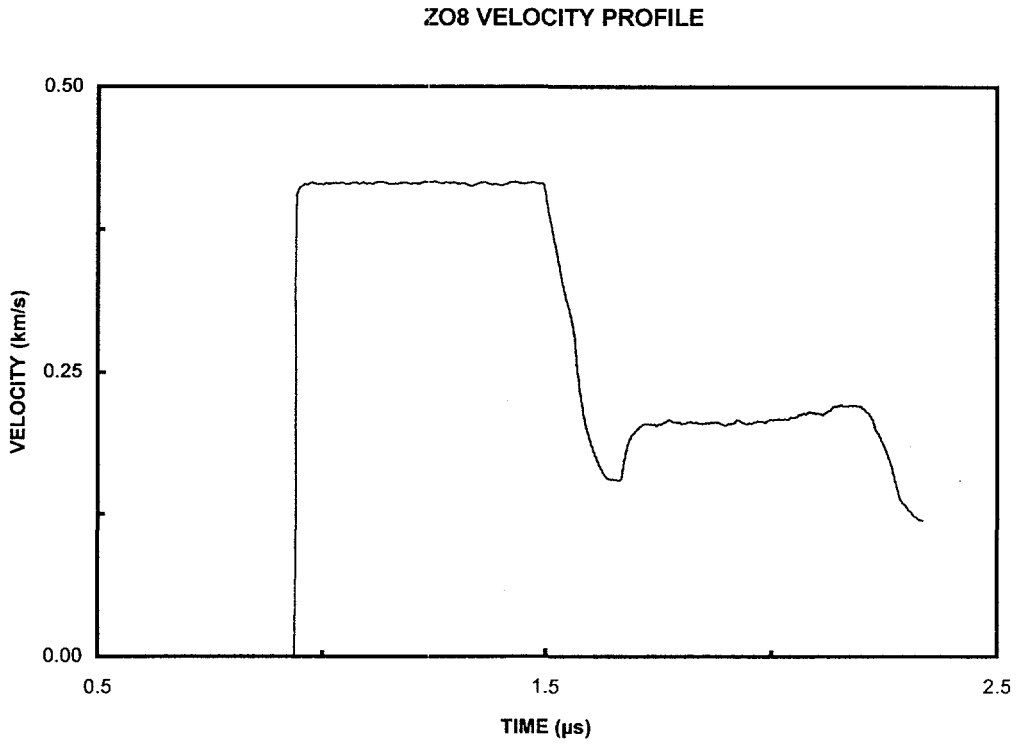

11. References

Ahrens, T. J., W. H. Gust and E. B. Royce, Material Strength Effects in Alumina, J. Appl. Phys., 39, 4610-4616, 1968.

Barker, L. M. and R. E. Hollenbach, Laser Interferometer for Measuring High Velocities of any Reflecting Surface. J. Appl. Phys., 43, 4669-4675, 1972.

Brar, N. S., S. J. Bless, and Z. Rosenberg, Response of Shock-Loaded AlN Ceramics Determined with In-Material Manganin Gauges, in Shock-Wave and High-Strain-Rate Phenomena in Materials, M. A. Meyers, et al. eds., Marcel Dekker, Inc., 1023-1030 (1992).

Cagnoux, J. and F. Longy, Spallation and Shock-Wave Behavior of Some Ceramics, DYMAT-88 - International Conference on Mechanical and Physical Behavior of Materials under Dynamic Loading, les Editions de Physique, 3-10 (1988).

Dandekar, D. P. and D. C. Benfanti, Strength of Titanium Diboride under Shock Wave Loading, J. Appl. Phys., 73, 673-679 (1993).

Dandekar, D. P., A. Abbate and J. Frankel, Equation of Aluminum Nitride and its Shock Response, J. Appl. Phys., 76, 4077-4085 (1994).

Dandekar, D. P and P Bartkowski, Shock Response of AD995 Alumina, in High Pressure Science and Technology - 1993, S. C. Schmidt, J. W. Shaner, G. A. Samara, M. Ross, eds., AIP Press, 733-736 (1994).

Emin, D., Icosahedral Boron-Rich Solids, Physics Today, 1, 1-8 (1987).

Grady, D. E., Shock-Wave Properties of High-Strength Ceramics, in Shock Compression of Condensed Matter, S. C. Schmidt, R. D. Dick, J. W. Forbes, D. G. Tasker, eds., North Holland, 455-458 (1992a).

Grady, D. E., Shock-Compression Properties of Ceramics, in Recent Trends in High-Pressure Research, A. K. Singh, ed., Oxford and IBH Publishing, 641-650 (1992b).

Grady, D. E. and T. Mashimo, Shock and Release Wave Properties of Yttria-Doped Tetragonal and Cubic Zirconia, J. Appl. Phys., 71, 4868-4874 (1992).

Grady, D. E. and M. E. Kipp, Shock Compression Properties of Silicon Carbide, Sandia National Laboratories Technical Report, SAND92-1832, July (1993).

Grady, D. E. and J. L. Wise, Dynamic Properties of Ceramic Materials, Sandia National Laboratories Technical Report, SAND93-0610, September (1993).

Grady, D. E., Dynamic Failure in Brittle Solids, in Fracture and Damage in Quasibrittle Structures: Experiment, Modeling and Computer Analysis, Z. P. Bazant et al. eds., E&FN Spon, 259-272 (1994a).

Grady, D. E., Shock-Wave Strength Properties of Boron Carbide and Silicon Carbide, in Proceedings of EuroDYMAT 94 - International Conference of Mechanical and Physical Behavior of Materials under Dynamic Loading, les Editions de Physique, 385-391 (1994b).

Grady, D. E., Dynamic Properties of Ceramic Materials, Sandia National Laboratories Technical Report, SAND94-3266, February (1995).

Graham, R. A. and W. P. Brooks, Shock-Wave Compression of Sapphire from 15 to 420 kbar: The Effects of Large Anisotropic Compressions, Phys. Chem. Solids, 32, 2311, 1971.

Gust, W. H. and E. B. Royce, Dynamic Yield Strengths of B_4C, BeO, and Al_2O_3 Ceramics, J. Appl. Phys., 42, 276-295 (1971).

Gust, W. H., A. C. Holt and E. B. Royce, Dynamic Yield, Compressional, and Elastic Parameters for Several Light Intermetallic Compounds, J. Appl. Phys., 44, 550-560 (1973).

Gust, W. H., Hugoniot Elastic Limits and Compression Parameters for Brittle Materials, in High Pressure Science and Technology, Vol. 2, B. Vodar and Ph. Marteau, eds., Pergamon Press, 1009-1016 (1980).

Kipp, M. E. and D. E. Grady, Shock Compression and Release in High-Strength Ceramics, Sandia National Laboratories Report, SAND89-1461, July (1989).

Kipp, M. E. and D. E. Grady, Shock Phase Transformation and Release Properties of Aluminum Nitride, in Proceedings of EuroDYMAT 94 - International Conference of Mechanical and Physical Behavior of Materials under Dynamic Loading, les Editions de Physique, 249-256 (1994).

Kondo, K., Sawaoka, A., Sato and M. Ando, Shock Compression and Phase Transformation of AlN and BP, AIP Conference Proceedings No. 78, Shock Waves in Condensed Matter - 1981 (Menlo Park), W. J. Nellis, L. Seaman, and R. A. Graham, eds., AIP Press, 303-305 (1982).

Marsh, S. P., LASL Shock Hugoniot Data, S. P. Marsh, ed., University of California Press, (1980).

Mashimo, T., Anomalously High Hugoniot Elastic Limit (35-39 GPa) of Y_2O_3-Doped Partially Stabilized Zirconia Ceramics, J. Appl. Phys., 63, 4747-4748 (1988).

Mashimo, T., Shock Compression Studies of Ceramic Materials, in Shock Wave in Materials Science, A. B. Sawaoka, ed., Springer-Verlag, 113-144 (1993).

McQueen, R. G., The Equation of State of Mixtures, Alloys, and Compounds, in Seismic Coupling, G. Simmons, ed., Proceedings of a Meeting sponsored by the Advanced Research Projects Agency at Stanford Research Institute, Menlo Park, California, January 15-16, (1968).

McQueen, R. G., S. P. Marsh, J. W. Taylor, J. N. Fritz, W. J. Carter, The Equation of State of Solids from Shock Wave Studies, in High-Velocity Impact Phenomena, R. Kinslow, ed., Academic Press, 293-417, 521-568 (1970).

McQueen, R. C. and S. P. Marsh, Handbook of Physical Constants, S. P. Clark Jr., ed., Geophysical Society of America, New York, Chapter 7, 1960.

Morris, C.E., LASL Shock Wave Profile Data, C.E. Morris, ed., Univ. of California Press, (1980).

Munson, D. E. and R. J. Lawrence, Dynamic Deformation of Polycrystalline Alumina, J. Appl. Phys, 50, 6272-6282 (1979).

Nahme, H., V. Hohler and A. Stilp, Dynamic Material Properties and Terminal Ballistic Behaviour of Shock-Loaded Silicon-Nitride Ceramics, in Proceedings of EuroDYMAT 94 - International Conference of Mechanical and Physical Behavior of Materials under Dynamic Loading, les Editions de Physique, 237-242 (1994).

Nakamura, A. and T. Mashimo, Shock-Induced Phase Transition of AlN, in High Pressure Science and Technology - 1993, S. C. Schmidt, J. W. Shaner, G. A. Samara, M. Ross, eds., AIP Press, 981-984 (1994).

Sato, T. and S. Akimoto, Hydrostatic Compression of Four Corundum-Type Compounds, J. Appl. Phys. 50, 5285-5291 (1979).

Staehler, J. M., W. W. Predebon and B. J. Pletka, The Mechanical Response of a High-Purity Alumina over the Strain Rate Range of 10^{-4} to 10^{-6} per Second, in Proceedings 13th Army Symposium on Solid Mechanics, S. C. Chou et al., eds., 493-504 (1993).

Steinburg, D.J., Equation of State and Strength Properties of Selected Materials, Lawerence Livermore Laboratories Report, UCRL-MA-106439 (1991).

Vanderwalker, D. M., Fracture in Titanium Diboride, Phys. Stat. Sol., 111, 119-126 (1989).

Vanderwalker, D. M. and W. J. Croft, Dislocations in Shock Loaded Titanium Diboride, J. Mater. Res., 3, 761-763 (1988).

Vollstädt, H., E. Ito, M. Akaishi, S. Akimoto, and O. Fukunaga, High Pressure Synthesis of Rocksalt Type of AlN, Proc. Japan Acad., 66 Ser. B, 7-9 (1990).

Winkler, W. D. and A. J. Stilp, Pressure-Induced Macro- and Micro-Mechanical Phenomena in Planar Impact in TiB_2, in Shock Compression of Condensed Matter, S. C. Schmidt, R. D. Dick, J. W. Forbes, D. G. Tasker, eds., North Holland, 555-558 (1992).

Wise, J. L. and L. C. Chhabildas, Laser Interferometer Measurements of Refractive Index in Shock-Compressed Materials, in Shock Waves in Condensed Matter - 1985, Y. M. Gupta, ed., Plenum Press, 441-445, 1986.

Yamakawa, A., T. Nishioka, M. Miyake, K. Wakamkori, T. Mashimo, Shock-Yielding Properties of Si_3N_4 Ceramics: Correlation with the Microstructure and Static Mechanical Strength, J. Ceramic Soc. Japan, 101, 1322-1326 (1993).

Yeshurun, Y., D. G. Brandon, A. Venkert and Z. Rosenberg, The Dynamic Properties of Two-Phase Alumina-Glass Ceramics, DYMAT-88 - International Conference on Mechanical and Physical Behavior of Materials under Dynamic Loading, les Editions de Physique, 11-18 (1988).

APPENDIX A

Table 1:
Ultrasonic and Elastic Properties[1]

Ceramic	Supplier[2]	ρ_o (kg/m^3)	C_l (km/s)	C_s (km/s)	C_o (km/s)	K (GPa)	G (GPa)	ν
AlN	Dow Chem.	3254	10.73	6.32	7.87	201.5	130.0	.235
AlN	Sumitomo	3236	10.80	6.34	7.94	204.0	130.1	.237
Al_2O_3	Industrie Bitassi	3555	9.28	5.47	6.80	164.4	106.4	.234
Al_2O_3	Coors (AD995)	3890	10.56	6.24	7.72	231.8	151.5	.232
Al_2O_3	Coors (AD999)	3948	10.85	6.38	7.97	250.8	160.7	.236
Al_2O_3	Mich. Tech.	3970	10.91	6.44	7.98	252.8	164.7	.232
B_4C	Eagle Picher	2517	14.04	8.90	9.57	230.5	199.4	.164
B_4C	Dow Chem.	2506	14.07	8.87	9.65	233.4	197.2	.170
SiC	Eagle Picher	3177	12.06	7.67	8.19	213.1	186.9	.161
SiC	Cercom (SiC-B)	3150	12.22	7.62	8.48	226.5	182.9	.182
Si_3N_4	Kyocera	3152	10.31	5.81	7.83	193.2	106.4	.267
TiB_2	Eagle Picher	4452	10.93	7.30	6.96	215.7	237.2	.098
TiB_2	Cercom	4509	10.79	7.43	6.54	192.9	248.9	.049
TiB_2	Ceradyne	4490	11.23	7.41	7.27	237.3	246.5	.114
TiB_2	Ernst-Mach	4360	10.80	7.30	6.75	198.7	232.3	.079
WC	Kennametal	14930	6.90	4.17	4.94	364.3	259.6	.212
WC	LANL	14910	6.92	4.15	4.99	371.3	256.8	.219
WC	Cercom	15560	7.04	4.30	4.99	387.4	287.7	.202
ZrO_2	Sumitomo (1)	5954	6.87	3.63	5.44	176.2	78.5	.306
ZrO_2	Sumitomo (2)	6028	7.11	3.72	5.67	193.8	83.4	.312
ZrO_2	McDonald	5602	6.61	3.54	5.19	150.9	70.2	.299

[1] Elastic properties are calculated assuming elastic isotropy. This is known to be incorrect for at least some of the hot pressed ceramics (notably the Cercom TiB_2).
[2] See Text.

APPENDIX B

In the present report a uniform system of test numbering was used which, in most cases, does not agree with the original test numbers assigned during the performance of the experiments. A number of the original test numbers appear in earlier reports and papers. For this reason the present appendix provides a cross reference between the numbering system in the present report and the original test numbers.

Aluminum Nitride (AlN)

AN1	CE33
AN2	CE34
AN3	CE35
AN4	CE36
AN5	CE37
AN6	CE43
AN7	CE44
AN8	CE47
AN9	CE48
AN10	CE52
AN11	CE53
AN12	AL01
AN13	AL02
AN14	AL03

Aluminum Oxide (Al_2O_3)

AO1	CE11
AO2	CE12
AO3	CE56
AO4	CE57
AO5	CE58
AO6	CE59
AO7	CE60
AO8	CE61
AO9	CE62
AO10	CE63
AO11	CE72
AO12	CE80
AO13	CE88
AO14	CE89
AO15	CE90
AO16	CE91
AO17	AO01
AO18	AO02
AO19	AO03
AO20	MT1
AO21	MT2

Boron Carbide (B_4C)

BC1	CE3
BC2	CE6
BC3	CE16
BC4	CE17
BC5	CE18
BC6	CE25

BC7	CE26
BC8	CE30
BC9	CE41
BC10	CE101
BC11	CE102

Silicon Carbide (SiC)

SC1	CE4
SC2	CE5
SC3	CE31
SC4	CE32
SC5	CE42
SC6	SC6
SC7	SC7
SC8	SC12
SC9	SC13
SC10	SC15
SC11	SC16
SC12	SC17
SC13	SC18
SC14	SC19
SC15	SC1
SC16	SC2
SC17	SC3
SC18	SC4
SC19	SC5

Silicon Nitride (Si_3N_4)

SN1	CE95
SN2	CE96
SN3	CE97
SN4	CE98
SN5	CE99
SN6	SIN1
SN7	SIN2
SN8	CE104

Titanium Diboride (TiB_2)

TB1	CE7
TB2	CE10
TB3	CE9
TB4	CE15
TB5	CE19
TB6	CE20
TB7	CE23
TB8	CE24
TB9	CE29
TB10	CE38
TB11	CE51
TB12	CE70
TB13	CE71
TB14	CE73
TB15	CE74
TB16	CE75
TB17	CE83
TB18	CE84
TB19	CE2
TB20	TE1
TB21	TE2

Tungsten Carbide (WC)

WC1	WC1
WC2	WC2
WC3	WC3
WC4	WC4
WC5	WC5
WC6	WC6
WC7	WC7
WC8	WC8
WC9	WC12
WC10	WC13

Zirconium Dioxide (ZrO_2)

ZO1	CE1
ZO2	CE8
ZO3	CE13
ZO4	CE14
ZO5	CE21
ZO6	CE22
ZO7	CE28
ZO8	CE39

DISTRIBUTION:

INTERNAL

MS 0100 Document Processing for DOE/OSTI (2)
MS 0619 Print Media
MS 0899 Technical Library (5)
MS 9018 Central Technical Files

MS 0321 W. J. Camp
MS 0458 J. R. Asay
MS 0821 J. A. Ang
MS 1111 S. S. Dosanjh
MS 1110 R. C. Allen
MS 1109 A. L. Hale
MS 0441 P. L. Stanton
MS 0819 J. M. McGlaun
MS 0819 E. S. Hertel
MS 0819 J. S. Peery
MS 0819 A. C. Robinson
MS 0819 T. G. Trucano
MS 0819 M. K. Wong
MS 0820 P. Yarrington
MS 0820 R. M. Brannon
MS 0820 H. E. Fang
MS 0820 A. V. Farnsworth
MS 0820 M. E. Kipp
MS 0820 S. A. Silling
MS 0820 P. A. Taylor
MS 0821 L. C. Chhabildas
MS 0821 M. D. Furnish
MS 0821 D. A. Crawford
MS 0821 D. E. Grady (25)
MS 0439 D. R. Martinez
MS 0834 A. C. Ratzel
MS 0443 H. S. Morgan
MS 0437 R. K. Thomas
MS 0437 J. W. Swegle
MS 0501 S. T. Montgomery
MS 0812 C. A. Harris
MS 0812 R. L. Moody (10)
MS 0861 J. T. Hitchcock
MS 0303 M. J. Forrestal
MS 1033 J. L. Wise

EXTERNAL

T. F. Adams
Los Alamos National Laboratory
MS F663
Los Alamos, NM 87545

T. J. Ahrens
Geophysics Division MS/252-21
California Institute of Technology
Pasadena, CA 91125

F. Allahdadi
Phillips Laboratory
PL/WSSD
Kirtland AFB, NM 87117-6008

M. L. Alme
102 Stevens Forrest Professional Center
9650 Santiago Road
Columbia, MD 21045

C. E. Anderson
Southwest Research Institute
6220 Culebra Road
San Antonio, TX 78284

J. A. Bailey
U.S. Army Research Office
P. O. Box 12211
Research Triangle Park, NC 27709

E. Baker
Army ARDE Center
SMCAR-AEE-WW
Picatinny Arsenal, NJ 07806-5000

D. W. Baum
Lawrence Livermore National Laboratory
L-35
Livermore,CA 94550

S. J. Bless
Institute for Advanced Technology
4030-2 W. Braker Lane
Austin, TX 78759-5329

S. Brar
Impact Physics Laboratory
University of Dayton Research Institute
300 College Park
Dayton, OH 45469-0182

W. J. Bruchey
Army Research Laboratory
Weapons Technology Directorate
AMSRL-WT
Aberdeen Proving Ground, MD
21005-5066

G. Bulmash
Army Research Laboratory
Weapons Technology Directorate
AMSRL-WT-TA
Aberdeen Proving Ground, MD
21005-5066

S. Chou
Army Research Laboratory
Materials Directorate
AMSRL-MA-PD
Aberdeen Proving Ground, MD
21005-5066

R. Clifton
Brown University
Division of Engineering
Providence, RI 02912

J. W. Coltman
Simula Inc.
10016 South 51st Street
Phoenix, AZ 85044

D. Curran
SRI International
333 Ravenswood Avenue
Menlo Park, CA 94025

D. Dandekar
Army Research Laboratory
Materials Directorate
AMSRL-MA-PD
Aberdeen Proving Ground, MD
21005-5066

J. Dehn
Army Research Laboratory
Weapons Technology Directorate
AMSRL-WT-TA
Aberdeen Proving Ground, MD
21005-5066

K. Epstein
DOW Chemical USA
Ordnance Systems, 800 Building
Midland, MI 48667

H. Espinoza
Purdue University
School of Aeronautics
1282 Grissom Hall
West Lafayette, IN 47907-1282

A. Ezis
CERCOM, Inc.
1960 Watson Way
P. O. Box 70
Vista, CA 92083

J. C. Foster, Jr.
U.S. Air Force Armament Laboratory
AD/MNW
Eglin Air Force Base, FL 32542-5434

K. Frank
Army Research Laboratory
Weapons Technology Directorate
AMSRL-WT-TD
Aberdeen Proving Ground, MD
21005-5066

G. Gazonas
Army Research Laboratory
Weapons Technology Directorate
AMSRL-WT-PD
Aberdeen Proving Ground, MD
21005-5066

W. Gillich
Army Research Laboratory
Weapons Technology Directorate
AMSRL-WT-TA
Aberdeen Proving Ground, MD
21005-5066

W. Gooch
Army Research Laboratory
Weapons Technology Directorate
AMSRL-WT-TA
Aberdeen Proving Ground, MD
21005-5066

Y. Gupta
Washington State University
Department of Physics
Pullman, WA 99163

G. T. Gray
Los Alamos National Laboratory
MS G755
Los Alamos, NM 87545

R. S. Hixson
Los Alamos National Laboratory
MS P952
Los Alamos, NM 87545

S. Howard
U.S. Army MICOM
Bldg. 5400, Rm. 314B
Redstone Arsonal, AL 35898

T. Holmquist
Alliant Techsystems
600 2nd St., NE.
MN11-1614
Hopkins, MN 55343

Y. Horie
North Carolina State University
Dept. of Civil Engineering
Raleigh, NC 27607

K. Iyer
U.S. Army Research Office
P. O. Box 12211
Research Triangle Park, NC 27709

G. Johnson
Alliant Techsystems
600 2nd St., NE.
MN11-1614
Hopkins, MN 55343

J. N. Johnson
Los Alamos National Laboratory
MS B221
Los Alamos, NM 87545

P. Kingman
Army Research Laboratory
Weapons Technology Directorate
AMSRL-WT
Aberdeen Proving Ground, MD
21005-5066

K. Kimsey
Army Research Laboratory
Weapons Technology Directorate
AMSRL-WT
Aberdeen Proving Ground, MD
21005-5066

R. W. Kocher
Advanced Research Projects Agency
Land Systems Office
3701 North Fairfax Drive
Arlington, VA 22203-1714

J. Lankford
Southwest Research Institute
6220 Culebra Road
San Antonio, TX 78284

D. Lassila
Lawrence Livermore National Laboratory
L-35
Livermore,CA 94550

K. T. Leighton
Lanxide Armor Products, Inc.
1300 Marrows Road
P. O. Box 6077
Newark, DE 19714-6077

D. Lovelace
Army Missile Command
AMSMI-RD-ST-WF
Redstone Arsenal, AL 35898-5240

D. Mandell
Los Alamos National Laboratory
MS F663
Los Alamos, NM 87545

M. Manghnani
Mineral Physics Group
University of Hawaii
2525 Correa Rd.
Honolulu, HA 96822

H. W. Meyer
Army Research Laboratory
Weapons Technology Directorate
AMSRL-WT-TA
Aberdeen Proving Ground, MD
21005-5066

M. Meyer
Univ. of Calif. at San Diego
Dept. of Applied Mech. & Eng. Sciences
La Jolla, CA 92093

J. D. Morrow
FMC Corporation
Ground Systems Division
1107 Coleman Avenue Box 367
San Jose, CA 95103

S. Nemat-Nasser
Univ. of Calif. at San Diego
Dept. of Applied Mech. & Eng. Sciences
La Jolla, CA 92093

T. Nicholas
Air Force Wright Aeronautical Labs.
Air Force Systems Command
Materials Laboratory
Wright-Patterson AFB, OH 45433

D. Orphal
International Research Associates, Inc.
4450 Black Ave./ Suite E
Pleasanton, CA 94566

R. Palicka
CERCOM, Inc.
1960 Watson Way
P. O. Box 70
Vista, CA 92083

R. Paricio
Coors Ceramics Company
600 Ninth Street
Golden, CO 80401

A. Prakash
Army Research Laboratory
Weapons Technology Directorate
AMSRL-WT-WD
Aberdeen Proving Ground, MD
21005-5066

W. W. Predebon
College of Engineering
Michigan Technological University
Houghton, MI 49931

E. Rapacki
Army Research Laboratory
Weapons Technology Directorate
AMSRL-WT-TA
Aberdeen Proving Ground, MD
21005-5066

A. M. Rajendran
Army Research Laboratory
Materials Directorate
AMSRL-MA-PD
Aberdeen Proving Ground, MD
21005-5066

G. Randers-Pehrson
Army Research Laboratory
Weapons Technology Directorate
AMSRL-WT
Aberdeen Proving Ground, MD
21005-5066

G. Ravichandran
Graduate Aeronautical Laboratories
California Institute of Technology
MS 105-50
Pasadena, CA 91125

J. V. Repa
Los Alamos National Laboratory
MS A133
Los Alamos, NM 87545

M. Scheidler
Army Research Laboratory
Weapons Technology Directorate
AMSRL-WT
Aberdeen Proving Ground, MD
21005-5066

S. Segletes
Army Research Laboratory
Weapons Technology Directorate
AMSRL-WT
Aberdeen Proving Ground, MD
21005-5066

M. Slavin
Army Research Laboratory
Materials Directorate
AMSRL-MA-PD
Aberdeen Proving Ground, MD
21005-5066

D. Steinberg
Lawrence Livermore National Laboratory
MS L35
Livermore, CA 94550

J. Thompson
U.S. Army Tank-Automotive Command
AMSTA-RSS
Warren, MI 48397-5000

L. T. Wilson
Naval Surface Warfare Center
Code G 22
Dahlgren, VA 22448-5000

T. Wright
Army Research Laboratory
Weapons Technology Directorate
AMSRL-WT
Aberdeen Proving Ground, MD
21005-5066